NAVAL POSTGRADUATE SCHOOL
Monterey, California

THESIS

HELICOPTER CONTROLLABILITY

by

Dean Carico

September 1989

Thesis Advisor: George J. Thaler

Approved for public release; distribution unlimited

90 04 04 0₀₀

REPORT DOCUMENTATION PAGE		Form Approved OMB No. 0704-0188

1a. REPORT SECURITY CLASSIFICATION Unclassified	1b. RESTRICTIVE MARKINGS

2a. SECURITY CLASSIFICATION AUTHORITY	3. DISTRIBUTION/AVAILABILITY OF REPORT Approved for public release Distribution is unlimited
2b. DECLASSIFICATION/DOWNGRADING SCHEDULE	

4. PERFORMING ORGANIZATION REPORT NUMBER(S)	5. MONITORING ORGANIZATION REPORT NUMBER(S)

6a. NAME OF PERFORMING ORGANIZATION Naval Postgraduate School	6b. OFFICE SYMBOL (If applicable) 62	7a. NAME OF MONITORING ORGANIZATION Naval Postgraduate School

6c. ADDRESS (City, State, and ZIP Code) Monterey, California 93943-5000	7b. ADDRESS (City, State, and ZIP Code) Monterey, California 93943-5000

8a. NAME OF FUNDING/SPONSORING ORGANIZATION	8b OFFICE SYMBOL (If applicable)	9. PROCUREMENT INSTRUMENT IDENTIFICATION NUMBER

8c. ADDRESS (City, State, and ZIP Code)	10 SOURCE OF FUNDING NUMBERS			
	PROGRAM ELEMENT NO.	PROJECT NO.	TASK NO.	WORK UNIT ACCESSION NO.

11. TITLE (Include Security Classification)

HELICOPTER CONTROLLABILITY

12. PERSONAL AUTHOR(S)
CARICO, G. Dean

13a. TYPE OF REPORT Master's Thesis	13b TIME COVERED FROM _____ TO _____	14. DATE OF REPORT (Year, Month, Day) 1989, September	15. PAGE COUNT 219

16 SUPPLEMENTARY NOTATION The views expressed in this thesis are those of the author and do not reflect the official policy or position of the Department of Defense or the U.S. Government.

17.	COSATI CODES		18. SUBJECT TERMS (Continue on reverse if necessary and identify by block number)
FIELD	GROUP	SUB-GROUP	Helicopter Controllability, Helicopter Automatic Flight Control Systems, Helicopter Flying Qualities, and Flying Qualities Specifications.

19 ABSTRACT (Continue on reverse if necessary and identify by block number)

The concept of helicopter controllability is explained. A background study reviews helicopter development in the U.S. General helicopter configurations, linearized equations of motion, stability, and piloting requirements are discussed. Helicopter flight controls, handling qualities and associated specifications are reviewed. Analytical, simulation, and flight test methods for evaluating helicopter automatic flight control systems are discussed. A generic simulation is also conducted. This thesis is intended to be used as a resource document for a helicopter stability and control course at the Naval Postgraduate School.

20 DISTRIBUTION/AVAILABILITY OF ABSTRACT ☒ UNCLASSIFIED/UNLIMITED ☐ SAME AS RPT ☐ DTIC USERS	21. ABSTRACT SECURITY CLASSIFICATION UNCLASSIFIED
22a NAME OF RESPONSIBLE INDIVIDUAL Prof George J. Thaler	22b TELEPHONE (Include Area Code) (408) 646-2134	22c OFFICE SYMBOL 62Tr

DD Form 1473, JUN 86   Previous editions are obsolete.   SECURITY CLASSIFICATION OF THIS PAGE

S/N 0102-LF-014-6603   Unclassified

Helicopter Controllability

by

Dean Carico
Aerospace Engineer
B.S., ASE, VPI and SU, 1967
M.S., ASE, Princeton University, 1976

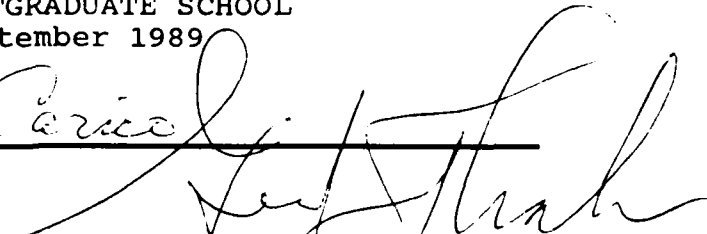Submitted in partial fulfillment of the requirements for the
degree of

MASTER OF SCIENCE IN ENGINEERING SCIENCE
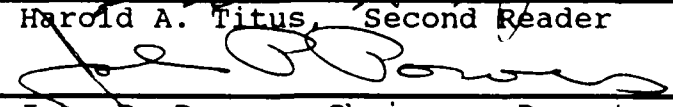
NAVAL POSTGRADUATE SCHOOL
September 1989

Author: _____
Dean Carico

Approved by: _____
George J. Thaler, Thesis Advisor

_____
Harold A. Titus, Second Reader

_____
John R. Powers, Chairman, Department of
Electrical and Computer Engineering

ii

ABSTRACT

The concept of helicopter controllability is explained. A background study reviews helicopter development in the U.S. General helicopter configurations, linearized equations of motion, stability, and piloting requirements are discussed. Helicopter flight controls, handling qualities, and associated specifications are reviewed. Analytical, simulation, and flight test methods for evaluating helicopter automatic flight control systems are discussed. A generic simulation is also conducted. This thesis is intended to be used as a resource document for a helicopter stability and control course at the Naval Postgraduate School.

TABLE OF CONTENTS

vii

ACKNOWLEDGEMENT

Powers, Prof. H. Titus, Prof. G. Thaler, Prof. L. Schmidt,
L. Corliss, E. Gulley, R. Miller, and Dr. L. Mertaugh for
their comments on the thesis.

I. INTRODUCTION

A. HELICOPTER CONTROLLABILITY DEFINED

Helicopter <u>controllability</u> refers to the ability of the pilot to fly a series of defined flight maneuvers required for a specific mission. The minimum time it takes to complete the flight maneuver profiles is a measure of the helicopter's <u>agility</u>. Helicopter <u>maneuverability</u> determines how closely the aircraft can follow rapidly varying flight profiles. The number and magnitude of tracking errors made in following the specified flight profiles is indicative of the <u>precision</u> with which the helicopter can be flown. The pilot effort expended in achieving the desired control is a measure of <u>pilot workload</u>. Ideally, the desired controllability can be achieved with minimum pilot workload. Both aircraft controllability and pilot workload will depend on the specific helicopter configuration, specific mission or task, and environmental conditions. Control of the helicopter will be a function of basic aircraft flying qualities and performance, level of augmentation, level of displays, task, environment, and pilot skill. For a given helicopter configuration the mission may require precise control of parameters like airspeed, altitude, and heading. Control may be required under visual meteorological conditions (VMC)

1

or under instrument meteorological conditions (IMC) under calm or turbulent atmospheric conditions, as illustrated in Table 1-1.

TABLE 1-1
RANGE OF GENERAL CONTROL PARAMETERS

	FLIGHT TIME
PILOT	HIGH <------> LOW
CURRENT	
STATE	SKILL LEVEL
	HIGH <------> LOW
	AUGMENTATION
	HIGH <------> LOW
BASIC	
HELICOPTER	DISPLAYS
	HIGH <------> LOW
	CALM <------> TURBULENT
ENVIRONMENT	DAY <------> NIGHT
	VMC <------> IMC
TASK	EASY <------> DIFFICULT
WORKLOAD LEVEL	LOW <------> HIGH
PERFORMANCE LEVEL	GOOD <------> BAD
TASK ACCOMPLISHED	YES OR NO

II. BACKGROUND

A. HELICOPTER DEVELOPMENT IN THE UNITED STATES

Man has always dreamed of soaring like the eagle and hovering like the hummingbird. It was not until the beginning of the twentieth century that science and technology in the United States progressed to the point where these dreams could become reality. The first Wright brothers flight at Kitty Hawk, North Carolina, on December 17, 1903, ushered in the era of fixed-wing flight. Development of these "conventional" aircraft progressed rapidly, leading to the barnstorming era of the 1920's and 1930's. Helicopter development proceeded much more slowly and it was not until the 1940's that rotary wing aircraft became practical. Reference 1 notes that initial helicopter pioneers had to advance technology in three primary areas:

      (1) Engines

      (2) Structures

      (3) Controllability

Helicopter development required light and reliable engines, light and strong aircraft structures, and a better understanding of helicopter controllability. Reference 2 presents a comprehensive history and References 1 and 3 present summarized histories of helicopter development.

Reference 4 discusses the history of U.S. Navy and Marine Corps helicopters, plus the history of major U.S. helicopter companies. A summary of helicopter development in the United States, based on References 1 through 4, is presented as background information to the study on helicopter controllability.

The helicopter concept is usually listed as having started with toy Chinese tops around 400 B.C. and with the Leonardo da Vinci screw-type propeller vertical lift machine sketches in the 15th century. In the U.S., the helicopter concept may have started with Thomas Edison's experiments with models in 1880. Reference 3 notes that Edison abandoned the experiments following a serious explosion while trying to develop a high power, light weight engine.

Helicopter flight hardware got its start in the U.S. with Emile and Henry Berliner in 1909. They built a two engine co-axial helicopter that lifted off the ground.

Reference 2 notes that the Leinweber-Curtiss helicopter was reported to have lifted off the ground in 1921. This aircraft had four rotors, two rotors above and two below the fuselage. The rotors each had three blades and the top and bottom rotors on each side were connected by a swiveling shaft.

The first US military contract for a helicopter was awarded to Professor Georges de Bothezat by the Engineering Division of Air Service, Technical Department for American

Reference 4 discusses the history of U.S. Navy and Marine Corps helicopters, plus the history of major U.S. helicopter companies. A summary of helicopter development in the United States, based on References 1 through 4, is presented as background information to the study on helicopter controllability.

The helicopter concept is usually listed as having started with toy Chinese tops around 400 B.C. and with the Leonardo da Vinci screw-type propeller vertical lift machine sketches in the 15th century. In the U.S., the helicopter concept may have started with Thomas Edison's experiments with models in 1880. Reference 3 notes that Edison abandoned the experiments following a serious explosion while trying to develop a high power, light weight engine.

Helicopter flight hardware got its start in the U.S. with Emile and Henry Berliner in 1909. They built a two engine co-axial helicopter that lifted off the ground.

Reference 2 notes that the Leinweber-Curtiss helicopter was reported to have lifted off the ground in 1921. This aircraft had four rotors, two rotors above and two below the fuselage. The rotors each had three blades and the top and bottom rotors on each side were connected by a swiveling shaft.

The first US military contract for a helicopter was awarded to Professor Georges de Bothezat by the Engineering Division of Air Service, Technical Department for American

Aeronautics, (US Army Air Corps) in June, 1921. The heli-copter fuselage was shaped like a cross, with a 6 bladed, 22 foot diameter rotor at each end of the cross. Controllability was achieved by varying the helicopter rotor blade pitch. Decreasing the front rotor pitch while increasing the aft rotor pitch would increase airspeed. Reference 3 notes that lateral flight was achieved by changing the right and left rotor blade pitch differentially. Increasing the pitch of all blades simultaneously would increase the total rotor thrust. Blade pitch could also be reduced to negative values for descent. An initial demonstration flight was made 18 Dec. 1922. The pilot performed a hover (at approximately 5 feet), an uncommanded displacement of about 300 feet, and a landing for a total flying time of one minute and 42 seconds. Reference 2 points out that this was the first time a helicopter had flown in front of witnesses for over a minute. Although other hovers were made in 1923, the project was canceled on 4 May, 1923. Reference 1 notes that the project was canceled, after $200,000.00 had been spent, because it was too complex mechanically. Reference 2 indicates that the cancellation resulted from poor performance and from potential safety problems which would result from a mechanical failure due to the helicopter configuration. A photograph of the de Bothezat helicopter is presented in Figure 2-1.

In 1922, the Berliner's built an aircraft with two vertical axis side-by-side counter-rotating rotors, plus a small vertical-axis rotor at the back of the aircraft. Control was achieved by tilting the two main rotors with respect to the fuselage. References 2 and 3 note that this machine achieved limited success in forward flight but disagree on whether or not it could hover.
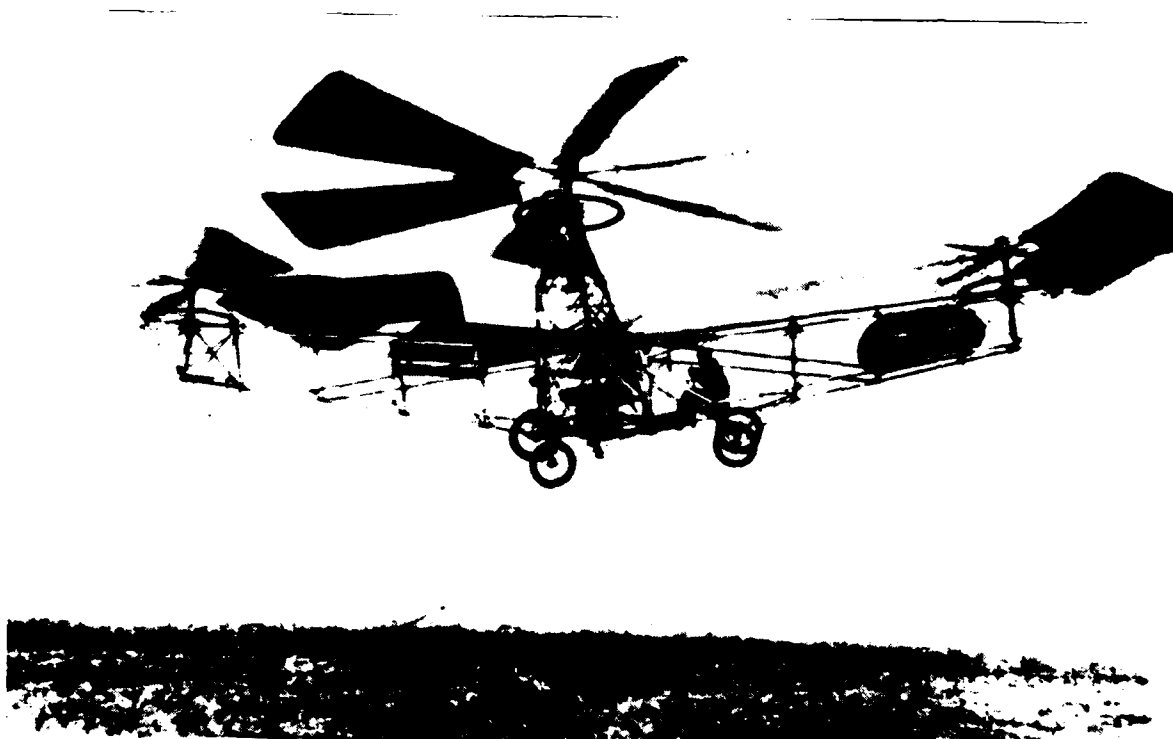

Figure 2-1 de Bothezat Helicopter
Courtesy American Helicopter Society (AHS)

Mr. M. B. Bleecker designed a four bladed main rotor helicopter in 1926 that had a propeller attached to each rotor blade. Power from the engine was fed to the propel-

lers and eliminated the torque balance problem of conventional single rotor helicopters. Control was achieved by using small airfoils attached to and below each rotor blade and by using a tail surface. Bleecker sold the design to the Curtiss-Wright Company and the aircraft was built in the early thirties. Reference 2 notes that although the aircraft made several turn-ups and hovers, it was abandoned because of vibration and stability problems.

The second US military contract for a helicopter was awarded by the Army Air Corps to Platt-LePage Aircraft Company of Eddystone, PA. in July, 1940. This helicopter was modeled after the earlier German Focke 61 (F61) and had two identical side-by-side rotors turning in opposite directions and a conventional airplane type tail. The aircraft, designated XR 1, weighted approximately 4800 lb and made its first flight (lifted off the ground, but was secured by ropes) on 12 May 1941. The aircraft achieved heights of approximately three feet and a flight duration of up to 30 sec during its first week but was damaged in a crash on 4 July, 1943. The second prototype, designated XR 1A, was completed in the fall of 1943. By Dec. 1943, it had flown across the Delaware River and returned, at an altitude of 300 feet. Reference 2 noted, that in April 1945, the Army withdrew its financial support and the company soon disappeared.

Igor Sikorsky of United Aircraft started the initial paper studies leading to the VS 300 helicopter in 1929; however, it was not built until the summer of 1939. The initial configuration had a single, three-bladed main rotor and a single anti-torque tail rotor. The initial VS 300 flight on 14 Sep., 1939, lasted only approximately 10 sec, although flights up to two minutes were achieved by the end of 1939. During the 1939-1941 period, Sikorsky decided to eliminate feathering (blade pitch) control from the main rotor and use two vertical axis propellers at the rear of the helicopter, one on each side, as shown in Figure 2-2. The change was made to improve control of the VS 300 and by May 6, 1941, a world helicopter endurance record of one hour, 32 min and 26 sec was established. Although the two small vertical axis propellers were satisfactory for hover and low speed flight, they presented problems in forward flight due to main rotor wake interference. Sikorsky decided to go back to main rotor feathering control at the end of 1941 and the final VS 300 configuration had a single main rotor and a single anti-torque tail rotor. Cyclic pitch control was used to tilt the main rotor and tail rotor pitch variation was used for directional control, establishing the standard to be used in future helicopters.
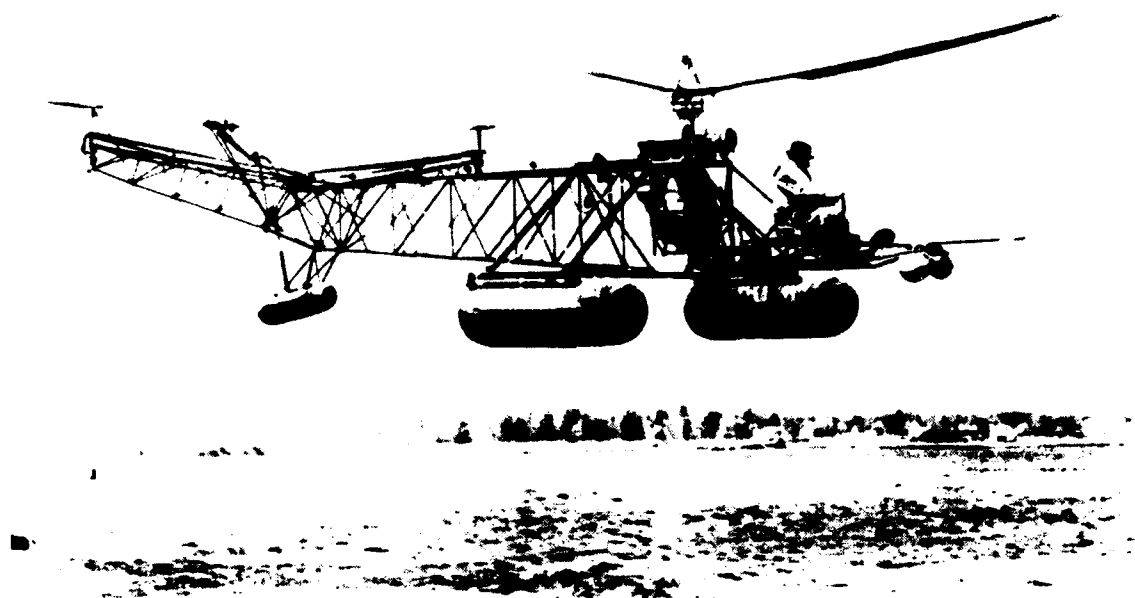
Figure 2-2   Sikorsky Flying Early VS 300 Helicopter
Courtesy AHS

The United Aircraft Company XR 4, a VS 300 derivative, made its first flight in Jan. 1942, and Reference 2 noted that a total of 126 XR 4 helicopters were built.   The Sikorsky R 4 aircraft is often considered the first successful helicopter.   Reference 1 contributes the success to three factors:

   (1)   Was mechanically simple

   (2)   Was controllable

   (3)   Entered production

A photograph of the Sikorsky R 4 helicopter is presented in Figure 2-3.

Figure 2-3   Sikorsky R 4 Helicopter
Courtesy Sikorsky Aircraft

A contract for the XR 6 helicopter was signed in Sep. 1942, with an initial flight on 15 Oct., 1943.   The XR 6 weighted 2600 lb, had R 4 blades, and a 245 HP 6 cylinder Franklin engine.   Reference 2 noted that United Aircraft Company built 416 aircraft for the Army by the end of World War II.   Sikorsky got a letter of intent from the Army in

June, 1943, for a helicopter bigger than the R 4. Having anticipated the requirement, Sikorsky had the XR 5 helicopter (Figure 2-4) completed by July, 1943. The XR 5 had a

Figure 2-4   Sikorsky R 5 Helicopter
Courtesy Sikorsky Aircraft

three bladed main rotor with wooden blade spars and ribs. It was powered by a 450 HP Pratt & Whitney Wasp Junior engine. The aircraft first flight occurred in August, 1943, but it crashed in October following a tail rotor failure. Sikorsky had the second XR 5 prototype flying in December, 1943, and according to Reference 2, had produced 123 XR 5 aircraft by the end of WW II. A photograph of the R 6 helicopter is presented in Figure 2-5.

Figure 2-5   Sikorsky R 6 Helicopter
Courtesy Sikorsky Aircraft

Arthur Young experimented with model helicopters for
about 10 years before coming up with the idea for the stabi-
lizer bar in 1940.   The stabilizer bar provided damping and
made the models much easier to fly.   He joined Bell Aircraft
in 1941, and by December, 1942, made the first teetered
flight (only three feet off the ground) with the initial
Bell Model 30 helicopter.   The initial Model 30 was a single
pilot helicopter with a two bladed main rotor, stabilizer
bar, four long legs for landing gear, and a non-enclosed

fuselage. A second Model 30, with two seats, was produced in August, 1943. The helicopter group at Bell Aircraft produced a third Model 30, incorporating lessons learned from the first two models. Reference 2 notes that the helicopter group built this aircraft in secret from the main company since they thought the main company version had no chance of succeeding. The third Model 30 turned out to be the prototype of the Bell 47. The Bell Model 47 received the first U.S. certificate of airworthiness. A photograph of the Bell Model 30 is presented in Figure 2-6.

Figure 2-6   Arthur Young Flying Bell Model 30 Helicopter
           Courtesy Bell Helicopter Textron

Frank Piasecki and Stanley Hiller were also involved in the early U.S. helicopter development. Frank Piasecki worked for the Platt-LePage Aircraft Company before forming his own company, the P. V. Engineering Forum. His first aircraft was the PV 2, a single main rotor and a single rigid tail rotor configuration, which flew in April, 1943 (see Figure 2-7). Piasecki built the tandem rotor PV 3 or

Figure 2-7   Frank Piasecki Flying PV 2 Helicopter
            Courtesy Piasecki Aircraft Company

XHRP-X helicopter on a Navy contract. This aircraft first flew in March, 1945, and was the beginning of the future Piasecki-Vertol tandem helicopters. A photograph of an HRP-1 tandem Piasecki helicopter conducting a mass rescue demonstration is presented in Figure 2-8.
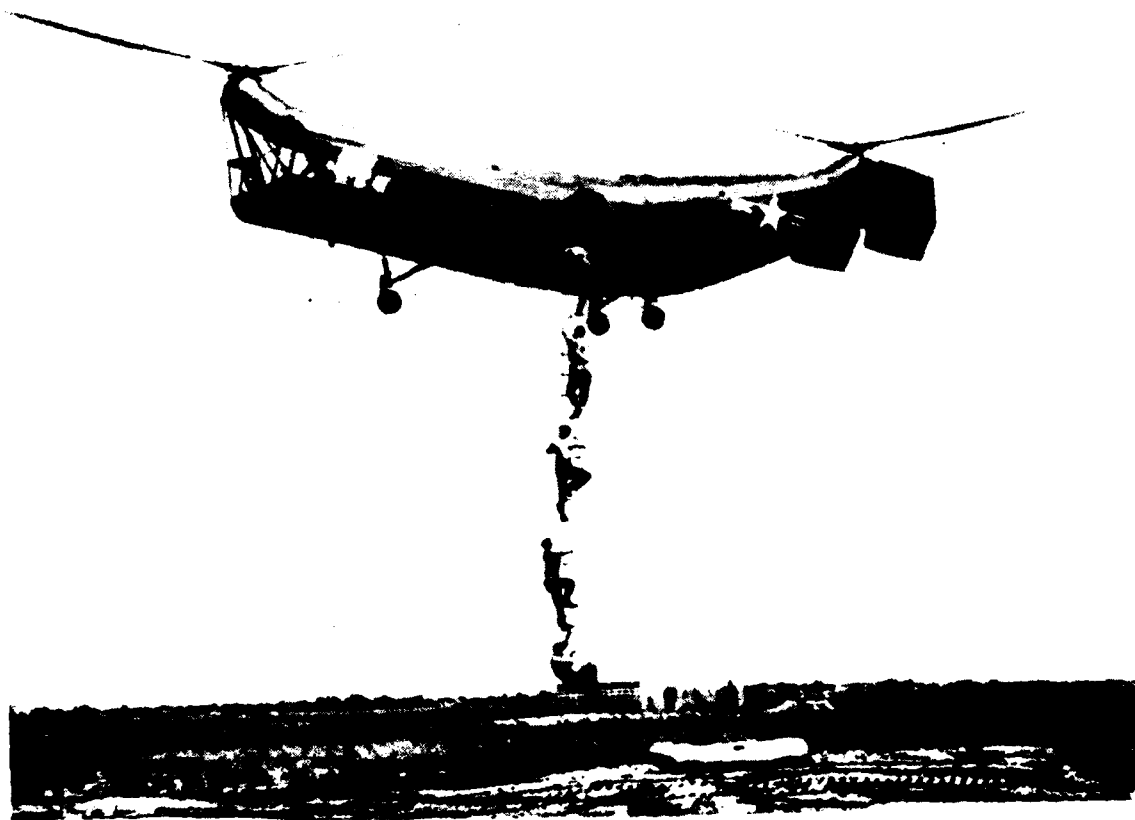

Figure 2-8 Piasecki HRP-1 Helicopter in Rescue Demonstration
Courtesy Piasecki Aircraft Company

Stanley Hiller's first helicopter, the XH-44, had a rigid coaxial rotor system with metal blades, a 90 HP

Franklin engine, and a single pilot cockpit. On its first free flight in 1944, the XH-44 rolled over after lifting off due to improper restraints. Hiller's third version of the XH-44 had a semi-rigid coaxial rotor system and was powered by a 125 HP Lycoming engine. Hiller joined Kaiser Company in 1944 and formed the Hiller Helicopter Division of Kaiser Cargo. His division produced two more coaxial helicopters, with two place cockpits, before he left Kaiser in 1945 and formed United Helicopters. A photograph of the XH-44 helicopter is presented in Figure 2-9.
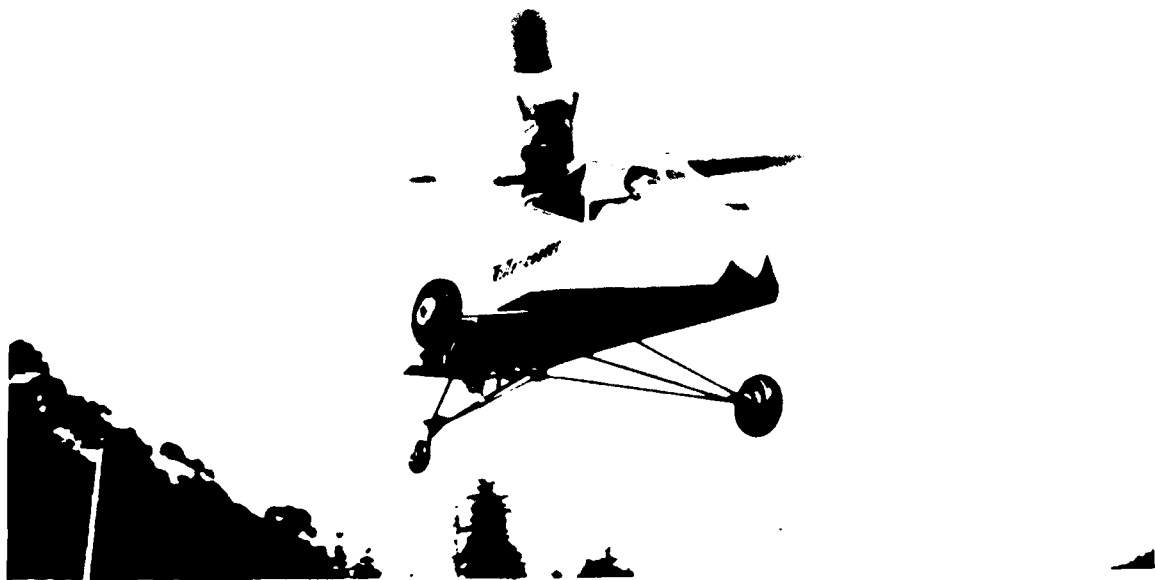

Figure 2-9   Hiller XH-44 Helicopter
Courtesy AHS

Reference 2 summarized the helicopter situation in the United States at the end of World War II (August, 1945) as follows:

"1.   Sikorsky had already produced hundreds of aircraft (580) of the following types: R4, R5, & R6;

2.   Bell was just completing its third prototype, the Model 30, which was the first prototype of the Bell 47;

3.   Piasecki was flying, since March 1945, the PV 3 tandem twin rotor, origin of the flying bananas;

4.   Hiller, a 20 year old engineer, had developed the first co-axial helicopter in the United States, the XH-44;

5.   Several other companies were developing some prototypes: Platt-LePage, Kellet, Bendix, Firestone, and Gyrodyne Company of America."

In addition, Charles Kaman started the Kaman Company in 1945 and had its first prototype helicopter with intermeshing rotors, the K-125 (see Figure 2-10), flying by January, 1947. The K-125 was followed by the K-190, K-225, and, eventually, the Air Force HH-43 Husky, all with intermeshing rotor systems. According to Reference 2, Kaman was the only helicopter company to put the intermeshing rotor into production. The Kaman K-225 was the first helicopter to fly with a gas turbine engine. The flight was made with a Boeing 502-2 gas turbine engine in December, 1951. Kaman also developed main rotor servo flaps to control the rotor blade angle of attack.

17
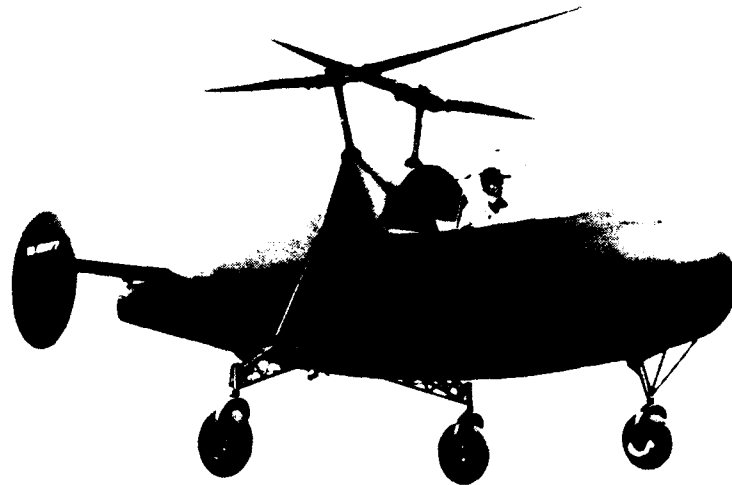
Figure 2-10   Kaman K-125 Helicopter
Courtesy AHS

The U.S. Navy experimented with autogyros in the early 1930's, but by 1938 Reference 4 points out that an official Navy Department memorandum had concluded: "Rotorplanes might be of some use in antisubmarine work when operated from auxiliaries. This appears to be a minor application, which hardly justifies expenditures of experimental funds at present." Helicopter/ship operations had their beginning in 1943 when a U.S. Army pilot landed the Sikorsky XR-4 helicopter on merchant tanker, S.S. BUNKER HILL (Figure 2-11).

Figure 2-11 Sikorsky XR-4 Operating Aboard S.S. BUNKER HILL
Courtesy Tommy Thomason, Bell Helicopter Textron

The shipboard applications of early helicopters were limited by inadequate engine power to carry required payloads or to follow a moving deck. The lack of endurance and controllability for extended hovers also limited its application to the antisubmarine warfare mission. As pointed out in Reference 4, the U.S. Navy considered the helicopter to have only minor applications in 1943, but ten years later no one could do without it.

The ten years following World War II witnessed the start and stop of a large number of companies attempting to manufacture and sell a variety of helicopter configurations. Reference 2 listed the American companies which appeared and disappeared or stopped producing helicopters between 1945 and 1956 as follows:

"Doman, created in 1945.

Pennsylvania-Brantly, created in 1945.

Hoppi-Copter Inc., created in 1945.

De Lacker, created in 1945.

Seibel-Cessna, created in 1946.

Gyrodyne Co. of America, created in 1946.

Rotorcraft Co., created in 1947.

American Helicopter Co., created in 1947.

Helicopter Engineering Research, created in 1948.

Jensen, created in 1948.

McCulloch, created in 1949.

Bensen, created in 1953.

Goodyear Aircraft Co., created in 1953.

Convertawings, created in 1954."

Helicopter development was spurred on by the Vietnam War during the late 1960's and early 1970's. Controllability was required for both gunship missions and confined area rescue missions. By this time, gas turbine engines were in wide use for helicopter applications. Use of composite

materials and fly-by-wire/light control system development
would not be emphasized until the late 1980's. With heli-
copter technology at its current state, the primary factor
in new helicopter development is program cost. The program
cost results in contractors teaming up to build new aircraft
like the V-22 (Bell/Boeing) and LHX (Bell/McDonnell or
Boeing/Sikorsky). The emphasis on new helicopter missions
like air-to-air combat and new flying qualities specifica-
tion efforts point to the importance of aircraft controlla-
bility in the future.

III. HELICOPTER DESIGN

A. HELICOPTER CONFIGURATIONS

1. General

The basic helicopter configuration determines how control is achieved about a given aircraft axis. Longitudinal, lateral, height, and directional control plus torque balancing is a function of the configuration, as shown in Table 3-1.

2. Rotor Systems

For a given configuration, controllability is primarily affected by the helicopter rotor type and level of augmentation. There are three primary types of helicopter rotor systems, as listed below and shown in Figures 3-1, 3-2, and 3-3.

(1) Teetering

(2) Articulated

(3) Hingeless

A teetering or two bladed "see-saw" type rotor system is shown in Figure 3-1. The rotor system is rigidly attached to the hub, but the hub is free to flap or tilt, as a unit, with respect to the rotor shaft. Teetering rotor systems often have an "underslung" configuration, with the blade root below the hinge point, to minimize the in-plane

TABLE 3-1   ROTORCRAFT FLIGHT CONTROL FUNCTIONS
Adapted from Reference 1

Helo Config	Torque Balance	Long Control	Lat Control	Height Control	Directional Control	Examples
single main rotor and tail rotor	tail rotor thrust	main rotor cyclic	main rotor cyclic	main rotor collective	tail rotor collective	Sikorsky R4-B SH-3H
tandem	main rotor differential	main rotor differential	main rotor cyclic	main rotor collective	main rotor differential	Boeing-Vertol UH-46E CH-47C
coaxial	main rotor differential torque	main rotor cyclic	main rotor cyclic	main rotor collective	main rotor differential collective	Hiller XH 44 Sikorsky ABC (XH-59)
side-by-side	main rotor differential torque	main rotor cyclic	differential collective	main rotor collective	main rotor differential cyclic	Platt-LePage XR-1 McDonnell XHJD1
tilt rotor	prop differential torque	prop cyclic + nacelle angle	prop differential collective	prop collective + nacelle angle	prop differential cyclic	Bell Textron XV-15 Bell-Boeing V-22
intermeshing	rotor differential torque	main rotors cyclic (servo flaps)	main rotors cyclic (servo flaps)	rotors collective	differential rotors collective + vertical tail	Kellett XH 10 Kaman HH-43B
tip jet	not required	main rotor cyclic	main rotor cyclic	main rotor collective	vertical tail	Hiller Hornet
stopped rotor	aux engine bleed air	cyclic blowing	cyclic blowing	collective blowing	tail rotor or aux engine bleed air	Sikorsky X-Wing

23

Coriolis forces. The teetering rotor design is relatively simple, aerodynamically clean, easy to maintain, and inexpensive. With zero hub offset, there is no average hub moment, making the configuration less prone to vibration feedback. Also, if the blades are made very stiff in the chordwise direction, ground resonance problems can be avoided. The teetering rotor system was standard on early Bell Helicopter Textron UH-1 "Hueys" and AH-1 "Cobras".

With a teetering rotor system, controllability is lost at zero g flight and the control sense is reversed at negative g flight. Large control inputs at a low g flight condition can lead to large rotor flap angles which could result in mast bumping and loss of the helicopter. Problems with teetering rotor controllability during low g Army flight maneuvers is documented in Reference 5. In addition, higher harmonic airloads and oscillatory moments can be transmitted to the shaft, since a teetering system has no lag hinge and the blades are not completely free to flap.

The articulated rotor system allows individual blade movement about the flap hinge, the lead-lag or drag hinge, and about the pitch change or feathering hinge, as shown in Figure 3-2. The articulated rotor system blade flap hinge offset distance from the hub has an important affect on control moments and controllability. Articulated rotor systems are very flexible in terms of design parameters like the number of blades, blade hinge offset location, and blade

hinge orientation. The rotor system may have an offset flapping hinge, an offset lead-lag hinge, or a combination offset flapping and lead-lag hinge. Reference 6 refers to these hinge configurations as Delta One (δ_1), Delta Two (δ_2), and Delta Three (δ_3) hinges, respectively. For example, a Delta Three hinge produces pitch-flap coupling which decreases the blade pitch and angle of attack when the blade flaps upward. The blade hinges also result in low inherent vibration since blade moments are not transmitted to the rotor hub. Helicopters with articulated rotor systems, like the CH-53, have been used to demonstrate loops and rolls.

Articulated rotor systems are, in general, mechanically complex and bulky, which implies a high drag configuration. The blades also experience high Coriolis forces which requires incorporating a lag or drag hinge. Lag hinge malfunction or improper design, by itself or in conjunction with landing gear problems, can lead to ground resonance. Ground resonance is a dynamic instability involving coupling between blade lag motion, fuselage, and landing gear (see Reference 1).

TEETERING
AXIS

ROTOR FEATHERING
AXIS

ROTOR BLADE

DRAG BRACE

PITCH ARM

PITCH LINK

ROTOR SHAFT

PITCH LINK

CENTER
OF
ROTATION

HINGE

ROTOR BLADE

SHAFT

CENTER
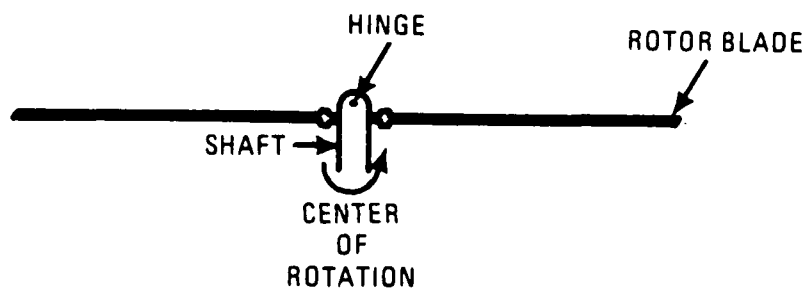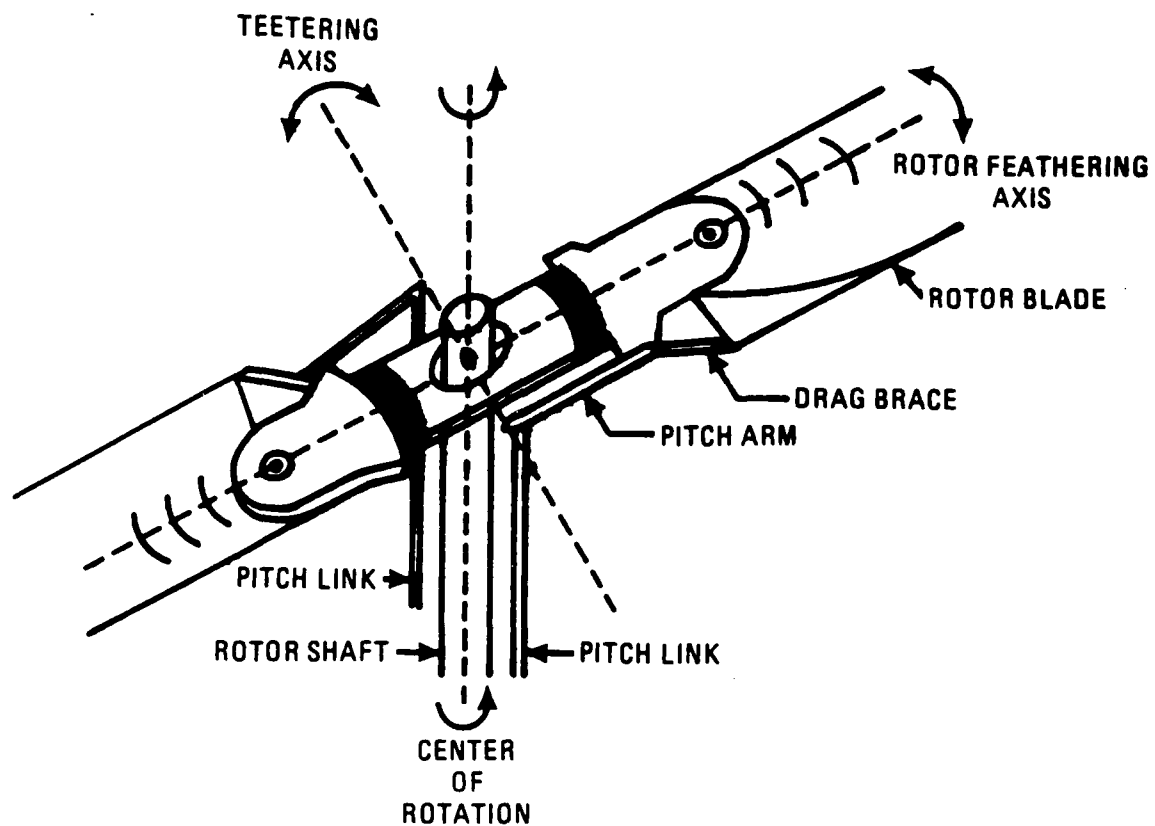OF
ROTATION

Figure   3-1   Sketch Showing Teetering Rotor Hub and
Underslung Teetering Rotor System

26
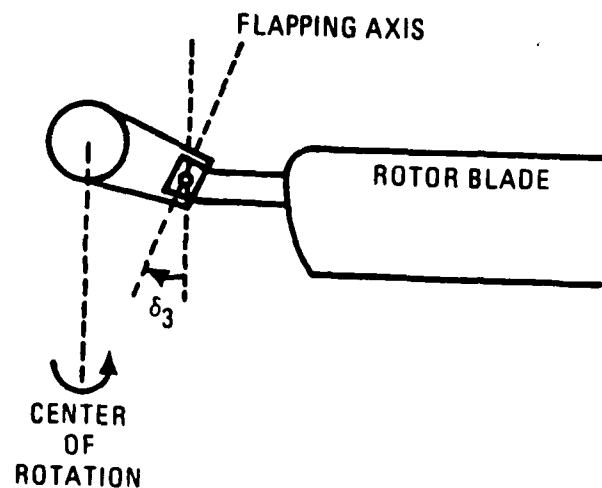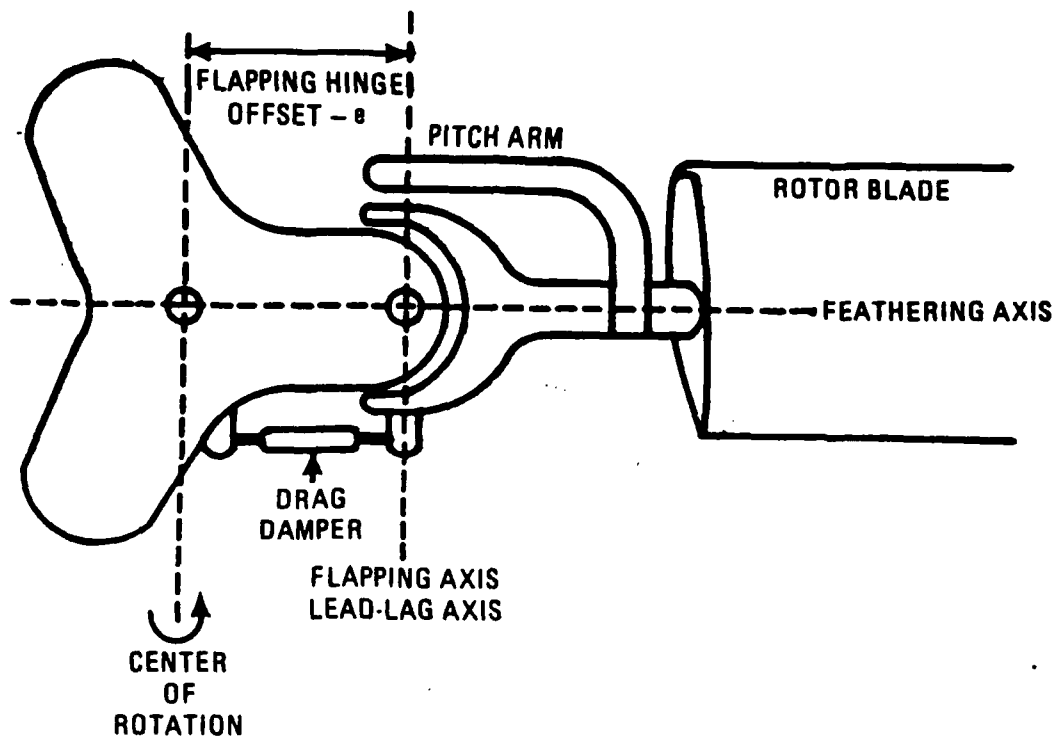
Figure 3-2   Sketch of Fully Articulated Rotor Hub Having
              Coinciding Hinge Locations, and Sketch of Delta
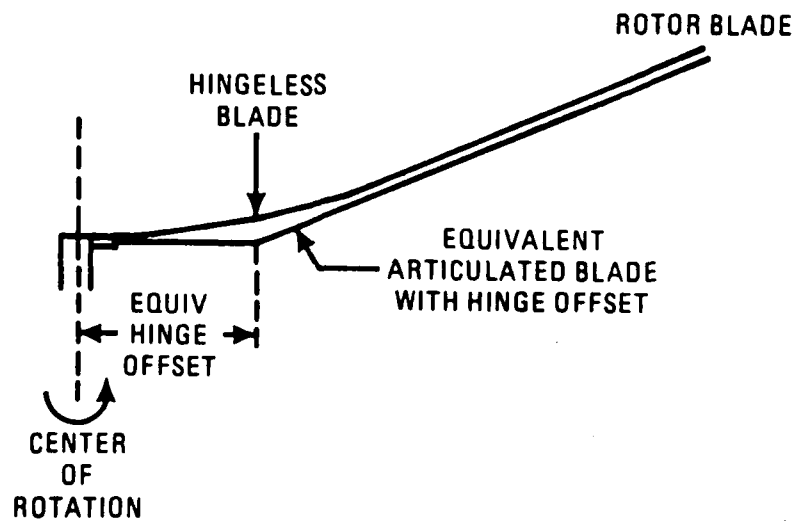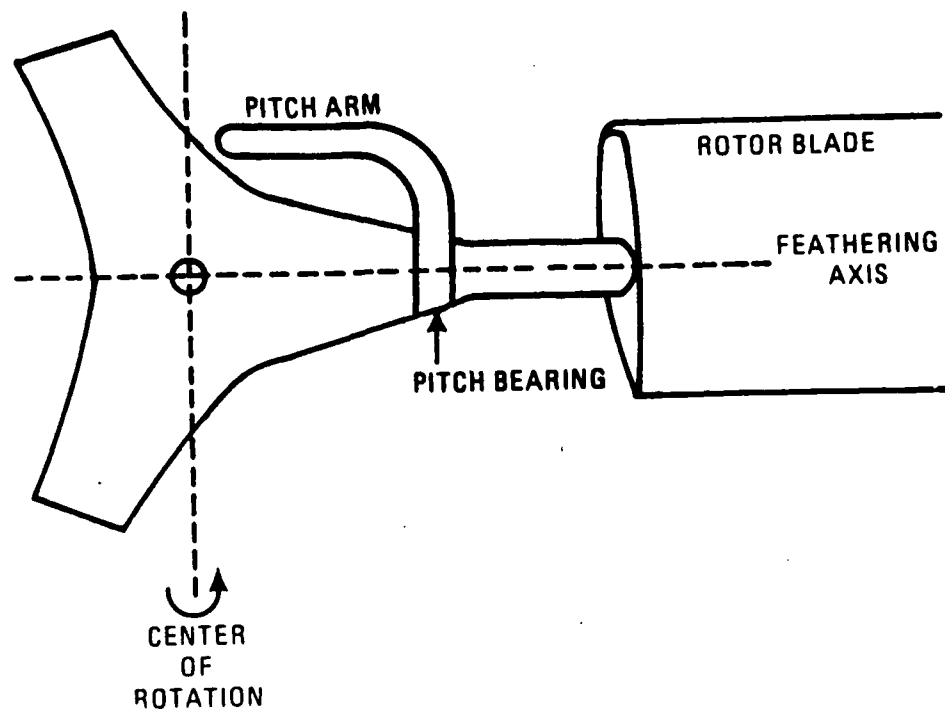   Three Hinge

27

Figure 3-3   Sketch Showing Hingeless Rotor Hub and Equivalent
              Articulated Blade Representation of a Hingeless Blade

28

The hingeless rotor system does not use flap or lag hinges, but attaches the rotor blades to the shaft like a cantilever beam, as shown in Figure 3-3. A flexible section, near the root of the blade, allows some flapping and lagging motion. The hingeless rotor system is relatively clean and simple in that it does not have the mechanical complexity of the articulated rotor system. Large hub moments resulting from tilting the TPP with a hingeless rotor produces high control power and damping compared to teetering and articulated rotor systems, as shown in Figure 3-4. A hingeless rotor system will produce a "crisper" response to pilot control inputs than other rotor types. A hingeless rotor system will also have controllability at low g flight conditions. Note that articulated rotor systems have physical flapping hinge offsets and a hingeless rotor can be thought of as having an effective hinge offset. A hingeless rotor is used on the BO-105 helicopter.

The hingeless rotor system airloads and moments are transmitted back to the hub. The hub loads and resulting vibration will, in general, be higher for a hingeless rotor system then for other type rotor systems. Reference 1 notes that the high damping of the hingeless rotor system implies high gust sensitivity which often requires an automatic flight control system. Reference 1 also points out that the angle of attack instability in forward flight is larger for a hingless rotor system than for an articulated

system, requiring a large horizontal tail or an automatic flight control system.
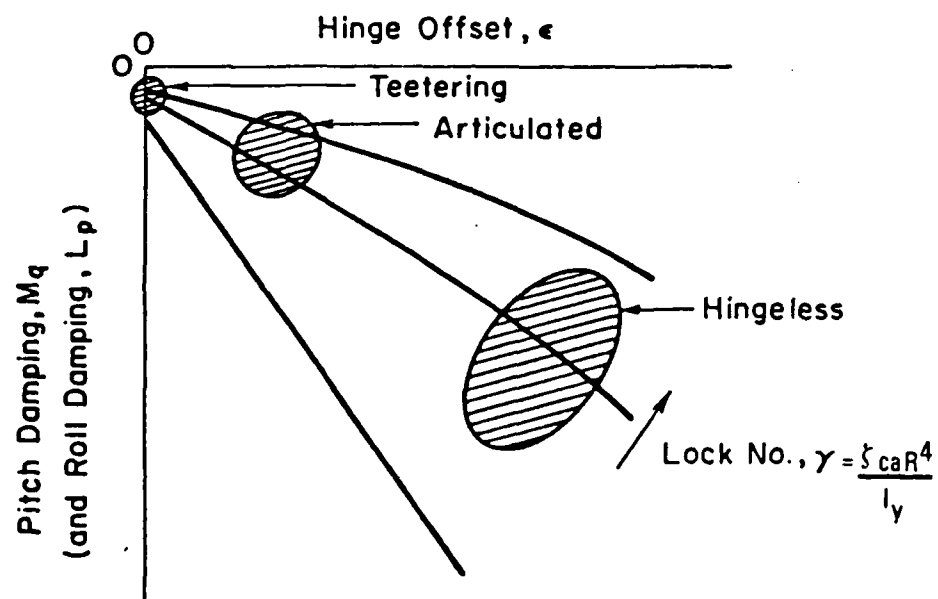
Figure 3-4   Helicopter Pitch and Roll Damping as a Function of Rotor Type, Hinge Offset, and Lock Number From Reference 7

B.   FORCE BALANCE

1.   General

Helicopter control requires a torque/force balance
for hover and a rotor thrust tilt to produce translation-
al flight.   Force and moment balance schematics for a
typical single main rotor, single tail rotor helicopter are
presented in Figures 3-5, 3-6, and 3-7.
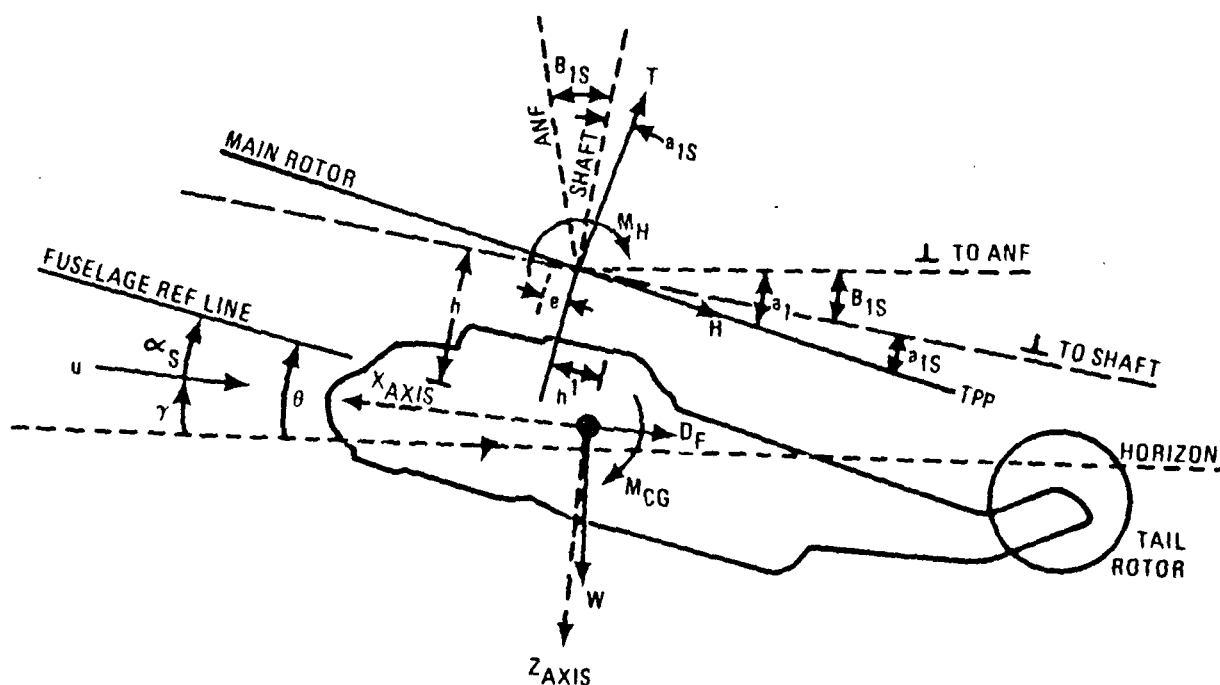
Figure 3-5   Longitudinal Force and Moment Diagram
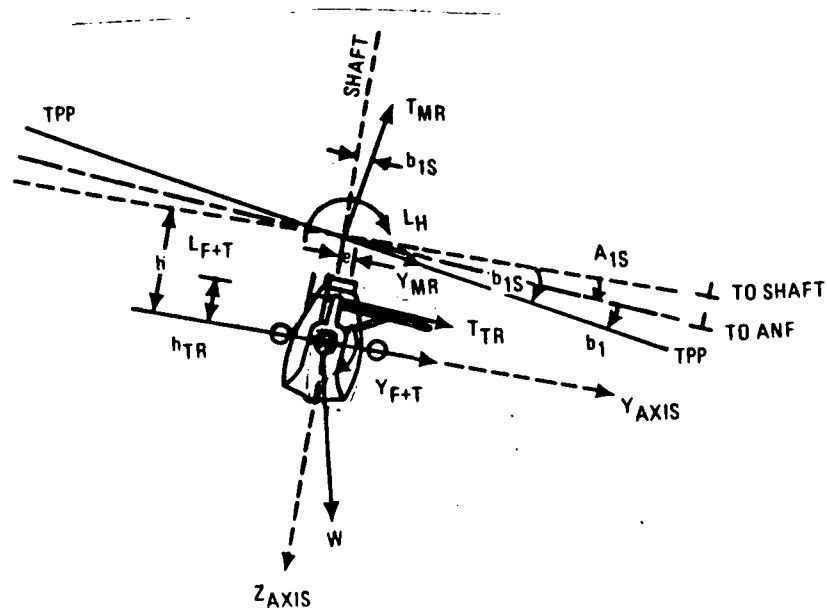
Figure 3-6 Lateral Force and Moment Diagram
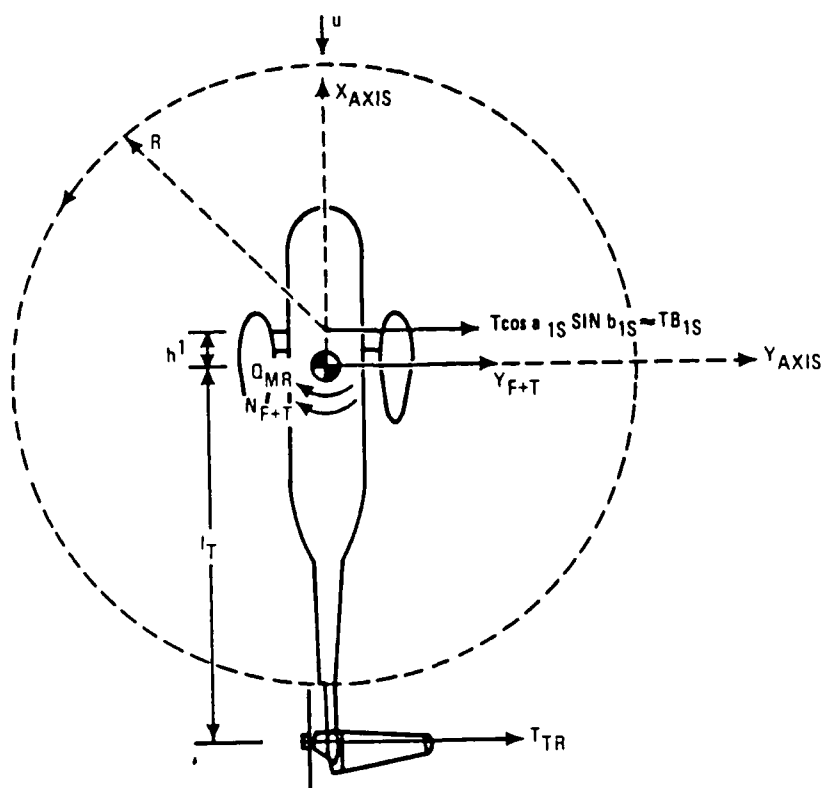
Figure 3-7 Directional Force and Moment Diagram

32

where the longitudinal parameters are defined as

ANF   - Axis of no rotor blade feathering or control axis

SHAFT - Rotor shaft or mast axis

TPP   - Tip path plane or axis of no flapping

a_1 - Angle between TPP and a perpendicular to ANF

a_{1S} - Angle between TPP and a perpendicular to shaft

B_{1S} - Angle between a $\perp$ to the shaft and a $\perp$ to ANF

D_F - Fuselage drag

e   - Flapping hinge offset from the shaft

H   - Rotor in-plane force

h   - Vertical distance from c.g. to hub

h^1 - Horizontal distance from c.g. to rotor shaft

M_{CG} - Moment about the c.g. due to fuselage and rotor

M_H - Moment due to rotor in-plane forces

T   - Rotor thrust, also T_{MR}

W   - Helicopter weight

V   - Free stream velocity

and the lateral-directional parameters are

A_{1S} - Angle between a $\perp$ to the shaft and a $\perp$ to the ANF

b_1 - Angle between TPP and a perpendicular to ANF

b_{1S} - Angle between TPP and a perpendicular to shaft

h_{TR} - Vertical distance from c.g. to tail rotor

l_T - Distance from the tail rotor to the c.g.

L_{F+T} - Rolling moment due to fuselage and tail

L_H - Rolling moment due to rotor in-plane forces

N_{F+T} - Yawing moment due to fuselage and tail

Q_{MR} - Main rotor torque

R - Main rotor radius

T_{TR} - Thrust of the tail rotor

V_T - Main rotor tip speed (hover)

Ω - Main rotor angular speed (hover)

Y_{F+T} - Sideforce due to fuselage and tail

Y_{MR} - Sideforce due to main rotor

From Figures 3-5, 3-6, 3-7, and following Reference 8, the basic force and moment perturbation equations can be expressed as:

$$\Delta X = -[\underset{(1)}{T \Delta a_{1s}} + \underset{(2)}{a_{1s} \Delta T} + \underset{(3)}{\Delta H_{MR}} + \underset{(4)}{\Delta D_F}] \tag{3-1}$$

$$\Delta Y = \underset{(1)}{T \Delta b_{1s}} + \underset{(2)}{b_{1s} \Delta T} + \underset{(3)}{\Delta Y_{MR}} + \underset{(4)}{\Delta Y_{F+T}} + \underset{(5)}{\Delta T_{TR}} \tag{3-2}$$

$$\Delta Z = \underset{(7)}{-\Delta T} \tag{3-3}$$

$$\Delta M = \underset{(1)}{[Th + M_H] \Delta a_{1s}} + \underset{(2)}{(h^1 + ha_{1s}) \Delta T} + \underset{(3)}{h \Delta H} + \underset{(4)}{\Delta M_{F+T}} \tag{3-4}$$

$$\Delta L = \underset{(1)}{[Th + L_H] \Delta b_{1s}} + \underset{(2)}{hb_{1s} \Delta T} + \underset{(3)}{h \Delta Y_{MR}} + \underset{(4)}{\Delta L_{F+T}} + \underset{(5)}{h_{TR} T_{TR}} \tag{3-5}$$

$$\Delta N = \underset{(1)}{h^1 T \Delta b_{1s}} + \underset{(2)}{h^1 b_{1s} \Delta T} + \underset{(3)}{h^1 \Delta Y_{MR}} + \underset{(4)}{\Delta N_{F+T}} - \underset{(5)}{\Delta T_{TR}} + \underset{(6)}{Q_{MR}} \tag{3-6}$$

where M_H $[L_H] = \dfrac{ebM_s\Omega^2}{2} \Delta a_{1s}$ $[\Delta b_{1s}]$ is the rotor offset hinge moment and the terms in equations 3-1 through 3-6 represent changes in moment due to

34

(1) Tilt of main rotor tip path plane

(2) Change in thrust and c.g. offset from the shaft

(3) Rotor in-plane force change

(4) Fuselage and tail pitching moment change

(5) Tail rotor thrust changes

(6) Change in main rotor torque

(7) Change in main rotor thrust

Equations 3-1 through 3-6 can be used to evaluate the helicopter stability derivatives.

2. Axis Systems

The axis system used to implement the equations of motion is usually a function of the type of problem being analyzed. An inertial or earth axis system is a right-handed orthogonal triad that has its origin at some point on the earth surface and is fixed with respect to space. In a space-fixed axis system, the moment of inertia about each axis will vary as the aircraft moves with respect to the origin of the axis system. This results in time-varying parameters in the equations of motion, which greatly complicate any analysis. Reference 9 notes that if the axis system is fixed in the aircraft, the measured rotary inertial properties are constant (assuming the aircraft mass is constant). Vehicle axis systems have coordinate systems fixed in the vehicle and may include the following, as illustrated in Figure 3-8.

- Body axis system

- Stability axis system

- Principal axis system

- Wind axis system

Additional axis systems used in helicopter analysis include:

- Shaft axis system

- Control axis system

- Tip-path-plane axis system

- Hinge axis system

- Blade axis system

The body axis system is a right handed orthogonal triad that has its origin at the aircraft center of gravity. This axis system is fixed to the aircraft making the inertia terms in the equations of motion constant and the aerodynamic terms depend only on the relative velocity vector. Since the body axis system is fixed to the aircraft, motion with respect to the body axis would be sensed by aircraft instrumentation and felt by the pilot.

The stability axis system is a right handed orthogonal triad that has its origin at the aircraft center of gravity and its x-axis aligned with the velocity vector. It is a special case of the body axis with the positive x-axis pointing into the relative wind. With a stability axis system, the moment and product of inertia terms vary with flight condition, and the axis system is limited to small disturbance motions. Estimation of the stability deriva-

tives is easier because of simplification of the aerodynamic terms. The stability axis system is used extensively in wind tunnel studies but loses its significance for helicopter hover studies, where the velocity vector is not defined.

The principal axis system is a right-handed orthogonal triad aligned the principal axis of the aircraft. Using the principal axis system implies that the product of inertia terms are identically zero, simplifying the equations of motion. When the stability axis is not aligned with the principal axis, cross product of inertia terms appear in the lateral equations of motion.

The wind axis system is a right-handed orthogonal triad that has its origin at the aircraft center of gravity and positive x-axis aligned with the aircraft flight path or relative wind. The wind axis system, like the inertial axis system, is not usually used in aircraft analysis since the moment and product of inertia terms in the rotational equations of motion vary with time, angle of attack, and angle of sideslip.

The shaft axis system, control axis system, and tip-path-plane (TPP) axis system are commonly referenced in helicopter texts (see References 3 and 9 through 11). These axes systems are right-handed orthogonal triads that have their origin at the rotor hub as shown in Figures 3-5 and 3-6. The helicopter rotor shaft and, thus, the shaft axis
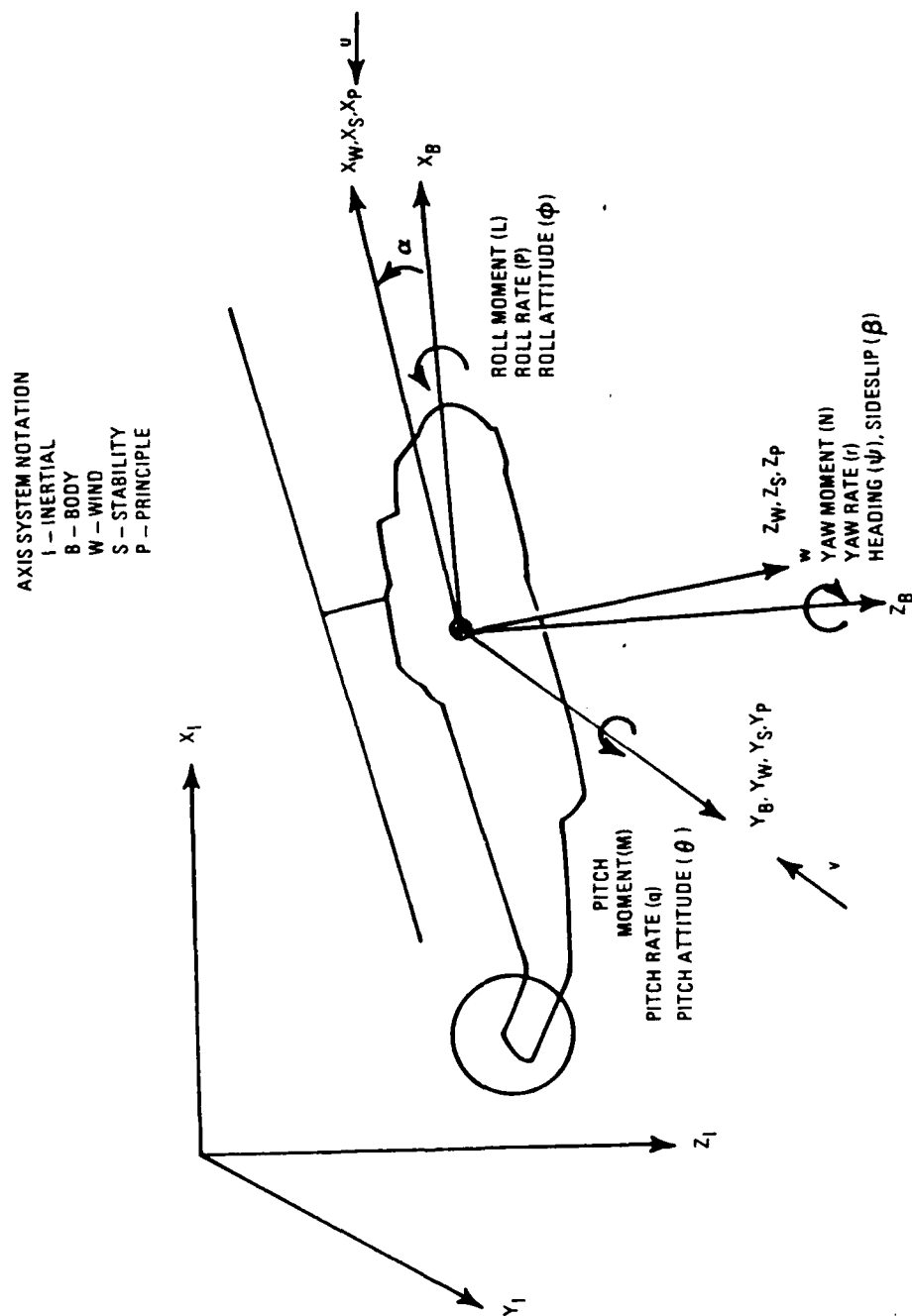
Figure 3-8   Inertial and Body Axis Systems, with Wind,
              Stability, and Principal Axis Coinciding

38

system may be tilted forward with respect to the fuselage to help produce a more level attitude in forward flight. Rotor force calculations are complicated because the blade incidence must be expressed in terms of both flapping and feathering. The control axis or axis of no feathering is normal to the swash plate, hence blade pitch is the constant collective value and no cyclic changes occur with respect to this axis. Reference 10 suggests that the control axis is normally used in American studies to express blade flapping. The TPP axis system is also referred to as the axis of no flapping since the blades change pitch periodically but do not flap with respect to this axis system. Reference 10 notes that the TPP axis system was used for most early British helicopter analysis.

The hinge and blade axis system have their origins at the rotor blade hinges. Hinge points for flapping, lead-lag, and feathering are often assumed to coincide for simplicity. The hinge and blade axes systems are used in studies analyzing the individual rotor blade dynamics.

Knowing the angle relations and origin location, transformations can be used to get from one axis system to another.

IV.   EQUATIONS OF MOTION

A.   ASSUMPTIONS

The complete nonlinear equations of motion describe
the helicopter flight trajectory resulting from pilot
control and environmental disturbances. These equations are
valid for analyzing both maneuvers and external disturbances
from a trim condition. Stability and control analysis is
usually concerned with small perturbations about a specified
trim condition. The goal is to simplify the equations of
motion to facilitate generic control system analysis, while
retaining essential elements to maintain the validity of the
analysis.

Reference 12 presents a detailed development of air-
plane/helicopter equations of motion. The development
includes a discussion of linear and angular motion plus
expansion of the inertial, gravity, and aerodynamic terms.
Reference 13 summarizes   the   equation   development and
presents basic discussions on linear and angular motion and
Coriolis forces and moments. Reference 9 implies that
helicopter and fixed-wing equations of motion are derived
the same basic way, but notes that with the helicopter,
rotor aerodynamics and hover capability should be consid-
ered. Reference 12   presents   twelve   assumptions   in

developing the aircraft equations of motion for control system analysis. These assumptions are summarized below:

Assumption 1: The airframe is a rigid body.

This implies that the airframe motion can be described by a translation of the center of mass and by a rotation about the center of mass. No attempt is made to include airframe bending or twisting or other aeroelastic effects. Actual helicopters do have major elements like rotor blades which move relative to each and to the fuselage.

Assumption 2: The earth is considered to be fixed in space.

This assumption implies that the inertial frame of reference is valid for the relatively short term analysis which is typical of control system design studies. This assumption may have limitations for long term navigation studies. Reference 12 notes that assumptions 2 and 1 provide an inertial reference frame in which Newton's laws are valid, and a rigid body to apply the laws. The development of the equations of motion start with Newton's second law on the motion of a particle:

The acceleration of a particle is proportional to the resultant force acting on it and the acceleration is in the direction of the force.

Assumption 3: The mass and mass distribution of the aircraft are assumed to be constant.

This assumption implies that no fuel is burned or stores expended, which is valid for control system analysis.

Assumption 4: The XZ plane is a plane of symmetry.

This assumption is very good for most fixed-wing aircraft and tandem rotor helicopters. The location and orientation of the tail rotor components on single main rotor, single tail rotor type helicopters are not symmetrical in the XZ plane. This assumption results in $I_{yz} = I_{xy} = 0$ and simplifies the moment calculations.

Assumption 5: Small disturbances are assumed to trimmed level flight conditions.

This assumption implies sine angle = angle and cosine angle = 1 and that higher order terms are negligible. It allows linearization of the equations of motion, thus simplifying the analysis. It also limits the equations to small perturbation analysis.

Assumption 6: The longitudinal forces and moments due to lateral perturbations are assumed negligible.

This assumption implies that if the aircraft is trimmed in steady, level flight, then initial roll and yaw angular velocities, initial lateral velocity and bank angle are zero. This assumption also decouples the longitudinal and lateral sets of equations.

Assumption 7: The flow is assumed to be quasi-steady.

This assumption implies that all derivatives with respect to the rate of change of velocities, except $\dot{w}$ and $\dot{v}$, are omitted.

Assumption 8:   Variations of atmospheric parameters are considered negligible.

This assumption is valid for helicopter control system studies, since the studies are concerned with operating about a trim point.

Assumption 9:   Effects associated with rotation of the vertical relative to inertial space are neglected and the trim body pitching velocity is zero.

The first part of this assumption does not apply to low speed, low altitude vehicles like helicopters. For control studies about an operating trim point the trim body axis pitching velocity should be zero. Reference 12 notes that assumption 9 corresponds to straight flight over an effectively flat earth.

    1.   <u>Complete Linearized Equations of Motion</u>

        The equations of motion can be further simplified by using a stability axis system with the X axis in steady-state pointing into the relative wind. With these assumptions, the complete linearized aircraft equations of motion, from Reference 12, are presented below.

Longitudinal/Vertical Equations
(4-1)

$$(S - X_u)u - (X_{\dot{w}}S + X_w)w + (-X_qS + g\cos\gamma_o)\theta =$$

$$X_\delta\delta - [X_u u_g + (X_{\dot{w}}S + X_w)w_g]$$

$$- Z_u u + (S - Z_{\ddot{w}}S - Z_w)w + [(-U_o - Z_q)S + g\sin\gamma_o]\theta =$$

$$Z_\delta\delta - [Z_u u_g + (Z_{\dot{w}}S + Z_w)w_g - Z_q\frac{Sw}{U_o}g]$$

$$- M_u u - (M_{\dot{w}}S + M_w)w + S(S - M_q)\theta =$$

$$M_\delta\delta - [M_u u_g + (M_{\dot{w}}S + M_w)w_g - M_q\frac{Sw}{U_o}g]$$

Lateral/Directional Equations
(4-2)

$$[S(1+Y_{\dot{v}}) - Y_v]v - (Y_pS+g\cos\gamma_o)(p/S)+[(U_o - Y_r)S - g\sin\gamma_o](r/S) =$$

$$Y_\delta\delta - [(Y_{\dot{v}}S + Y_v)v_g + Y_pp_g - Y_r\frac{Sv}{U_o}g]$$

$$-(L'_{\dot{v}}S + L'_v)v + (S - L'_p)p - L'_r r =$$

$$L'_\delta\delta - [(L'_{\dot{v}}S + L_v)v_g + L'_pp_g]$$

$$-(N'_{\dot{v}}S + N'_v)v - N'_p p + (S - N'_r)r =$$

$$N'_\delta\delta - [(N'_{\dot{v}}S + N'_v)v_g + N'_pp_g - (N'_r)g\frac{Sv}{U_o}g]$$

44

where the terms will be defined following simplification of the equations.

2. Simplified Equations of Motion

These equations are still not convenient for transfer function computations and can be simplified.

Assumption 10: It is assumed that $X_{\dot{w}} = X_q = Z_{\dot{w}} = Z_q = 0$

Reference 12 bases this assumption on a general relative order of magnitude discussion and notes that these stability derivatives rarely appear in technical literature. The validity of neglecting these terms should be checked for each specific configuration and flight condition.

Assumption 11: The aircraft steady flight path angle, γ_c', is assumed to be zero.

This assumption precludes the requirement for   in the transfer functions, thus simplifying the analysis.

Assumption 12: It is assumed that $Y_{\dot{v}} = Y_p = Y_r = L_{\dot{v}}' = N_{\dot{v}}' = 0$

Reference 12 notes that this assumption is good for most configurations. However, the validity of neglecting these terms should be checked for each aircraft configuration and flight condition.

Based on these assumptions, and neglecting gust inputs $(u_g, w_g, p_g,$ and $v_g)$, the linearized longitudinal and lateral equations of motion for forward flight (from Reference 12) can be expressed as:

LONGITUDINAL

$$(S - X_u)u \quad - \quad X_w w \quad + \quad g\theta = X_\delta \delta$$

$$-Z_u u \quad + \quad (S - Z_w)w \quad - \quad U_O S\theta = Z_\delta \delta \quad (4\text{-}3)$$

$$M_u u \quad - \quad (M_{\dot{w}}S + M_w)w \quad + \quad S(S - M_q)\theta = M_\delta \delta$$

LATERAL

$$(S - Y_v)\beta \quad - \quad (g/U_O)(p/S) \quad + \quad r = Y_\delta^* \delta$$

$$- L_\beta' \beta \quad + \quad (S - L_p')p \quad - \quad L_r' r = L_\delta' \delta \quad (4\text{-}4)$$

$$- N_\beta' \beta \quad - \quad N_p' p \quad + \quad (S - N_r')r = N_\delta' \delta$$

3. <u>Definitions</u>

The terms in the above equations are defined as

S = LaPlace Operator = d/dt

u = Forward speed (ft/sec)

w = Vertical speed (ft/sec)

θ = Pitch angle (rad)

β = Sideslip angle (rad)

p = Roll rate (rad/sec)

r = Yaw rate (rad/sec)

δ = Control deflection (rad)

g = Gravitational constant (32.2 ft/sec^2)

U_O = Trim true airspeed (ft/sec)

Y_δ^* = Y_δ/U_O ; $L_v' v = L_\beta' \beta$; $N_v' v = N_\beta' \beta$

Reference 12 defines the primed terms as

$$L_i = \frac{L_i + I_X N_i \dfrac{I_{XZ}}{}}{1 - \dfrac{I^2_{XZ}}{I_X I_Z}} \quad ; \quad N_i = \frac{N_i + I_Z L_i \dfrac{I_{XZ}}{}}{1 - \dfrac{I^2_{XZ}}{I_X I_Z}}$$

and the prime terms eliminate product of inertia terms in the equations. The product of inertia terms appear when the stability axis is not aligned with the aircraft principal axis. If the stability axis system is assumed to be aligned with the aircraft principal axis, there is no need to distinguish between the primed and unprimed derivatives. A brief description of the stability derivatives is presented below. Additional information is available in References 7 through 12.

$$X_u = \text{Velocity damping} = \frac{1}{m} \frac{\partial X}{\partial u}$$

Velocity damping is also referred to as drag damping and the fuselage contribution is proportional to dynamic pressure. The derivative, consisting of fuselage and rotor contributions, is typically negative corresponding to a forward tilt of the rotor tip path plane as speed increases. Reference 9 notes that X_u has a weak but stabilizing effect on the helicopter long term stability.

$$Z_u = \text{Lift due to forward speed} = \frac{1}{m} \frac{\partial Z}{\partial u}$$

47

Reference 9 notes that the lift due to velocity derivative for fixed-wing aircraft is always negative (increased lift for increased airspeed). The primary contribution comes from the main rotor and the derivative is negative at low speed and positive at high speed.

X_w = Drag due to Vertical Velocity or Angle of Attack = $\dfrac{1}{m}\dfrac{\partial X}{\partial w}$

The drag due to changes in vertical velocity or angle of attack has little affect on the helicopter statics or dynamics according to Reference 9.

Z_w = Vertical Velocity Damping = $-\dfrac{1}{m}\dfrac{\partial T}{\partial w}$

The vertical velocity damping derivative is the reciprocal of the vertical response time constant in hover.

M_u = Speed Stability = $\dfrac{1}{I_y}\dfrac{\partial M}{\partial u}$

The speed stability or velocity stability is the change in pitching moment caused by a change in forward speed. Reference 9 notes that for most helicopter configurations, M_u is positive in hovering and at very low speed flight.

$M_{\dot{w}}$ = Angle of Attack Damping = $\dfrac{1}{I_y}\dfrac{\partial M}{\partial w}$

The angle of attack damping is negative and affects only the helicopter short period pitch damping.

48

M_w = Angle of Attack stability = $\dfrac{1}{I_y}\dfrac{\partial M}{\partial w}$

M_w is the pitching moment derivative with respect to vertical velocity or angle of attack and a negative value corresponds to positive stability.

M_q = Pitch Rate Damping = $\dfrac{1}{I_y}\dfrac{\partial M}{\partial q}$

M_q or M_θ is the pitching moment derivative with respect to pitch rate and considered very important to stability and control analysis. Reference 9 notes that most helicopters require angular damping augmentation for good handling qualities and that the augmentation may be either mechanical or autopilot-type devices.

Y_v = Sideforce due to sideslip = $\dfrac{1}{M}\dfrac{\partial Y}{\partial v}$

The sideforce due to sideslip or sideward velocity will act to resist or damp sideward motion.

Y_r = Side force due to yaw rate = $\dfrac{1}{m}\dfrac{\partial Y}{\partial r}$

The primary contribution to side force due to yaw rate will be from the tail rotor for conventional helicopters. The vertical tail fin will also affect the side force due to yaw rate.

Y_p = Side force due to roll rate = $\dfrac{1}{m}\dfrac{\partial Y}{\partial p}$

Both main and tail rotors will contribute to the side force due to roll rate.

$Y_{\delta A_{1s}}$ = Sideforce due to lateral control = $\dfrac{1}{M}\dfrac{\partial Y}{\partial A_{1s}}$

The side force due to lateral control results from tilting the rotor tip path plane to the side.

$Y_{\theta_{TR}}$ = Side force due to directional control = $\dfrac{1}{m}\dfrac{\partial T_{TR}}{\partial \theta_{TR}}$

The side force due to directional control will be a function of tail rotor thrust resulting from a rudder pedal control input.

L_v = Rolling moment due to sideslip = $\dfrac{1}{I_{XX}}\dfrac{\partial L}{\partial v}$

The rolling moment due to sideslip is also called dihedral effect and a negative value implies positive dihedral effect. Primary contributions to dihedral effect come from the main and tail rotors.

L_r = Roll due to yaw rate = $\dfrac{1}{I_{XX}}\dfrac{\partial L}{\partial r}$

Reference 8 notes that the fuselage does not contribute very much to this derivative, but that the tail rotor contribution is very important.

L_p = Roll damping = $\dfrac{1}{I_{XX}}\dfrac{\partial L}{\partial p}$

L_p is the rolling moment due to roll rate or roll damping with primary contributions from the main and tail rotors.

$$L_{\delta_{A_{1S}}} = \text{Lateral control derivative} = \frac{1}{I_{XX}} \frac{\partial L}{\partial A_{1s}}$$

The lateral control derivative is primarily a function of the rate of change of rotor tip path tilt with lateral cyclic input. Reference 8 notes that it is independent of airspeed.

$$N_v = \text{Directional stability derivative} = \frac{1}{I_{ZZ}} \frac{\partial N}{\partial v}$$

The directional stability derivative is primarily a function of the tail rotor with additional contributions from the fuselage and vertical tail.

$$N_r = \text{Yaw rate damping derivative} = \frac{1}{I_{ZZ}} \frac{\partial N}{\partial r}$$

The yaw rate damping derivative is primarily due to the tail rotor contribution.

$$N_p = \text{Yaw due to roll rate} = \frac{1}{I_{ZZ}} \frac{\partial N}{\partial p}$$

The yaw due to roll rate derivative depends primarily on the height of the tail rotor with some contribution from the vertical stabilizer.

$$N_\delta = N_{\theta_{TR}} = N_{PED} = \text{Directional control derivative} = \frac{1}{I_{ZZ}} \frac{\partial N}{\partial \theta_{TR}}$$

51

The directional control derivative is the tail rotor effectiveness or yawing moment resulting from rudder pedal inputs.

Reference 8 summarizes the relative importance of the helicopter major components to the lateral/directional stability derivatives. The summary focuses on the fuselage and tail, main rotor, and tail rotor, as shown in Table 4-1.

4. Stability Derivative Calculations

Values for stability derivatives can be calculated for each helicopter at specific flight conditions

TABLE 4-1   SUMMARY OF RELATIVE IMPORTANCE OF LATERAL/DIRECTIONAL STABILITY DERIVATIVES (FROM REFERENCE 8)

Derivative	Relative Importance To Derivative (A,B,C)		
Symbol (Sign)	Fuselage	Main Rotor	Tail Rotor
N_v (+)	B (VFS)	–	A
N_r (–)	B	–	A
N_p	B (VFS,VFH)	–	A (TRH)
$N_{A_{1s}}$	–	Small	–
$N_{\theta TR}$ (–)	–	–	A
L_v (–)	B	A	A (TRH)
L_r (+)	B (VFS,VFH)	C	A (TRH)
L_p (–)	B	A	A (TRH)
$L_{A_{1s}}$ (+)	–	A	–
$L_{\theta TR}$ (+)	–	–	A (TRH)
Y_v (–)	A	A	A
Y_r (–)	B (VFS)	–	A
Y_p (–)	B (VFS,VFH)	–	A (TRH)
$Y_{A_{1s}}$ (+)	–	A	–
$Y_{\theta TR}$ (+)	–	–	A

VFS = Vertical Fin Size; VFH = Vertical Fin Height
TRH = Tail Rotor Height

by evaluating the terms in equations 3-1 through 3-6. Equations for helicopter stability derivatives are also presented in References 8 through 11. Sample calculations and calculator programs for determining the derivatives are given in Reference 13. Stability derivative values for a single main rotor helicopter are presented in Reference 12. Reference 7 presents stability derivatives for OH-6A, BO-105, AH-1G, UH-1H and CH-53D helicopters. Stability derivatives for the CH-46 and UH-60 helicopters are presented in References 14 and 15, respectively.

   5.   Hover Case

Helicopter stability derivatives in forward flight will not be the same as for the hover case since many are a function of forward velocity. In addition, the derivatives $M_{\dot{w}}$, M_w, X_w, Z_u, and $Z_{B_{1c}}$ are usually neglected in hover due to symmetry as noted in References 9 and 12. For the hover case, the longitudinal equations of motion presented in Equations 4-3 reduce to:

$$(S - X_u)u + \qquad 0 \qquad + \qquad g\theta = X_\delta\delta$$
$$0 \qquad + (S \quad - \quad Z_w)w \quad + \qquad 0 \qquad = Z_\delta\delta \qquad (4-5)$$
$$-M_u u + \qquad 0 \qquad + \quad (S - M_q S)\theta = M_\delta\delta$$

For the lateral equations of motion, Reference 12 points out that N_p, L_r, N_v, Y_p, and Y_r are usually assumed to be zero. Reference 12 notes that the assumption applies well to

hovering vehicles without a tail rotor or with a tail rotor of high disk loading. For the hover case, the lateral equations of motion presented in equations 4-4 reduce to

$$
\begin{aligned}
(S - Y_v)v &- &g\phi &+ &0 &= Y_\delta \delta \\
-L_v v &+ &S(S - L_p)\phi &+ &0 &= L_\delta \delta &\quad (4-6) \\
0 &+ &0 &+ &(S - N_r)r &= N_\delta \delta
\end{aligned}
$$

6.   Summary Equations

In matrix form, the equations of motion can be expressed as follows:

Longitudinal/ Vertical

Forward Flight

$$
\begin{bmatrix}
S-X_u & -X_w & g \\
-Z_u & (S - Z_w) & -U_oS \\
-M_u & -(M_{\dot{w}}S + M_w) & S(S - M_q)
\end{bmatrix}
\begin{bmatrix}
u \\
w \\
\Theta
\end{bmatrix}
=
\begin{bmatrix}
X_\delta \\
Z_\delta \\
M_\delta
\end{bmatrix}
\begin{bmatrix}
\delta \\
\delta \\
\delta
\end{bmatrix}
\quad (4-7)
$$

Hover

$$
\begin{bmatrix}
S - X_u & 0 & g \\
0 & S - Z_w & 0 \\
-M_u & 0 & S^2 - M_qS
\end{bmatrix}
\begin{bmatrix}
u \\
w \\
\Theta
\end{bmatrix}
=
\begin{bmatrix}
X_\delta \\
Z_\delta \\
M_\delta
\end{bmatrix}
\begin{bmatrix}
\delta \\
\delta \\
\delta
\end{bmatrix}
\quad (4-8)
$$

Equation 4-8 shows that, for the hover case, the vertical motion is independent of longitudinal and pitching motion. The collective control (Z_δ) only affects the vertical Z force or, in this case, the vertical damping (Z_w).

Lateral - Directional

Forward Flight

$$
\begin{bmatrix} S - Y_v & - & g/U_o S & + & 1 \\ - L_\beta & + & S - L_p & - & L_r \\ - N_\beta & - & N_p & + & S - N_r \end{bmatrix}
\begin{bmatrix} \beta \\ p \\ r \end{bmatrix}
=
\begin{bmatrix} Y_\delta \\ L_\delta \\ N_\delta \end{bmatrix}
\begin{bmatrix} \delta \\ \delta \\ \delta \end{bmatrix}
\qquad (4-9)
$$

Hover

$$
\begin{bmatrix} S - Y_v & - & g & + & 0 \\ - L_\beta & + & S(S - L_p) & + & 0 \\ 0 & + & 0 & + & S - N_r \end{bmatrix}
\begin{bmatrix} \beta \\ \phi \\ r \end{bmatrix}
=
\begin{bmatrix} Y_\delta \\ L_\delta \\ N_\delta \end{bmatrix}
\begin{bmatrix} \delta \\ \delta \\ \delta \end{bmatrix}
\qquad (4-10)
$$

Equation 4-10 shows that, for the hover case, the yaw motion is independent of sideslip and bank angle. Thus, a pedal input (N_δ) produces a pure yaw response with no cross coupling.

V.   SYSTEM CHARACTERISTICS

A.   CHARACTERISTIC EQUATION (CE)

The CE gives information on both the stability and the characteristic motion of the system. It is obtained by setting the denominator of the system polynomial equal to zero or by solving the determinant of the system matrix with zero inputs. Solving equation 4-8 for zero inputs and expanding the determinant gives the longitudinal CE for hover.

$$
\begin{vmatrix}
S - X_u & g \\
- M_u & S^2 - M_q S
\end{vmatrix} = 0 \tag{5-1}
$$

$$
[(S - X_u)(S^2 - M_q S) + M_u g] = 0 \tag{5-2}
$$

$$
[S^3 - (X_u + M_q)S^2 + X_u M_q S + M_u g] = 0 \tag{5-3}
$$

In a hover, the vertical response is decoupled from the longitudinal response in equation 4-8, and can be expressed as:

$$
(S - Z_w)w = Z_\delta \delta \tag{5-4}
$$

where $\delta = \Theta_c$ is the collective control.

Solving equation 4-10 for zero inputs and expanding the determinant gives the lateral CE for hover.

$$\begin{vmatrix} S - Y_v & -g \\ -L_\beta & S(S - L_p) \end{vmatrix} \quad = \quad 0 \qquad (5\text{-}5)$$

$$S(S - L_p)(S - Y_v) - L_\beta g \quad = \quad 0 \qquad (5\text{-}6)$$

$$S^3 - (Y_v + L_p)S^2 + Y_r L_p S - L_\beta g = \quad 0 \qquad (5\text{-}7)$$

The yaw response in hover is decoupled from sideslip and bank angle in equation 4-10 and can be expressed as:

$$(S - N_r)r = N_\delta \delta \qquad (5\text{-}8)$$

where $\delta = \delta_r$ is the rudder pedal input.

In forward flight the longitudinal and vertical motion is coupled (equation 4-7) and so is the lateral and directional motion (equation 4-9). The CE is obtained by solving the determinants of equations 4-7 and 4-9. This results in fourth order equations of the form

$$CE_{fwd.\ flt.} = AS^4 + BS^3 + CS^2 + Ds + E \qquad (5\text{-}9)$$

where in the longitudinal/vertical case, equation 4-7 can be expanded by cofactors to give:

$$CE_{Long} = (S-X_u) \begin{vmatrix} S-Z_w & -U_oS \\ -M_{\dot{w}}S-M_w & S(S-M_q) \end{vmatrix} - (-Z_w) \begin{vmatrix} -X_w & g \\ -M_{\dot{w}}S-M_w & S(S-M_q) \end{vmatrix}$$

$$+ (-Mu) \begin{vmatrix} -X_w & g \\ s-Z_w & -U_oS \end{vmatrix} \qquad (5\text{-}10)$$

$$= (S - X_u)[(S - Z_w)S(S - M_q) - (U_oS)(M_{\dot{w}}S + M_w)]$$

$$+ Z_u[- X_wS(S - M_q) + M_{\dot{w}}Sg + M_wg]$$

$$- M_u(X_wU_oS - gS + Z_wg) \tag{5-11}$$

$$= S^4 - M_qS^3 - Z_wS^3 + Z_wM_qS^2 - M_{\dot{w}}U_oS^3 - M_wU_oS^2 - X_uS^3 +$$

$$X_uM_qS^2 + X_uZ_wS^2 - X_uZ_wM_qS + X_uM_{\dot{w}}U_oS^2 + X_uM_wU_oS - X_wZ_uS^2 +$$

$$X_wZ_uM_ug + Z_uM_wgS + Z_uM_wg - X_wM_uU_oS + M_ugS - Z_wM_ug \tag{5-12}$$

Equating like power terms in equations 5-12 and 5-9 gives the coefficients to the forward flight longitudinal characteristic equation. These coefficients are given below and are also presented in Reference 12.

$$A = 1 \tag{5-13}$$

$$B = -(M_q + Z_w + M_{\dot{w}}U_o + X_u)$$

$$C = Z_wM_q - X_wZ_u - M_wU_o + X_u(M_q + Z_w + M_{\dot{w}}U_o)$$

$$D = Z_u(X_wM_q + M_{\dot{w}}g) + X_u(M_wU_o - Z_wM_q) + M_u(g - X_wU_o)$$

$$E = g(Z_uM_w - Z_wM_u)$$

The lateral characteristic equation for forward flight can be obtained using the same procedure. Reference 12 presents the coefficients for the lateral characteristic equation as:

$$A = 1 \tag{5-14}$$

$$B = - Y_v - L_p - N_r - N_p - L_r$$

$$C = N_\beta + L_p(Y_v + N_r) + N_p(Y_v - L_r) + Y_v(L_r + N_r) + L_\beta$$

$$D = - N_\beta L_p + Y_v(N_pL_r - L_pN_r + N_pL_\beta) - (g/U_o)(L_\beta + N_\beta)$$

$$E = (g/U_o)(L_\beta N_r - N_\beta L_r)$$

58

B. TRANSFER FUNCTIONS

A transfer function (TF) is the ratio of the system output to the system input with zero initial conditions.

Using Laplace notation:

$$\text{Input} \quad I(S) \longrightarrow \boxed{\begin{array}{c}\text{TRANSFER} \\ \text{FUNCTION TF(S)}\end{array}} \longrightarrow \text{OUTPUT} \quad O(S)$$
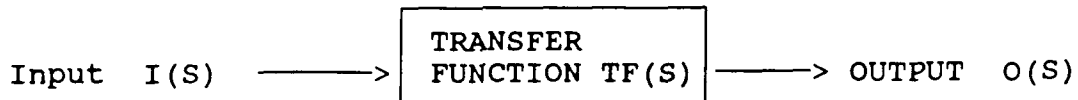
and

$$TF(S) = \frac{O(S)}{I(S)} \tag{5-15}$$

This relation applies to linear time-invariant systems with zero initial conditions. (For certain nonlinear control systems see Reference 16, Chapter 11.) The TF can also be expressed as the ratio of a zero or numerator polynomial to a characteristic denominator polynomial.

$$TF(S) = \frac{N(S)}{D(S)} = \frac{N(S)}{(S)} = \frac{b_m S^m + b_{m-1} S^{m-1} + \ldots + b_1 S + b_0}{S^n + a_{n-1} S^{n-1} + \ldots + a_1 S + a_0} \tag{5-16}$$

$$= \frac{b_m (S - Z_1)(S - Z_2) \ldots (S - Z_m)}{(S - P_1)(S - P_2) \ldots (S - P_n)} \tag{5-17}$$

where

$m \leq n$

Z = Zeroes (roots) of the numerator polynomial

P = Poles (roots) of the characteristic polynomial

The characteristic equations have already been presented for hover and forward flight, (see equations 4-7 through 4-10). The denominator, or characteristic polynomial, is common to all helicopter transfer functions and determines the stability (frequency and damping) of the response. The numerator, or zero polynomial, is obtained by replacing the specified motion column in the equation of motion with the specified control column (Cramer's rule). For example, to look at the forward speed (u) to control input (δ) TF, replace the u column in equation 4-3 with the δ column

$$\frac{u(S)}{\delta(S)} = \frac{\begin{vmatrix} X_\delta & -X_w & g \\ Z_\delta & S - Z_w & U_oS \\ M_\delta & -(M_wS + M_w) & S(S - M_q) \end{vmatrix}}{\triangle(S)} = \frac{N_\delta^u(S)}{\triangle(S)} \quad (5\text{-}18)$$

where $N_\delta^u(S)$ is the notation used in Reference 12 for a forward speed (u) to control input (δ) numerator.

1. Block Diagrams

Block diagrams are shorthand or pictorial representations of linear control processes which facilitate

60

analysis, especially in control system design. Block diagram algebra may be used to reduce complicated aircraft control system block diagrams to forms that are more easily analyzed. Most control theory texts (see References 16, 17, and 18) contain summaries of the theorems used for block diagram manipulation. Key points to remember include:

- Series or cascade blocks can be combined by multiplication
- Parallel blocks can be combined by addition
- Minor feedback loops may be eliminated by manipulation

A block diagram of a control system with feedback is presented in Figure 5-1 (Reference 18).
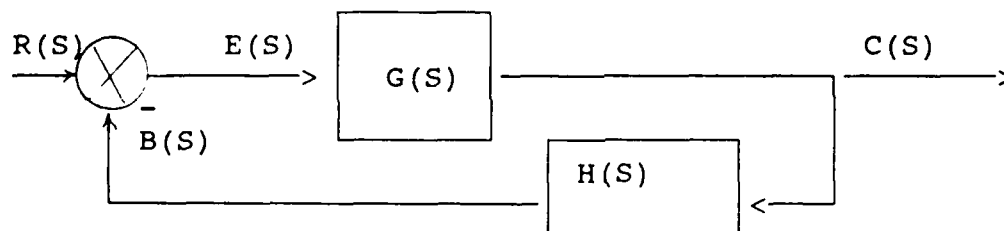

Figure 5-1 Block Diagram of Feedback Control System

where

$R(S)$ = System input (no feedback)

$C(S)$ = System output (no feedback)

$E(S)$ = Error signal

$G(S)$ = Forward transfer function

$H(S)$ = Feedback transfer function

$G(S)H(S)$ = Open loop transfer function

$\dfrac{C(S)}{R(S)}$ = Closed loop transfer function

$\dfrac{E(S)}{R(S)}$ = Error or actuating signal ratio

$\dfrac{B(S)}{R(S)}$ = System feedback ratio

The system output, C(S)H(S), is fed back and compared to the input R(S). The difference, E(S), is the error signal which drives the loop transfer function. From Figure 5-1:

$$E(S) = R(S) - C(S)H(S) \tag{5-19}$$

$$C(S) = E(S)G(S) \tag{5-20}$$

combining equations 5-19 and 5-20

$$C(S) = G(S)[R(S)-C(S)H(S)] = G(S)R(S) - G(S)C(S)H(S) \tag{5-21}$$

$$C(S)[1 + G(S)H(S)] = G(S)R(S) \tag{5-22}$$

$$\frac{C(S)}{R(S)} = \frac{G(S)}{1 + G(S)H(S)} \tag{5-23}$$

$$\frac{E(S)}{R(S)} = \frac{1}{1 + G(S)H(S)} \tag{5-24}$$

$$\frac{B(S)}{R(S)} = \frac{G(S)H(S)}{1 + G(S)H(S)} \tag{5-25}$$

Note that the denominator is the same for equations 5-23 through 5-25. The term "1 + G(S)H(S) = 0" is the characteristic equation for the system in Figure 5-1 and determines the stability of the system.

C.   STABILITY

The concept of stability is very important to helicopter controllability and to automatic flight control system design requirements. In general, the helicopter should be

stable, but not so stable as to appear overly sluggish to the pilot. As previously noted, the amount of stability and agility required for a specific helicopter will be a function of the mission being considered. Stability can be discussed in terms of what happens to a helicopter when it is disturbed from a trimmed flight condition with no pilot or automatic flight control systems corrective inputs. Static stability is concerned with the initial tendency of the helicopter motion following the disturbance. If the helicopter tends to return to the original trim condition, it is said to exhibit positive static stability. If it tends to diverge from the trim condition, it is said to exhibit negative static stability. If the helicopter tends to remain at the new position with no tendency to return to the original trim condition or to diverge, it is said to possess neutral static stability. The degree of static stability or instability will have an effect on the helicopter automatic flight control system (AFCS) design and gain selection. Static stability options are illustrated in Figure 5-2.

Dynamic stability is concerned with the resulting motion of the helicopter following a disturbance from trim condition. The resulting motion can be either oscillatory (periodic) or non-oscillatory (aperiodic). It may also be convergent, divergent, or neutral. Static stability is

required for dynamic stability, but a system may be statically stable and dynamically unstable. Dynamic stability motion options are also illustrated in Figure 5-2.

1.   <u>Stability In The S Plane</u>

The helicopter stability can also be analyzed by examining the location of the roots of a linear closed loop system in the complex or S plane. Stability in the S plane is illustrated in Figure 5-3. The figure shows that if all the system closed loop poles lie in the left half of the S plane the system will be stable. If any of the close loop poles lie in the right half of the S plane the system will be unstable. If the roots lie on the real axis, the system will be either non-oscillatory (left half S plane) or aperiodic divergent (right half S plane). The radial distance out from the origin to the roots determines the natural frequency (w_n) of the system. The angle of the roots from the imaginary axis (θ_d) determines the damping ( ). For example, consider the case of a hovering helicopter. The characteristic equations for longitudinal and lateral motion were presented in equations 5-3 and 5-7, and are repeated below.

Longitudinal: $s^3 - (X_u + M_q)s^2 + X_u M_q S + M_u g = 0$ (5-3)

Lateral: $s^3 - (Y_v + L_p)s^2 + Y_v L_p S - L_\beta g = 0$ (5-7)
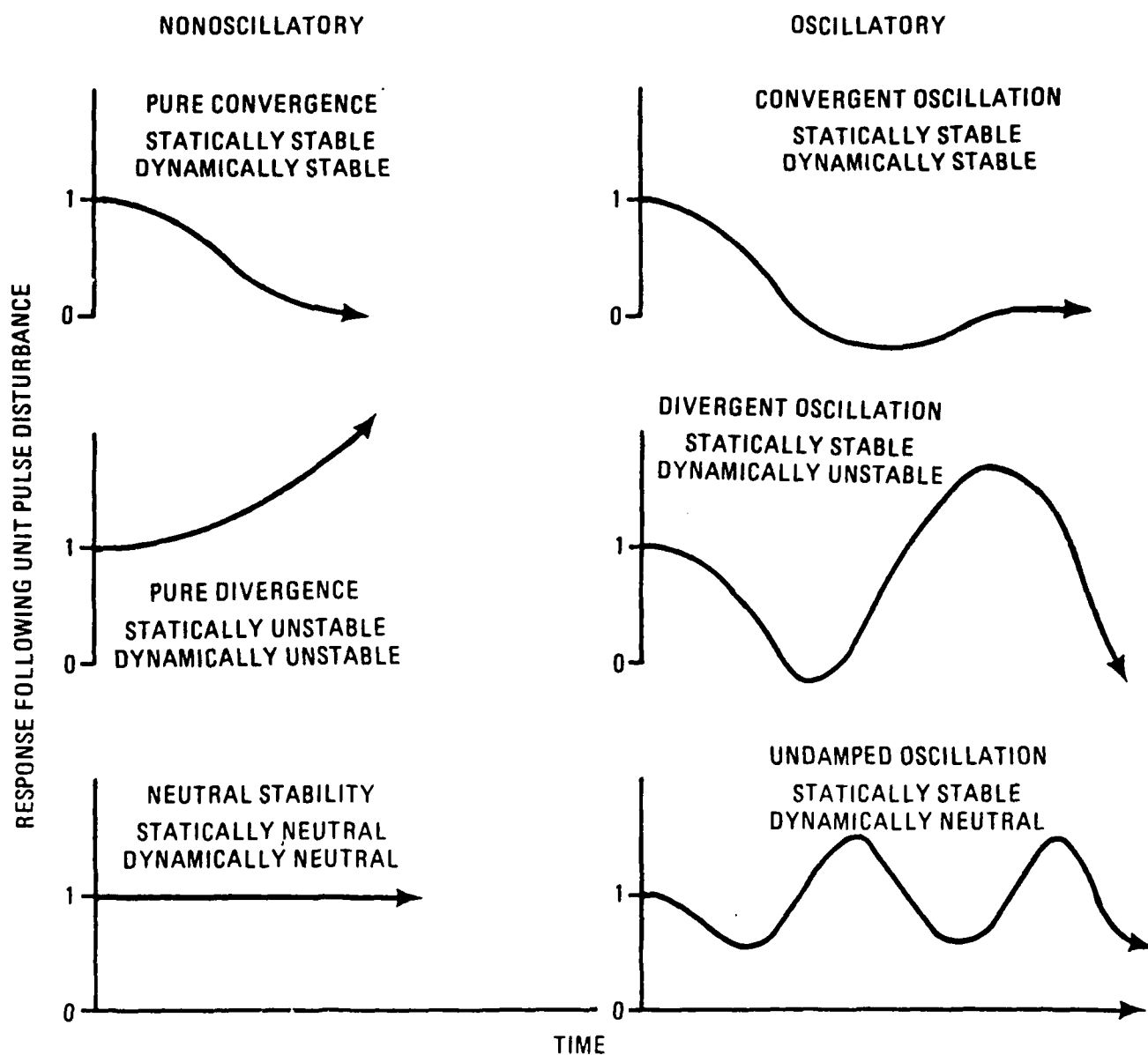
Figure 5-2   Illustration of Stability Options

65

The hovering cubics presented in equations 5-3 and 5-7 can be solved by hand using a trial and error process, but a hand calculator or personal computer makes the task much easier. Conventional single rotor and tandem rotor helicopter stability derivatives from Reference 19 are presented below.

<div align="center">Hover</div>

Conventional Rotor		Tandem Rotor	
Longitudinal Roots	Lateral Roots	Longitudinal Roots	Lateral Roots
$X_u = -.0284$	$Y_v = -\ .0731$	$X_u = -\ .019$	$Y_v = -\ .0282$
$M_q = -.610$	$L_p = -\ 3.18$	$M_q = -\ 1.98$	$L_p = -\ 1.612$
$M_u = \ .00609$	$L_\beta = -\ .052$	$M_u = \ .0348$	$L_v = -\ .0342$
Vertical Root	Directional Root	Vertical Root	Directional Root
$Z_w = -.69$	$N_r = -\ 1.1$	$Z_w = -\ .82$	$N_r = -\ .0535$

Both conventional and tandem rotor type helicopters have a pair of roots in the right hand plane. The longitudinal roots are shown in Figure 5-4. Both longitudinal and lateral hover modes will be unstable and stability will have to be provided by the pilot or by some form of automatic flight control system.
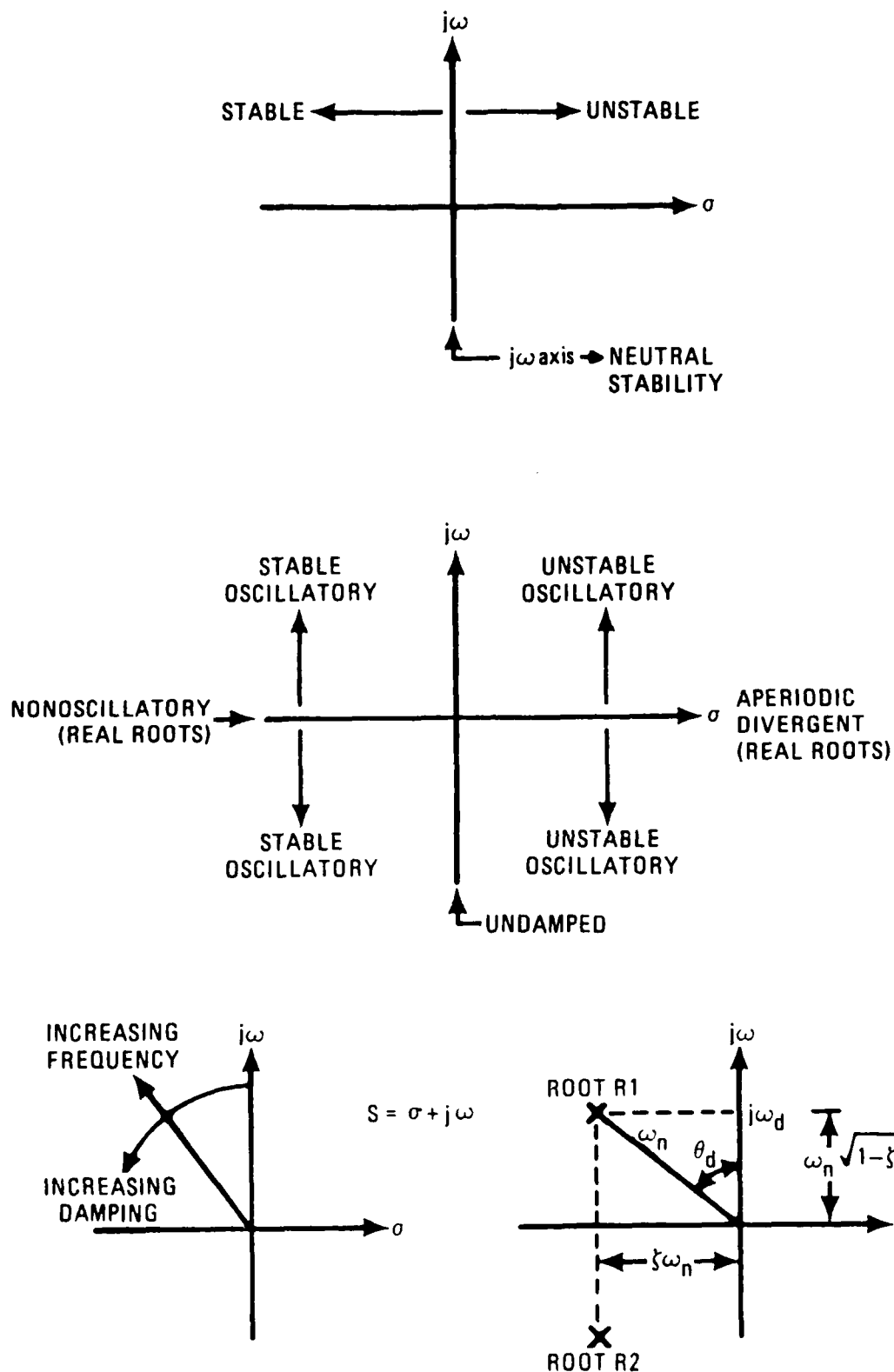
Figure 5-3   Effect of Root Location on Stability in the S Plane

Conventional Helicopter Longitudinal/Vertical Motion Hover	Tandem Helicopter Longitudinal/Vertical Motion Hover

$$S^3+.6384S^2+.0173S+.1961=0 \qquad S^3+1.999S^2+.0376S+1.1206=0$$

$C_1=-.8748$; $C_{2,3}=.1182 \pm j.4585$ $T_1=-2.211$; $T_{2,3}=.1061 \pm j.7039$
$C_4= Z_w = -.69$, (equation 5-4) $T_4= Z_w = -.82$, (equation 5-8)
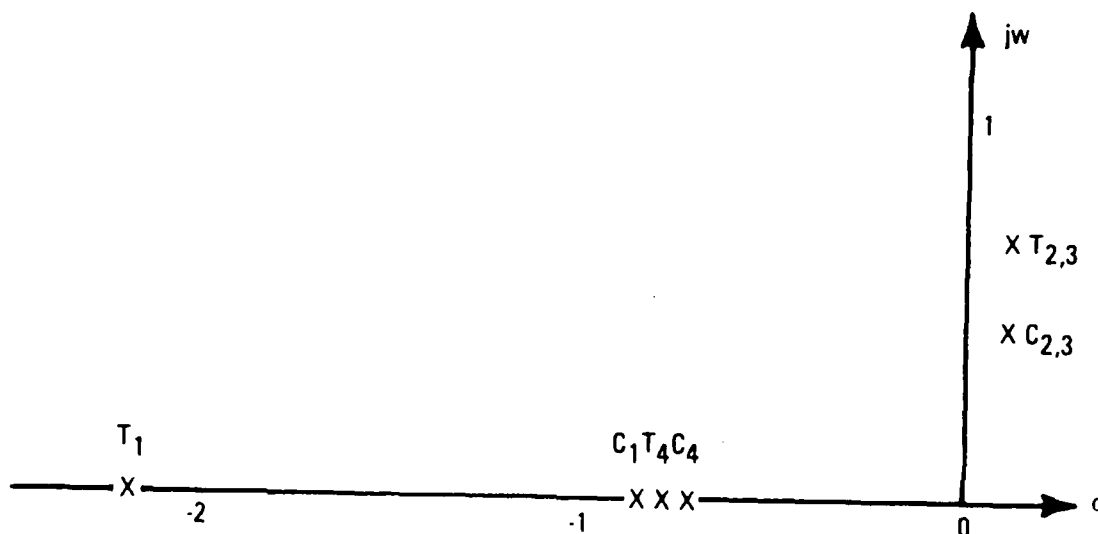
Figure 5-4   Hover Longitudinal/Vertical Roots

As previously noted, the characteristic equation determines the character or stability of the system response. Descarte's Rule of Signs tells us that the number of unstable or positive real roots equals the number of consecutive sign changes in the characteristic equation or is less than this minus an even number. A fourth order characteristic equation of a single rotor helicopter in forward flight is presented as equation 5-26. Note that the equation has two

consecutive sign changes which implies two positive or unstable roots.

$$s^4 + 1.874S^3 - 5.916S^2 - 5.910S + .011 = 0 \qquad (5\text{-}26)$$

Another method of determining the number of closed loop poles lying in the right half of the S plane without having to factor the polynomial is Routh's Stability Criterion. This method is also referred to as the Routh-Hurwitz Stability Criterion since both Routh and Hurwitz independently developed similar methods for determining the number of roots in the right hand plane. Equation 5-26 can be written in the form:

$$a_n s^n + a_{n-1} s^{n-1} + \dots + a_1 s + a_o = 0 \qquad (5\text{-}27)$$

One necessary, but not sufficient, condition for stability is that the coefficients in the above equation be positive with no missing terms (recall Descarte's Rule). The sufficient condition for stability involves setting up a Routh array or table and verifying that all elements in the first column of the array are nonzero and that they have the same sign. The criteria also tells us that the number of first column element sign changes in the array is equal to the number of roots in the right hand plane. The Routh Array is set up in rows and columns as shown below:

Row					
1	s^n	a_n	a_{n-2}	a_{n-4}	$\ldots$ (5-28)
2	s^{n-1}	a_{n-1}	a_{n-3}	a_{n-5}	$\ldots$
3	s^{n-2}	b_1	b_2	b_3	$\ldots$
4	s^{n-3}	c_1	c_2	c_3	$\ldots$
.	.	.	.		
.	.	.			
n	s^1				
n+1	s^0				

where
$$b_1 = \frac{(a_{n-1}\, a_{n-2}) - (a_n\, a_{n-3})}{a_{n-1}}$$

$$b_2 = \frac{(a_{n-1}\, a_{n-4}) - (a_n\, a_{n-5})}{a_{n-1}}$$

$$b_3 = \frac{(a_{n-3}\, a_{n-6}) - (a_{n-2}\, a_{n-7})}{a_{n-1}}$$

$$c_1 = \frac{(b_1\, a_{n-3}) - (a_{n-1}\, b_2)}{b_1}$$

$$c_2 = \frac{(b_1\, a_{n-5}) - (a_{n-1}\, b_3)}{b_1}$$

$$d_1 = \frac{c_1 b_2 - b_1 c_2}{c_1}$$

and the rows are constructed until zero value elements are obtained except in the first column. Equation 5-26 can be used to illustrate the Routh array, as shown below.

70

$$s^4 \qquad 1 \qquad\qquad -5.916 \qquad\qquad .011 \qquad\qquad (5\text{-}28)$$

$$s^3 \qquad 1.874 \qquad -5.910 \qquad\qquad 0$$

$$s^2 \quad \frac{(1.874)(-5.916)-(1)(-5.910)}{1.874} \qquad \frac{(1.874)(.011)-(1)(0)}{1.874S}$$

$$s^2 \quad = -2.76 \qquad\qquad = .011$$

$$s^1 \quad \frac{(-2.76)(-5.916)-(1.874)(.011)}{-2.76} \qquad\qquad 0$$

$$s^1 \quad = -5.91 \qquad\qquad = 0$$

$$s^0 \quad \frac{(-5.91)(.011)-(5.91)(0)}{-5.91}$$

$$s^0 \quad = \quad .011$$

The first column had two sign changes, implying that there are two roots with positive real parts. The Routh criteria was published in 1877 and provided a way of determining the stability of systems without having to factor high order characteristic equations. As a result of modern hand calculators and personal computers, the need for using the Routh criteria has gone the way of the slide rule. It is much easier to find the roots of characteristic equations using a root finding algorithm. The "POLY" function of the Hewett-Packard HP41CV hand calculator gives the roots of equation 5-26 as

$R1 = 2.1515, R2 = 0.0019, R3 = -0.8723, R4 = -3.155$

This confirms that two of the roots are located in the right half of the S plane.

D.   PILOTING REQUIREMENTS

Piloting requirements for helicopter control system evaluations include both open and closed loop tasks. Open loop tasks are oriented primarily at specification compliance and may include observing the aircraft response to a unit step control input. Closed loop requirements include mission oriented tasks, where pilot input/feedback is required. Aircraft flying qualities can be considered an open loop function, where specification compliance is the driving factor. Aircraft handling qualities implies a closed loop function, where the pilot is using a vehicle with a given level of flying qualities to accomplish a specific task. Note that some sources, like Reference 8, consider both flying qualities and handling qualities to imply closed loop functions. Piloting tasks are performed by trained test pilots using standard procedures like those outlined in Reference 8. Pilot ratings for a specific task are assigned using the Cooper-Harper Handling Qualities Rating (HQR) scale presented in Figure 5-5.

Helicopter controllability testing is conducted to determine the aircraft response quality and control effectiveness. Response quality is primarily a function of system lags, and control sensitivity/damping. Control system lags can have a very adverse affect on pilot ratings, especially for high workload tasks. Testing has shown that

control system lags on the order of 200 msec can cause pilot induced oscillations (PIO) for VMC hover tasks. Control system mechanical characteristics testing must consider current conventional cyclic/collective/pedal displacement systems and possible sidearm force controllers in the future.

Control sensitivity is usually defined as the control moment generated per unit of control displacement. Control power is defined as the total moment available about a given axis. Damping is the moment that tends to resist the initial rotor acceleration caused by a control moment. For the basic airframe, sensitivity and damping are primarily affected by the rotor configuration. Reference 1 notes a hingeless rotor system gives high control power compared to an articulated rotor and even larger increases in pitch and roll damping. Damping helps the pilot to predict the resulting motion following a control input. Control sensitivity affects the initial aircraft acceleration following a control input. Control sensitivity and damping allow the pilot to predict the altitude change and resulting steady state rate resulting from control input.

AIRCRAFT CHARACTERISTICS	DEMANDS ON THE PILOT IN SELECTED TASK OR REQUIRED OPERATION*	PILOT RATING
EXCELLENT HIGHLY DESIRABLE	PILOT COMPENSATION NOT A FACTOR FOR DESIRED PERFORMANCE	1
GOOD NEGLIGIBLE DEFICIENCIES	PILOT COMPENSATION NOT A FACTOR FOR DESIRED PERFORMANCE	2
FAIR — SOME MILDLY UNPLEASANT DEFICIENCIES	MINIMAL PILOT COMPENSATION REQUIRED FOR DESIRED PERFORMANCE	3
MINOR BUT ANNOYING DEFICIENCIES	DESIRED PERFORMANCE REQUIRES MODERATE PILOT COMPENSATION	4
MODERATELY OBJECTIONABLE DEFICIENCIES	ADEQUATE PERFORMANCE REQUIRES CONSIDERABLE PILOT COMPENSATION	5
VERY OBJECTIONABLE BUT TOLERABLE DEFICIENCIES	ADEQUATE PERFORMANCE REQUIRES EXTENSIVE PILOT COMPENSATION	6
MAJOR DEFICIENCIES	ADEQUATE PERFORMANCE NOT ATTAINABLE WITH MAXIMUM TOLERABLE PILOT COMPENSATION CONTROLLABILITY NOT IN QUESTION	7
MAJOR DEFICIENCIES	CONSIDERABLE PILOT COMPENSATION IS REQUIRED FOR CONTROL	8
MAJOR DEFICIENCIES	INTENSE PILOT COMPENSATION IS REQUIRED TO RETAIN CONTROL	9
MAJOR DEFICIENCIES	CONTROL WILL BE LOST DURING SOME PORTION OF REQUIRED OPERATION	10

*DEFINITION OF REQUIRED OPERATION INVOLVES DESIGNATION OF FLIGHT PHASE AND/OR SUBPHASES WITH ACCOMPANYING CONDITIONS.

ADEQUACY FOR SELECTED TASK OR REQUIRED OPERATION*

DEFICIENCIES WARRANT IMPROVEMENT

DEFICIENCIES REQUIRE IMPROVEMENT

IMPROVEMENT MANDATORY

IS IT SATISFACTORY WITHOUT IMPROVEMENT?

IS ADEQUATE PERFORMANCE ATTAINABLE WITH A TOLERABLE PILOT WORKLOAD?

IS IT CONTROLLABLE?

YES   NO

PILOT DECISIONS

Figure 5-5   Cooper-Harper Rating Scale

VI.   HELICOPTER FLIGHT CONTROL SYSTEMS

A.   GENERAL

Automatic flight control systems (AFCS), as described in Reference 12, have been around much longer than practical helicopters. The primary concern of the early helicopter inventors was to get their machines off the ground. Once adequate engine power was available, the pioneer aviators had to worry about the controllability of their aircraft. Basic helicopter instabilities and requirements, like over water hovers and night/IMC operations, emphasized the need for automatic flight control systems.

A summary of helicopter automatic flight control system development by selected companies is presented in Appendix A. Early helicopter stabilization systems were either mechanical or analog. Helicopter development was gaining momentum during the 1950's, but recall that electronically the 1950's can be referred to as the time of vacuum tube technology. Discrete solid state technology came about in the 1960's. The 1970's are referred to as the time of integrated solid state technology. As technology improved, digital AFCS started replacing analog systems during the late 1970's and during the 1980's.

The V-22 tiltrotor aircraft has a triply redundant hybrid Fly-By-Wire (FBW) system. Fly-By-Light (FBL) flight control system technology has also been demonstrated (see References 20 and 21). Reference 21 summarizes a series of simulations and flight tests under the Advanced Digital Optical Control (ADOCS) program that were conducted to determine the optimum side arm controller configuration for specific mission tasks.

B. IMPLEMENTATION OPTIONS

1. Digital Systems

Digital systems are very popular today, both in terms of new helicopter AFCS, and as replacements for existing analog systems in helicopters involving service life extension programs. The advantages of digital systems center primarily around the flexibility in development, the ability to use more complex functions, and improved self-test capability. Reference 22 noted that Sikorsky studies in the early 1970's showed that two digital computers could be used to replace six analog subsystems on the YCH-53E. The studies also showed that compared to an analog system, a digital system would provide the following:

- Significant weight, size, and power reductions
- Improvements in reliability, logistics, and spares
- Improved development flexibility
- Improved system growth potential
- Reduced life cycle cost

Reference 23 lists the advantage of digital systems as:

- Flexibility

- Accuracy

- Noise rejection

- Long-term stability

- Simplicity of binary systems

- Physical characteristics

The disadvantages of digital systems are listed as:

- Susceptibility to gross errors

- Difficult software validation

- Sampled-data effects

- Quantization effects

- Analog/digital conversions

- Slow integration

- Large number of elements

2.   Fly-by-Wire and Fly-by-Light Systems

References 24 through 26 review flight control system criteria for advanced aircraft and new flight control technologies for future naval aircraft. Fly-by-wire (FBW) systems offer advantages such as:

- Installation options

- Preprogrammed product improvement easily done

- Weight savings

Negative points for FBW systems include:

- Electromagnetic Interference (EMI) susceptibility,

especially for composite aircraft, from lightning strikes or electronic equipment radiation

. Susceptibility to fire

Fly-by-light (FBL) systems have the following primary advantages:

. Reduced EMI susceptibility

. Reduced weight (about one half the weight of current systems)

The primary negative points for FBL include the following:

. Susceptibility to gamma radiation

. Susceptibility to fire (not as bad as for FBW)

FBL systems have two primary advantages over FBW systems:

. Weight savings

. Reduced EMI problems

C.   MECHANICAL SYSTEMS

Helicopters primarily use mechanical linkages to transmit pilot control system movement to the main rotor, to the tail rotor, and, often, to the horizontal stabilizer. The flight control system for a typical teetering rotor helicopter is presented in Figure 6-1. Cyclic control movements are transmitted, via mixing units and the hydraulic system, to the swash plate assembly. The swash plate assembly consists of two concentric rings which move up and down and tilt with respect to the shaft in response to control inputs. The lower concentric ring does not rotate but does transmit inputs to the upper rotating ring which transmits the input

to the blades via the blade pitch links. Moving the cyclic control forward changes the rotor pitch cyclically and results in the rotor tip path plane tilting forward. The tip path plane produces a force/moment unbalance in the longitudinal axis which results in the helicopter accelerating forward. Moving the cyclic control left or right changes the rotor pitch cyclically and results in the rotor tip path plane tilting left or right with the helicopter banking and moving in the corresponding direction. Moving the rudder pedals right or left increases or decreases the collective pitch of the tail rotor blades. The change in tail rotor pitch produces more (right pedal) or less (left pedal) thrust than required to balance the main rotor torque. The unbalanced torque produces a yaw angular acceleration which results in a yaw rate and an aircraft heading change. Moving the collective control up or down increases or decreases the pitch on the rotor blades collectively and results in the aircraft moving up or down. A synchronized elevator is often connected to the fore and aft cyclic system at the swashplate to help with longitudinal trimming as a function of airspeed.

Rotor forces on all but the smallest helicopters (e.g., McDonnell-Douglas OH-6, Robinson, etc.) are reduced to zero by hydraulic servo cylinders and do not feed back into the pilot's controls. The servo cylinders are powered by trans-

mission driven hydraulic pumps. Force trims (bungees) are commonly used to induce force gradients in the cyclic and directional controls. The force trims are electromechanical units and are also used to keep the flight controls from moving by themselves.

D. MECHANICAL STABILITY

Mechanical stability devices are simple and reliable but are limited in the stability improvement they can provide. Three examples of mechanical gyros include the Bell bar, the Hiller airfoil, and the Lockheed gyro.

1. Bell Bar

The Bell Bar, see Figure 6-1, was used on all early Bell helicopters with teetering rotor systems. The stabilizer bar is pivoted to the main rotor mast in a plane above and at 90 degrees to the main rotor blades. If the helicopter attitude is disturbed while hovering, the bar tends to remain in its current plane causing the blades to feather and return the rotor to its initial plane of rotation. The mast following characteristic of the bar is regulated by the hydraulic (viscous) dampers shown in Figure 6-1. The bar provides lagged rate damping where the equation of motion can be approximated by a first order lag as

$$A_{1s} = \frac{K_p}{S + 1/t} \quad \text{and} \quad B_{1s} = \frac{K_q}{S + 1/t} \quad (6-1)$$
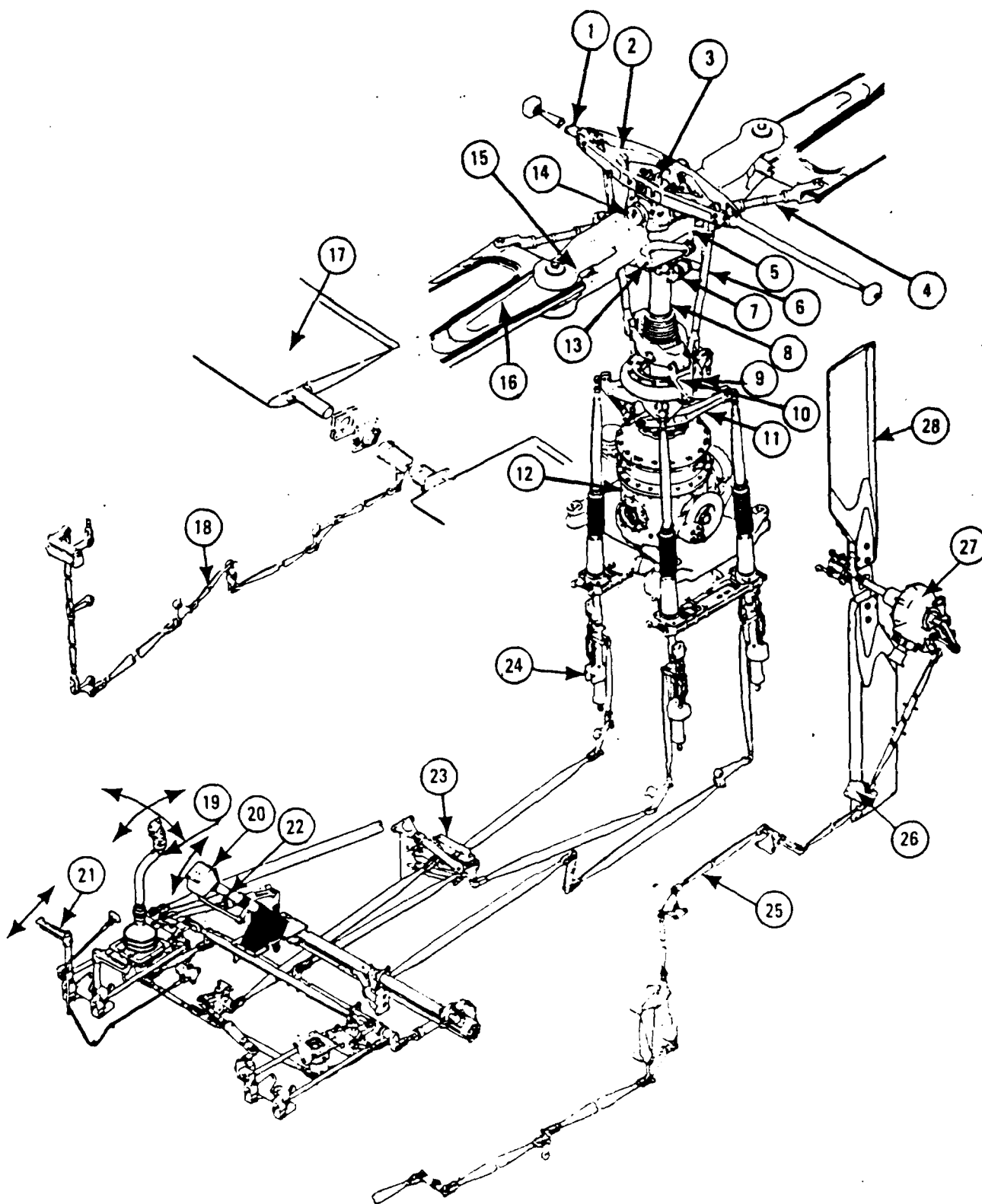
Figure 6-1 Mechanical Flight Control System
From Reference 27

81

Figure 6-1 shows the following parts:

1. Stabilizer Bar
2. Mixing Lever
3. Mast Retaining Nut
4. Drag Brace
5. Pitch Change Link
6. Control Tube
7. Hydraulic Damper
8. Mast
9. Swashplate and Support Assembly
10. Drive Link
11. Collective Lever
12. Transmission
13. Pitch Horn
14. Main Rotor Grip Reservoir
15. Main Rotor Hub
16. Main Rotor Blade
17. Synchronized Elevator
18. Elevator Linkage
19. Cyclic Control
20. Collective Control
21. Rudder Pedals
22. Twist-Grip Throttle
23. Control Mixing Unit
24. Hydraulic Servos
25. Tail Rotor Linkage
26. 42° Gear Box
27. Tail Rotor 90° Gear Box
28. Tail Rotor Blade

where for equation (6-1), Reference 7 notes that for the UH-1H, $t = 3$ sec and 0.16 degrees of cyclic control results in the same blade feathering angle as one degree of stabilizer bar angle. Figure 6-2 shows the roll rate response to a lateral step input for the UH-1H bar on, UH-1H bar canceled analytically, and the UH-1N and Bell 205A with the stabilizer bar removed.
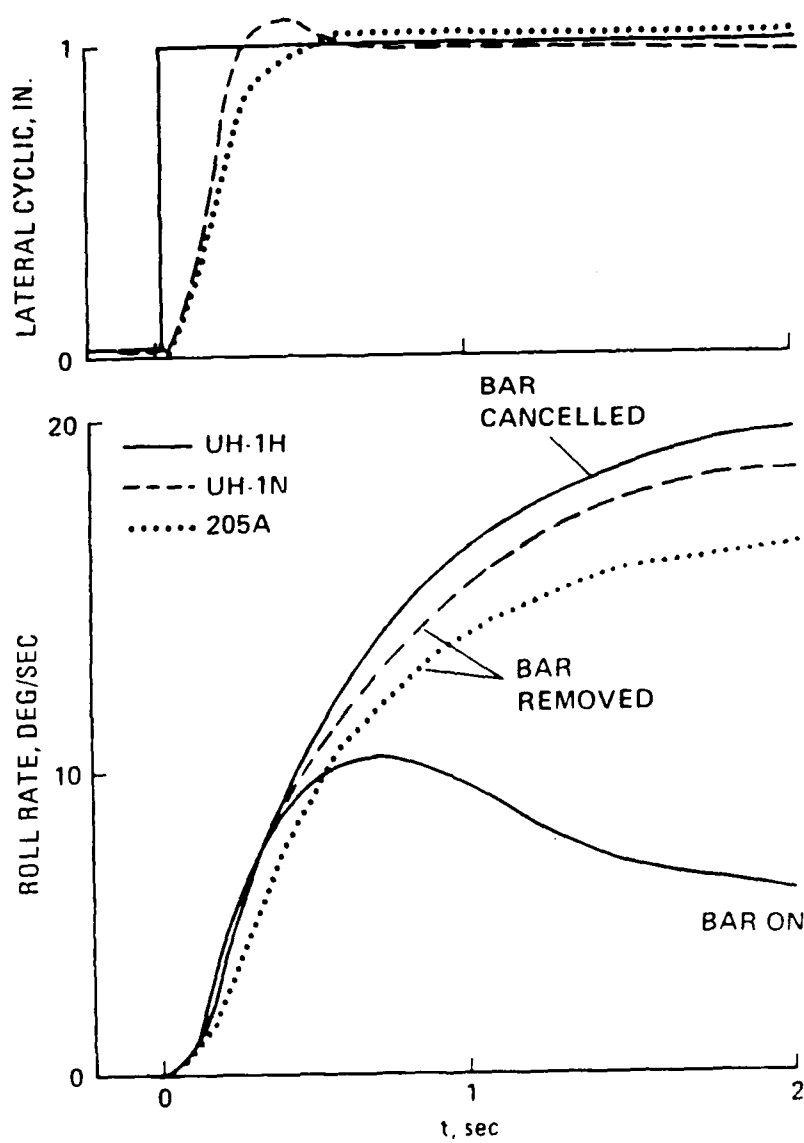
Figure 6-2   Roll Rate Response With and Without Bell Bar
From Reference 28

2. Hiller Airfoil

Hiller helicopters featured a gyro bar with small airfoils or paddles at the ends of the bar. The paddle bar was oriented perpendicular to the main rotor blades. The Hiller airfoil or control rotor operates like the Bell bar except that it uses aerodynamic damping from the airfoils rather than viscous damping. The pilot input goes through mechanical linkage to the swashplate and from the swashplate directly to the control rotor. The control rotor generates the moment required to change the pitch of the main rotor blades. Both the Bell bar and the Hiller paddle bar require a compromise in that only one gain can be used for both pitch and roll stabilization. The bars provide rate damping, but are relatively heavy and are high drag items.

3. Lockheed Gyro

The Lockheed stabilizing bar was used on the XH-51A and AH-56A hingeless or rigid rotor helicopters. The Lockheed system featured one bar for each rotor blade, spaced as shown in Figure 6-3. Reference 10 notes that, since the Lockheed rotor blade span axis is swept forward of the feathering axis, a component of aerodynamic flapping moment is applied to bar. The bar is excited by gyroscopic, inertia, and aerodynamic forces. This gives the designer more options when trying to match the rate response from the gyro to the high control power and damping of the hingeless rotor system. With the gyro bar, control phasing, and cross

coupling problems can occur because of large blade pitching moments at high speed flight.
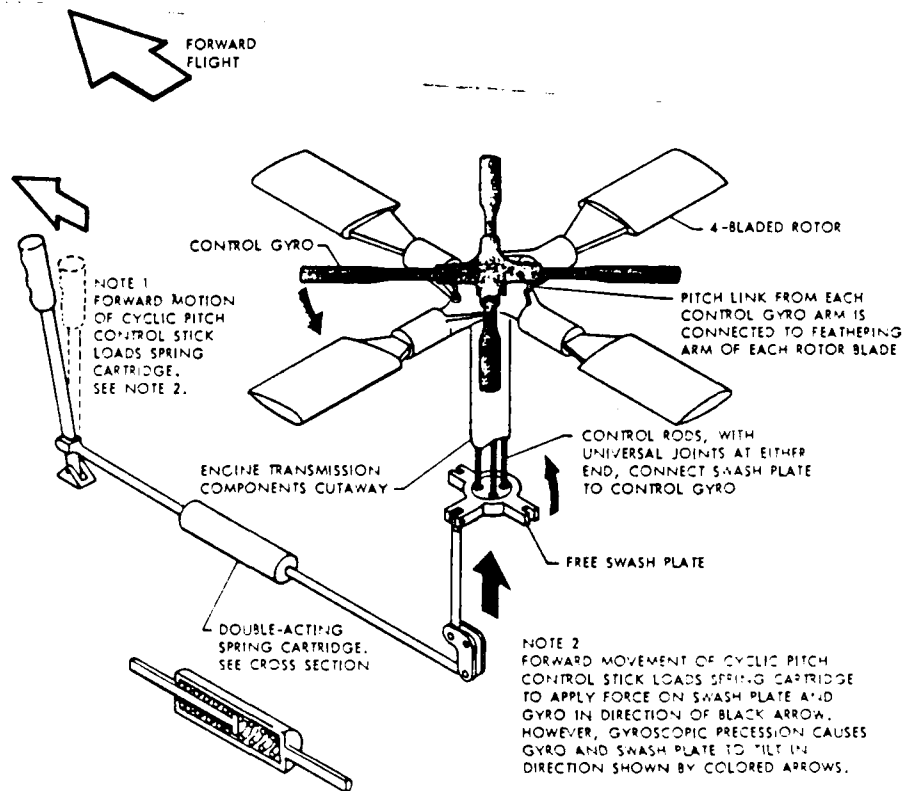
FORWARD
FLIGHT

NOTE 1
FORWARD MOTION
OF CYCLIC PITCH
CONTROL STICK
LOADS SPRING
CARTRIDGE.
SEE NOTE 2.

CONTROL GYRO

4-BLADED ROTOR

PITCH LINK FROM EACH
CONTROL GYRO ARM IS
CONNECTED TO FEATHERING
ARM OF EACH ROTOR BLADE

ENGINE TRANSMISSION
COMPONENTS CUTAWAY

CONTROL RODS, WITH
UNIVERSAL JOINTS AT EITHER
END, CONNECT SWASH PLATE
TO CONTROL GYRO

FREE SWASH PLATE

DOUBLE-ACTING
SPRING CARTRIDGE.
SEE CROSS SECTION

NOTE 2
FORWARD MOVEMENT OF CYCLIC PITCH
CONTROL STICK LOADS SPRING CARTRIDGE
TO APPLY FORCE ON SWASH PLATE AND
GYRO IN DIRECTION OF BLACK ARROW.
HOWEVER, GYROSCOPIC PRECESSION CAUSES
GYRO AND SWASH PLATE TO TILT IN
DIRECTION SHOWN BY COLORED ARROWS.

Figure 6-3   Lockheed Rigid-Rotor Control System
From Lockheed Brochure

E.   **ELECTROMECHANICAL STABILITY**

Electromechanical stability devices provide more stabilization options than the simple mechanical devices, ranging from basic rate damping to complete automatic flight control systems.   Electromechanical stability devices include:

85

- Stability Augmentation System (SAS)

- Command Augmentation System (CAS)

- Stability and Control Augmentation System (SCAS)

- Automatic Stabilization Equipment (ASE)

- Autopilot

- Automatic Flight Control System (AFCS)

1. Stability Augmentation Systems

Previous flight tests and simulations (see References 7 through 11) have shown that increased damping or increased control power and damping result in improved aircraft handling qualities including controllability. Vehicle damping can not be improved much with the basic airframe. Increased damping can be readily provided with a SAS. A simplified block diagram of a SAS is shown in Figure 6-4.

The rate gyro senses aircraft attitude rate and commands a servo actuator position. The SAS may use both attitude and rate to command the servo actuator position and may have limiting circuits to prevent actuator saturation in a steady turn. The SAS thus provides basic rate damping about a particular axis, but will not return the aircraft to the reference datum following a disturbance.
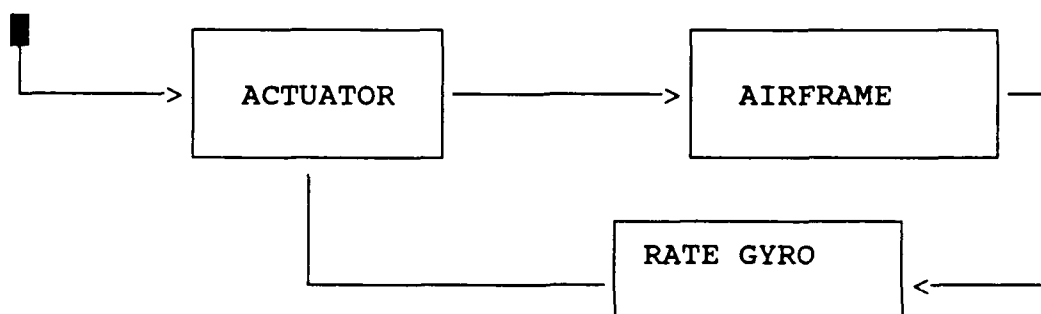
Pilot Control Input

Figure 6-4   Functional Block Diagram of SAS

The CAS senses pilot control position and can be used
to help shape the response to a control input or to decouple
the response to a control input.   The SCAS provides basic
rate damping feedback like a SAS, and provides a pilot
control input feed-forward loop like a CAS.   The pilot
control input feed-forward loop also provides a means of
differentiating between pilot control inputs and external
disturbances.   An example of the SCAS design for the AH-1G
Huey Cobra is presented in Reference 29.   A functional block
diagram of the AH-1G SCAS is presented in Figure 6-5.

2.   Automatic Stabilization Equipment

ASE provides long term hold of established or set
helicopter flight reference conditions.   A basic SAS can
provide improved short term handling qualities by increasing
the aircraft rate damping, but will not return the aircraft
to a reference datum following a disturbance.   The ability
of the aircraft to return to trim following a disturbance or
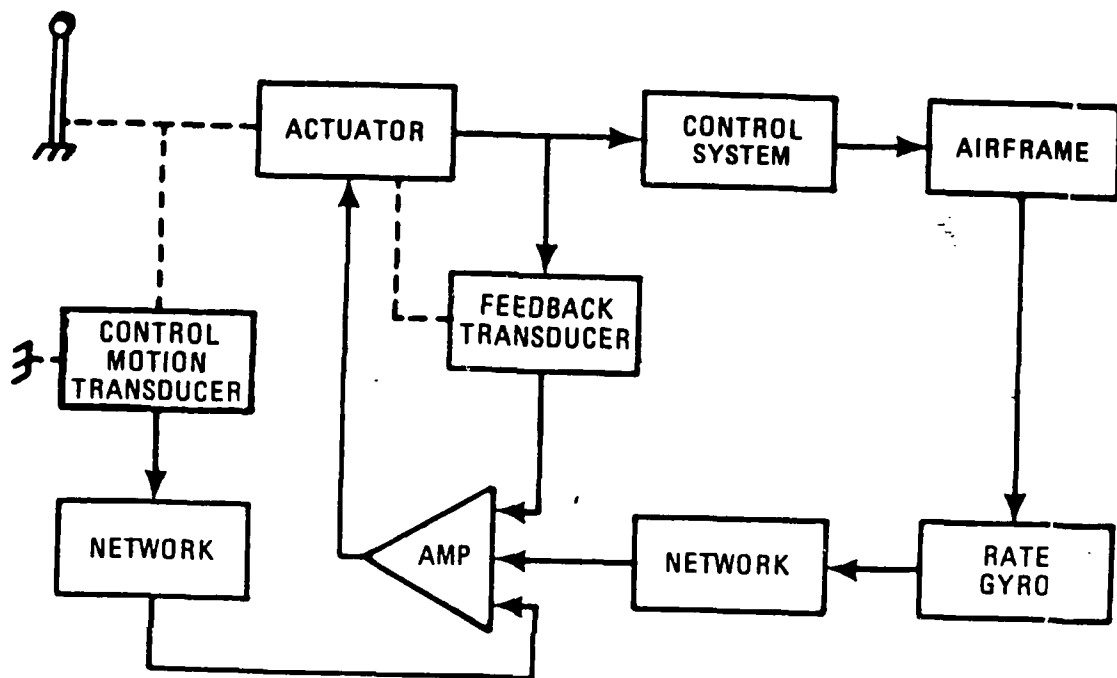
Figure 6-5   Block Diagram of AH-1G SCAS
From Reference 29

pilot release of the controls is very important at night or
during flight under IMC. ASE provides this ability and also
permits the pilot to introduce his own inputs through the
aircraft primary flight control system.

3. Autopilot

An autopilot is basically an electromechanical device designed to perform some repetitive pilot task without continual pilot assistance. Reference 12 describes a C-54 equipped with Sperry automatic pilot and approach coupler and Bendix throttle controls, making a complete flight from Newfoundland to England, including takeoff and landing, on 21-22 September 1947. An autopilot would typically use both SAS and ASE to accomplish specific functions like attitude/altitude hold, automatic steering and navigation, etc. The pilot engages the autopilot using switches and not through the primary flight control system.

4. Automatic Flight Control System

AFCS is basically an electromechanical (optical, hydraulic, pneumatic, etc.) device designed to enhance or correct the basic airframe dynamics for satisfactory mission task accomplishment and/or specification compliance. The AFCS must provide the required level of stability, controllability, and pilot assistance. An AFCS will have both inner and outer loop functions. The inner loops are typically SAS and provide short term rate damping. The SAS has limited-authority (usually ± 10%), fast responding series actuators. Movement of the series actuators does not move the pilot flight controls.

The outer loop typically employs ASE or autopilot functions to provide long term memory to maintain selected

conditions. The outer loop may use parallel actuators with 100% authority (rate limited) to perform the ASE functions. The parallel actuators may move the primary flight controls as they work to maintain specific flight conditions. A modern digital AFCS can provide a variety of functions to help the helicopter pilot accomplish a given task. The CH-53E dual-digital AFCS has functions like those listed below:

- Stability Augmentation System (SAS)
- Hover Augmentation and Gust Alleviation
- Roll Control Augmentation
- Force Augmentation System (FAS)
- Autopilot
- Turn Coordination
- Autobank
- Pedal Force Limiting
- Longitudinal Bias
- Trim

As helicopter FBW and FBL control systems, and advanced technology controllers and displays become more commonplace, the AFCS options will increase.

F. FLIGHT SPECIFICATIONS

1. Background

Flight specifications are written by the procuring activities to ensure that the aircraft they buy are "acceptable". Military aircraft specifications date back to the

early 1900's, and these early documents could be considered rather primitive (like the aircraft) by today's standards. Reference 30 notes that the first military specification for a heavier-than-air flying machine was the one page, 14 requirements Signal Corps Specification No. 486 of 20 January 1908. The flying qualities requirements of this specification were stated as follows: "Before acceptance a trial endurance flight will be required of at least one hour during which time the flying machine must remain continuously in the air without landing. It shall return to the starting point and land without damage that would prevent it immediately starting upon another flight. During this trial flight of one hour it must be steered in all directions without difficulty and at all times under perfect control and equilibrium." Pilot workload requirements, in a generic sense, were addressed indirectly as follows: "It should be sufficiently simple in its construction and operation to permit an intelligent man to become proficient in its use within a reasonable length of time." As discussed previously, it was not until the mid to late 1940's that the helicopter became widespread in military applications. Specifications addressing helicopter handling qualities, and related documents, did not appear until the early 1950's as shown in the Table 6-1 summary.

TABLE 6-1
HELICOPTER HANDLING QUALITIES SPECIFICATION DEVELOPMENT

1952 MIL-H-8501   Helicopter Flying and Ground Handling Qualities; General Requirements

1961 MIL-H-8501A   Helicopter Flying and Ground Handling Qualities

1962 NATO AGARD REPORT NO. 408, Recommendation for V/STOL Handling Qualities, Oct 1962

1965 Suggested Requirements for V/STOL Flying Qualities, USAAML TR65-45 RTM, Curry, P.R. and Matthews, J.T., of Jun 1965

1967 Analytical Review of Military Helicopter Flying Qualities, STI Technical Report No 143-1, Walton, R.P. and Ashkenas, I.L., of Aug 1967

1968 A Graphical Summary of Military Flying and Ground Handling Qualities of MIL-H-8501A, Technical Report ASNF TN 68-3; Griffin, John and Bellaire, Robert of 15 Sep 1968

1968 MIL-H-8501B (Proposed, not adopted)

1970 Agard Report No. 577   V/STOL Handling Dec 1970

1970 MIL-F-83300, Flying Qualities of Piloted V/STOL Aircraft   3 Dec 1970

1971 UTTAS Prime Item Development Specification (PIDS)

1972 A Review of MIL-F-83300 for Helicopter Applications, AHS Reprint 643, Green, D.L., May 1972

1973 AAH PIDS

1984 MIL-H-8501A Revision   Phase I awarded to STI to establish new specification structure

1985 Proposed MIL-H-8501B and Background Information and User's Guide (BIUG), STI Tech. Rpt. 1194-2 and 1194-3 of Dec. 1985

1986   Phase II (LHX) initiated

TABLE 6-1 (CONTINUED)
HELICOPTER HANDLING QUALITIES SPECIFICATION DEVELOPMENT

1986   Phase II (Generic)
                                              initiated

1988   Draft MIL-H-8501B and BIUG, Hoh, Rodger H., et al,
         USAAVSCOM Technical Report 87-A-3 of May 1988

1989   Technical review at AHS 45th Annual Forum, Boston,
         MA., May 1989

   2.   Handling Qualities Specifications

        The initial helicopter handling qualities specifi-

cation, MIL-H-8501, dates back to 1952. It was based pri-

marily on flight research performed at NASA Langley during

this time frame. Variable stability helicopters were used

to determine the best range of parameters such as control

power and damping. An example of early NASA Langley control

power and damping study using a variable stability R 5

helicopter is discussed in Reference 31. The handling

quality boundaries from Reference 31 as a function of damp-

ing and control power are presented in Figure 6-6. This

study noted that increasing damping improved helicopter

handling qualities. Reference 32 superimposes MIL-H-8501A

requirements on the early NASA Langley data in Figure 6-7.

Note that MIL-H-8501 is a 13 page document with a minor

revision (MIL-H-8501A) in 1961. The specification require-

ments are listed in terms of aircraft axis and special
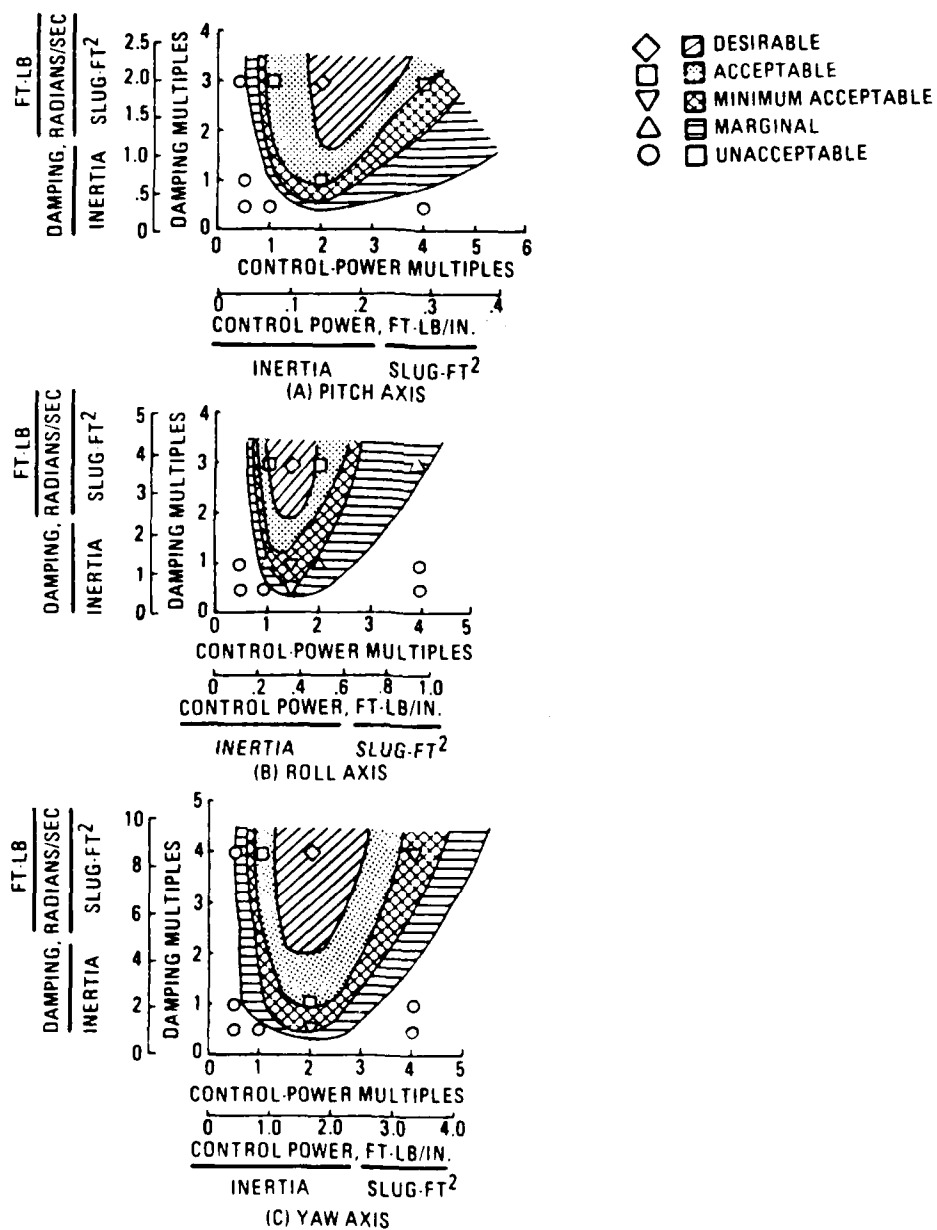
flight conditions as summarized below:

Figure 6-6   Handling Qualities Boundaries as a Function of
Damping and Control Power (From Reference 31)

MIL-H-8501A

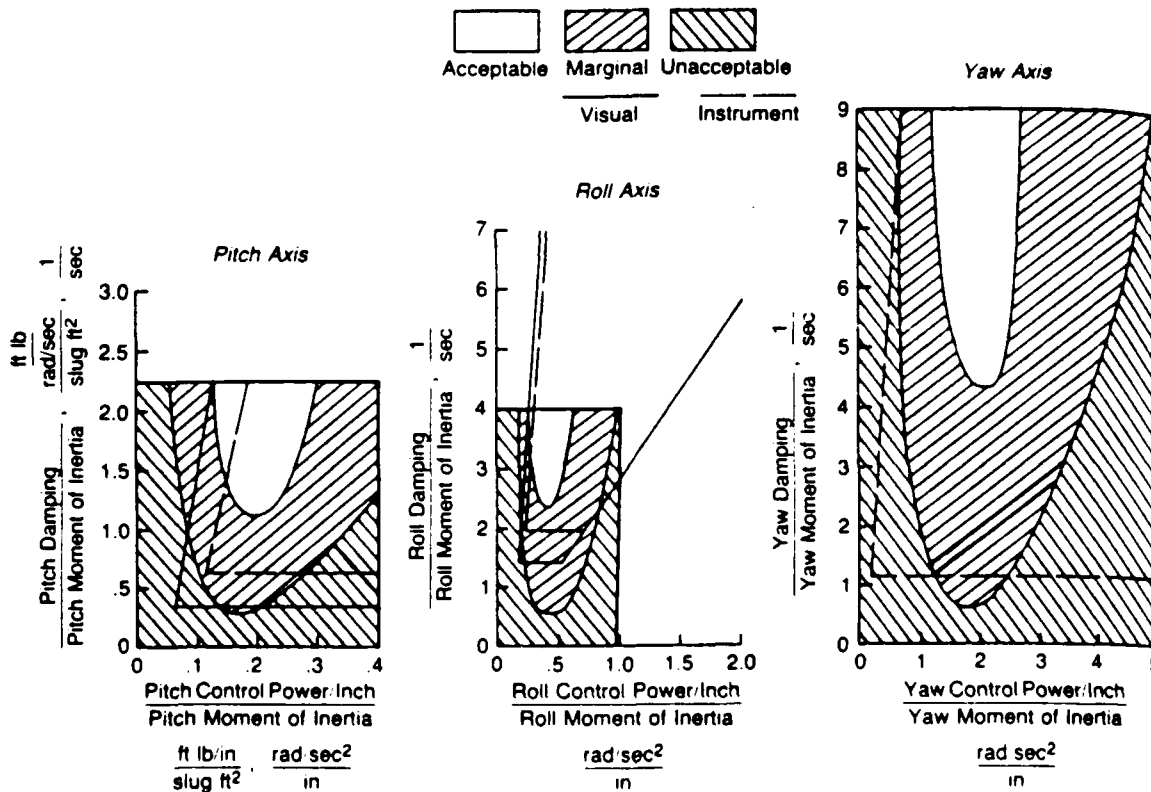| Paragraph	Topic
3.1	General
3.2	Longitudinal characteristics
3.3	Directional and lateral characteristics
3.4	Vertical characteristics
3.5	Autorotation, rotor characteristics, and miscellaneous requirements
3.6	Instrument flight characteristics

Figure 6-7   Damping and Control Power for Acceptable
              Handling Qualities (From Reference 11)

Individual MIL-H-8501A requirements are presented in Appendix B, along with the test that a flight test activity would use to verify that the requirement was met. Helicopter technology, including aircraft subsystems, and mission applications developed rapidly during the 1960's and 1970's. Reference 31 indicates that by the early 1970's government test activities were finding shortcomings in MIL-H-8501A for specific helicopters and specific mission applications. Attempts have been made to develop a database to update MIL-H-8501A. Reference 32 compares MIL-H-8501A, AGARD 577, and MIL-F-83300 requirements to selected SH-60B, CH-53D, CH-46A, XH-59A, and XV-15 data. The results of this study are presented in Figures 6-8 and 6-9 and summarized below:

MIL-H-8501A does not give adequate guidence in

> Distinguishing between hover and forward flight conditions
> Helicopter degraded AFCS flying qualities
> Mission and configuration differences in hover control power criteria

and also,

> Dynamic response criteria is very lenient

Reference 32 also notes the following points:

Hover Roll Response

> Substantiates low rating (level 2) given XV-15 with AFCS off
> CH-53D AFCS on response described as quite adequate for assault mission, yet does not satisfy MIL-F-83300
> Big difference in response between rotorcraft of approximately same weight (SH-60B & CH-46A)

Yaw Rate versus Control Sensitivity (Hover)

> Neither XV-15 nor ABC AFCS off met MIL-H-8501A or MIL-F-83300 requirements
>> ABC yaw response described as crisp
>> XV-15 yaw response described as sluggish

Pitch Rate versus Pitch Control Sensitivity (Hover)

> XV-15 pitch response meets MIL-H-8501A, but is still considered level 2
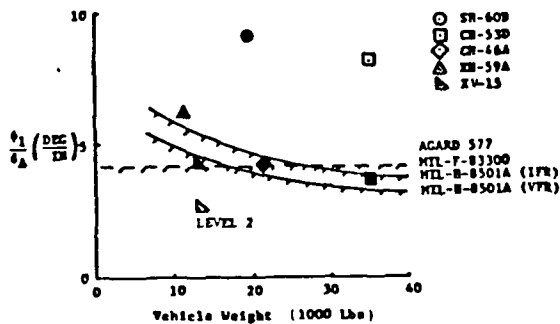
Hover Longitudinal Dynamic Stability

> Only MIL-H-8501A shows both VFR and IFR boundaries (MIL-F-83300 assumes aircraft have IFR capability)

The current rotorcraft handling qualities revision effort is designated MIL-H-8501B. Emphasis has been placed on developing a structure for MIL-H-8501B similar to that of MIL-F-8785C (fixed wing flying qualities specification) and MIL-F-83300 (V/STOL flying qualities specification). Levels of handling qualities are based on the Cooper-Harper scale presented in Figure 5-5 where:

```
        Level I   <----------->  HQR    1 - 3.5
        Level II  <----------->  HQR   3.5 - 6.5
        Level III <----------->  HQR   6.5 - 8.5
```

Reference 34 defines levels as follows:

Level 1   Safisfactory without improvement, and therefore handling qualities are adequate for the Mission Task Element (MTE)

Level 2   Deficiencies warrent improvement, but do not require improvement. Interpretation is that handling qualities are adequate to complete the MTE, but with some increase in workload and/or reduced task performance.

Level 3   Deficiencies require improvement and control can be retained with considerable compensation. Interpreted to imply that the MTE cannot be completed.
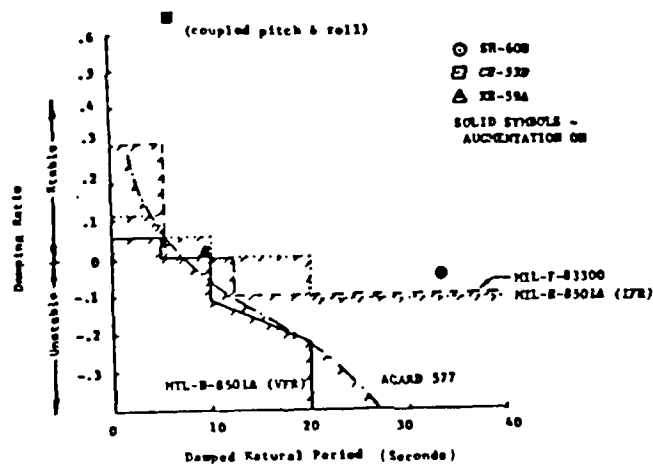
Hover roll response comparisons
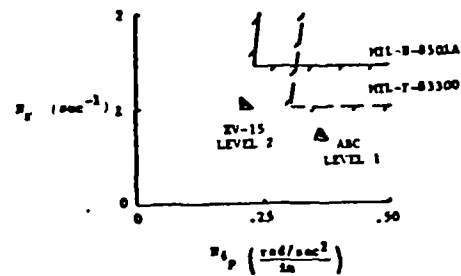
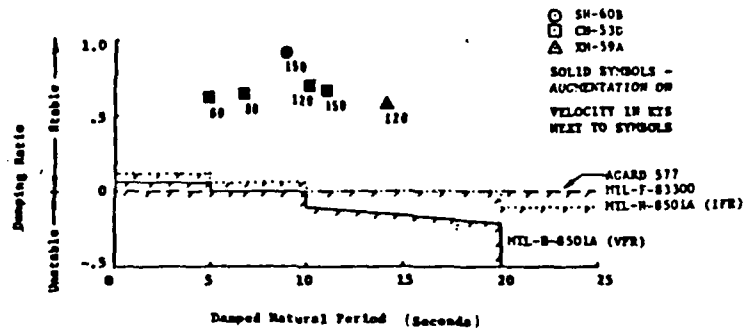Yaw rate vs. sensitivity comparisons
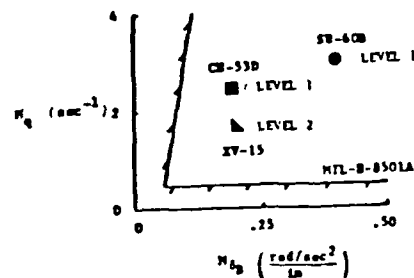
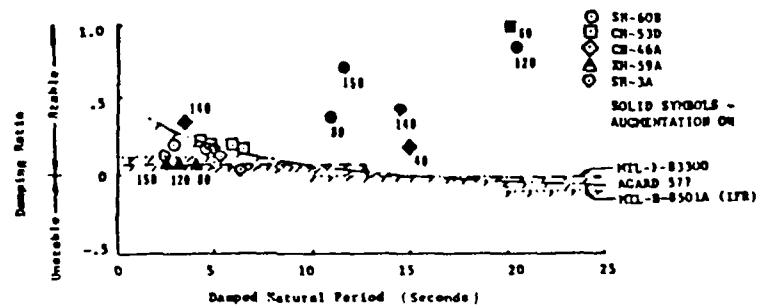Pitch rate vs. sensitivity comparisons

Hover longitudinal dynamic
stability requirements

Figure 6-8   Rotorcraft Hover Response Compared to
Specification Requirements (Reference 32)

Forward flight longitudinal dynamic stability requirements

Forward flight lateral-directional
dynamic stability requirements

Figure 6-9 Rotorcraft Forward Flight Dynamic Stability
Compared to Specifications (Reference 32)

MIL-H-8501B (Proposed) requires a minimum of level 1 handling qualities within the aircraft operational flight envelope (OFE). Level 2 handling qualities are required within the service flight envelope (SFE). The SFE is based on aircraft flight limits specified by the airframe manufacturer. The procuring activity specifies the OFE based on required aircraft missions. The OFE will be within the SFE.

Figure 6-10 presents a MIL-H-8501B flowchart. The mission and mission task element are first defined, and the mission task element defines the minimum required aircraft response type as discussed in Reference 34. A mission task element like shipboard landing might require a rate command type response. Mine sweeping may require attitude command, attitude hold for pitch and roll; rate command, heading hold in yaw; and rate command, altitude hold for height control. A basic assumption is that, if the visual cues are reduced, then the aircraft augmentation or display/vision aids must be increased to maintain the required level of flying qualities. Reference 34 also defines Usable Cue Environment (UCE) levels in an attempt to measure the pilot's ability to fly in a precise and aggressive manner with reduced visual cues. Degraded UCE may require an upgraded control system response type. With the minimum response type and UCE defined, the quantitative requirements of Section 3 and the flight test requirements of Section 4 of the proposed MIL-H-8501B may be addressed.
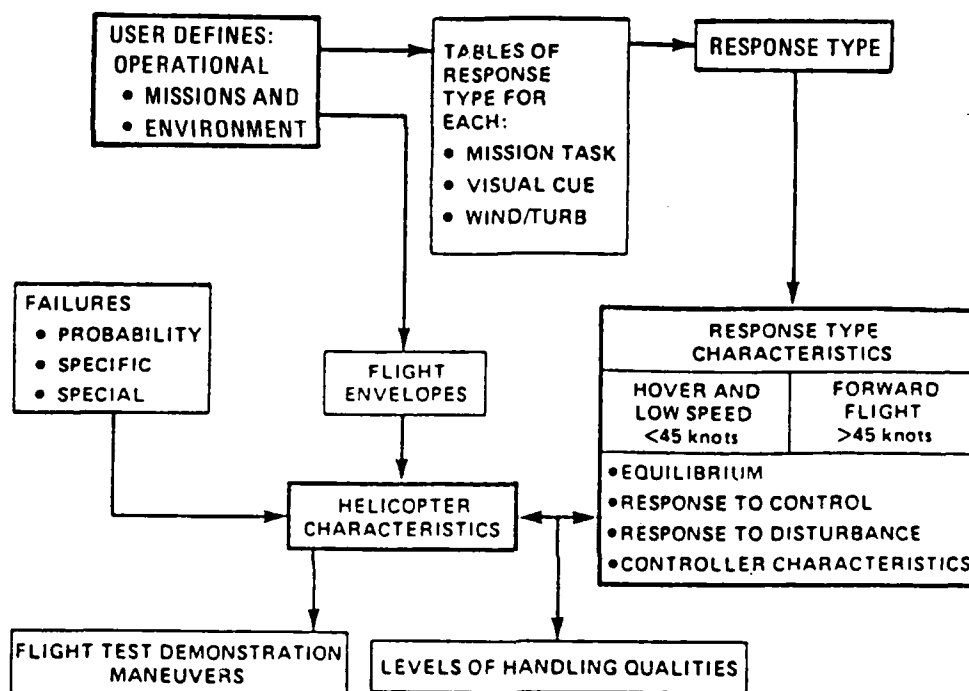
Figure 6-10   MIL-H-8501B Flowchart Summary
From Reference 34

MIL-H-8501B (Proposed) requires demonstration maneuvers by three pilots at the most critical aircraft configuration with respect to handling qualities. The average handling qualities rating (HQR) for the three pilots flying the maneuvers must be·level I or 1 < HQR < 3.5 to meet the specification requirements.

The flight test demonstration maneuvers include:

Precision Tasks

- Precision hover
- Precision hover in simulated wind
- Rapid hover turn
- Rapid hover turn in simulated wind
- Rapid vertical landing
- Precision slope landing

Aggressive Tasks

- Rapid acceleration/deceleration
- Lateral unmask/remask
- Bob-up/bob-down
- Vertical displacement and terrain avoidance
- Slalom
- Translational turn
- Roll reversal

Deceleration to Hover

MIL-H-8501B was developed primarily by research activities and departs significantly from the traditional flight test way of doing business with MIL-H-8501A. An on-going effort is being made to present the proposed new requirements to helicopter-related activities and to get feedback from these activities. It often appears that specification revision must be controversial by nature. The tendency is for one organization to propose something new or different and for another activity to shoot it down. This starts a vicious circle and often delays acceptance of a proposed specification for years, if it is accepted at all. The goal is always to come up with the best criteria for both helicopter user and designer, and something that everyone can agree upon. The proposed handling qualities specification,

MIL-H-8501B, will require more exposure to flight test activities and more flight test activity feedback before it is finally accepted.

3. Flight Control Systems Specifications

Like the flying qualities specifications, the flight control systems specifications also date back to the mid-fifties. Also like the flying qualities specification revision effort, the Navy is in the process of revising its flight control system specification. In a third similarity, the Air Force have their own rotorcraft flight control system specification as well as their rotorcraft flying qualities specification. Military Specification MIL-F-18372 (Aer) covered mechanical flight control systems and was published on 31 March 1955, superseding SR-169A of 1 July 1953. Military Specification MIL-C-18244A (WEP) covered automatic flight control systems and was published on 1 December 1962, superseding MIL-C-18244 (AER) of 16 March 1955. A Navy/NASA V/STOL Flying Qualities Workshop at Monterey, Ca., reviewed the status of AFCS specifications in 1977. The follow-up Grumman Aircraft Company, Inc., study (Reference 35) concluded that MIL-C-18244A (WEP) and MIL-F-18372 (Aer) did not reflect state-of-the-art design philosophy. Technology advances from early flight control system specifications include fly-by-wire and fly-by-light systems, plus sidearm controllers. Funding constraints have hampered

the Navy flight control system specification update effort. The current Navy flight control system specification revision effort will only cover conventional control system design requirements. Plans include a follow-on program to identify advanced flight control system requirements. A chronology of events leading up to the current Air Force flight control system specification (MIL-F-87242) is given in Appendix C.

VII. METHODS OF EVALUATING HELICOPTER AFCS

A. COMPUTATIONAL OPTIONS

1. General

Computational requirements for helicopter control system analysis will depend on the complexity of the problem. Options range from simple hand sketches to complex control system analysis programs on mainframe computers. Commercially available personal computer (PC) software is a good compromise between the two extremes listed above. PC programs can provide a quick solution for roots of a CE and can display various plot options. This gives the designer physical insight into the problem that, in the past, would have taken considerable more time to obtain from hand sketches. PC programs can provide analysis tools for complex multi-input non-linear digital systems requiring optimization studies. It is also important to question any computer results, realizing an incorrect answer is still incorrect even though it may be displayed with six or more digits to the right of the decimal point.

Control system or stability and control text books often refer to a computer program to aid the analysis and may include a listing of the program code. Professor G. Thaler of the Navy Postgraduate School (NPS) goes beyond

this to include a PC disk in his control systems book (Reference 36). He also dedicates a chapter in the book to describing the program.

2. ALCON

The Automatic Linear Control (ALCON) System analysis and design software was originally developed by Mr. Roy Wood in Reference 37 as a thesis topic at NPS. The program was developed as a learning tool to supplement basic control system courses in Electrical Engineering Department at NPS. ALCON manipulates block diagrams and determines system stability in the form of root locations, including root locus, Bode, Nyquist and time history plots, plus tabular data. The program is menu-driven and block input data can be in either factored or polynomial form. The program is valid for individual block numerators or denominators up to the eighth order and with no single block polynomial exceeding twenty-fifth order. ALCON makes no attempt to address digital control systems or state space analysis. Alcon is inexpensive, easy to use, and is highly recommended for basic linear automatic control systems analysis. The program graphic options should be improved in future versions. Similar programs should be developed as teaching aids for digital, optimal, and other specialized control system analysis courses and included with texts.

3.   Program CC

Systems Technology, Inc. (STI) of Hawthorne, CA.,
develops and markets PC control system analysis and design
software including Program CC (Version 4, Reference 38) and

• Parameter Identification (PIM, by Adaptech of France)

• Linear Systems Modeling Program   (LSMP)

• Frequency Domain Analysis Routine (FREDA)

• Model Fitting Program (MFP)

Program CC is a comprehensive control systems analysis
software package for PCs.   It includes frequency domain
analysis, time domain analysis, stochastic analysis, classi-
cal systems, sampled data systems, multi-output systems,
state space methods and optimal control procedures. It
features extensive graphics capabilities with the ability to
interactively change the plot or call up specific item of
interest from the plot.   Program CC can be extended to
system identification using the PIM program. LSMP program
can be used to input and analyze transfer function matrices,
like equations 4-7 - 4-10, without having to get them into
state space format. FREDA can be used for frequency domain
system identification with LSMP. The MFP program can be
used to fit the frequency responses of multiple measured
systems to one or more continuous transfer function models.
Program CC by itself, or especially in conjunction with the

other STI programs listed, forms a very powerful set of software for linear control system analysis using a PC. These programs are expensive for an individual looking for PC control system analysis software, and are normally used by companies, government agencies, and colleges. Although Program CC comes with considerable documentation, it is the author's opinion that the biggest weaknesses of the program are the lack of complete examples and the lack of an applications manual. The biggest program limitation is the inability to solve non-linear problems. Most of the examples in this study involve the use of Program CC.

4.   TUTSIM

The TUTSIM PC program is marketed in Palo Alto, Ca., by Applied i and can be used for both linear and non-linear control system analysis. Using TUTSIM involves developing the control system equations or mathematical model, setting up the model in a analog computer type simulation block diagram, and finally inputting the model. Models can be readily set-up using elements like integrators, summers, attenuators, and gains in a numbered sequence. The input or output of each numbered element can be tabular or graphical. The TUTSIM program comes in a Short Form which allows 15 blocks, a Collegiate Form which allows 35 blocks, and the Professional Form which allows 999 blocks

per model. Cost of the program is a function of the form selected. TUTSIM is well suited for control system problems set up in the time domain and containing nonlinear elements. It has first and second order Laplace blocks, but is not as convenient for solving linear problems expressed in the Laplace or S domain as the previous PC programs.

An ideal Control System PC program would incorporate the best features of Program CC and TUTSIM and retain the user friendliness and low price characteristics of ALCON. Many other PC controls programs are available and are often listed in control system magazines.

B. ANALYTICAL PROCEDURES

1. General

The helicopter AFCS is designed to improve the flight characteristics or controllability of the basic airframe and thus improve the pilot's ability to perform a specified task. Helicopter AFCS's can be evaluated analytically in the pre-design or design stages. The AFCS can also be evaluated by using simulation, with or without a pilot in the loop. The final evaluation, prior to acceptance, must include a flight test program.

Several graphical analytical procedures are available to evaluate control systems. The procedures center around S

plane analysis, frequency response analysis, and transient response analysis.   The primary approaches are summarized below:

  S Plane Analysis

   • Root locus

  Frequency Response Analysis

   • Bode
   • Nyquist
   • Nichols

  Transient Response Analysis

No attempt is made to derive these methods, since the information is available in References such as 16 through 18.   The techniques are summarized and enough information is presented to provide a quick reference to a person designing or evaluating a helicopter AFCS.

2.   S Plane Analysis

a. Root Locus. The root locus method, developed by W.R. Evans, shows the variation of the closed loop poles of the CE as the open loop gain is varied. The location of the closed-loop poles in the S plane determines the transient response of the system. Recall that Figure 5-3 shows the stability region of the S plane and illustrates system frequency and damping. Root locus plots of simple systems with factored transfer functions can be readily constructed by hand. Higher order systems and specific closed-loop pole

location in the S plane as a function of gain can be determined with a personal computer. Higher order transfer functions may also be partitioned and two-parameter root locus plots constructed as shown in Reference 36. General rules for constructing root locus plots include:

- **Root locus plots are symmetrical with respect to the real axis**
- **There are as many root locus branches as there are open loop poles**
- **The root loci originates at the open loop pole**
- **The root loci terminate at the open loop zero or at infinity**

Specific rules/parameters used in constructing a root locus graph are presented below:

(1) **Angle and Magnitude Criteria**

As noted above, any point on the root locus must satisfy the angle and magnitude criteria:

Angle

$$\frac{N(S)}{D(S)} = \frac{180(2k+1)}{180(2k)} \text{ for } K > 0 \quad k = 0 \pm 1, \pm 2, \dots \quad (7\text{-}1)$$

Magnitude

$$|G(S)H(S)| = 1 \quad \text{or} \quad |K| = \left|\frac{D(S)}{N(S)}\right| \quad (7\text{-}2)$$

111

(2)   **Number of Loci**

The number of loci is equal to the number of open-loop transfer function poles.

If the transfer function is $GH(S) = \dfrac{K(S + 1)}{S(S + 2)}$ (7-3)

then it has two poles ($p_1 = 0$ and $p_2 = -2$) and hence two loci paths in the root locus plot.

(3) **Real Axis Loci**

For K > 0, the real axis loci are located to the left of an odd number of finite poles and zeros.

For K < 0, the real axis loci are located to the left of an even number of finite poles and zeros.

If $GH(S) = \dfrac{K(S+1)}{S(S+2)} = \dfrac{K(Z_1)}{(P_1)(P_2)}$ (7-4)
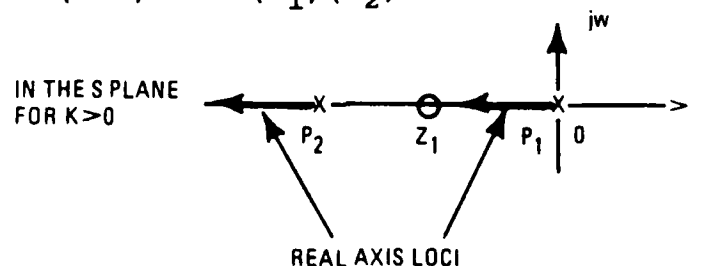

Figure 7-1   Root Locus Plot Showing Real Axis Loci

(4)   **Asymptotes**

As the system gain (K) is increased, the branches of the root locus plot approach straight line asymptotes. The gravity centroid (σ_{cg}) can be calculated as

112

$$\sigma_{cg} = \frac{\sum\limits_{i=1}^{n} p_i - \sum\limits_{i=1}^{m} z_i}{n - m} \qquad (7\text{-}5)$$

where p_i = poles
z_i = zeroes
n = number of poles
m = number of zeroes

If

$$GH(S) = \frac{K(S + 1)}{S(S + 2)} \qquad (7\text{-}6)$$

then

$$\sigma_{cg} = -\frac{2 + 0 - 1}{2 - 1} = -1 \qquad (7\text{-}7)$$

(5) **Breakaway Points**

Breakaway points are points on the real axis where two or more branches of the root locus arrive or depart. The location of the breakaway points (σ_b) can be determined by differentiating the open loop transfer function or

$$\frac{d}{ds} \, GH(S) = \sigma_b \qquad (7\text{-}8)$$

If

$$GH(S) = \frac{K}{S(S+1)} = K[S(S+1)]^{-1} = K(uv)^{-1} \qquad (7\text{-}9)$$

113

$$\frac{d}{ds} GH(S) = K[S^{-1}(S+1)^{-2}(1) + (S+1)^{-1} S^{-2}] \qquad (7\text{-}10)$$

$$\frac{d}{ds} = \frac{K}{S(S+1)^2} + \frac{K}{(S+1)S^2} = \frac{1}{S+1} + \frac{1}{S} \qquad (7\text{-}11)$$

and $S = -\dfrac{1}{2}$ which is the long way to show the obvious!

The breakaway points can also be obtained by solving the following equation

$$\sum_{i=1}^{n} \frac{1}{\sigma_b + p_i} = \sum_{i=1}^{m} \frac{1}{\sigma_b + z_i} \qquad (7\text{-}12)$$

where $- p_i$ and $- z_i$ are the poles and zeroes of GH.
This equation requires factoring an $n + m - 1$ order polynomial and it is suggested, that if possible, to let the computer solve for the breakaway points on higher order systems.

(6) Departure and Arrival Angles

The angle at which the root locus departs a complex pole (θ_D) is given by

$$\theta_D = 180° + \text{arg } GH \qquad (7\text{-}13)$$

The angle at which the root locus arrives at a complex poles (θ_A) is given by

$$\theta_A = 180° - \text{arg } GH \qquad (7\text{-}14)$$

Arg GH is the phase angle of GH calculated at a complex pole or zero while ignoring the effect of that pole or zero.

114

3.   Frequency-Response Analysis

Frequency-response analysis involves evaluating the system response to sinusoidal inputs of varying frequency. Sinusoidal inputs or frequency sweeps are used for aircraft automatic flight control system evaluations and for obtaining aircraft parameter identification data. Frequency-response analysis data are usually presented graphically and shows the relative or absolute stability of the system. The graphs can be constructed by hand for relatively simple systems to give quick approximations needed in initial studies. Constructing the graphs by hand can become very time consuming, especially if several iterations are required for the final design. Frequency-response analysis can be readily performed using a personal computer. A personal computer, with frequency analysis software, facilitates analysis of more complex systems, including compensation requirements for the systems. Personal computer control system software can be used for Bode, Nyquist, or Nichols analysis.

a. **Bode Analysis.** Bode or logarithmic plots consist of the magnitude of GH(jw) in decibels and the phase angle of GH(jw) in degrees, plotted as a function of logarithmic frequency (w). Certain basic factors occur very frequently in transfer functions. Understanding these basic factors

115

can make sketching a Bode plot very easy. Adding the curves
on the logarithmic Bode plot corresponds to multiplying the
factors of the transfer function. Bode factors commonly
found in transfer functions are summarized in Table 7.1.
The straight line factors in Table 7-1 are asymptotic ap-
proximations to the actual Bode curves. The difference
between the actual curve and asymptotic approximation is a
function of the type factor, damping ratio, and specific
frequency. With a first order factor the maximum magnitude
variation between the two curves is 3 db and it occurs at
the corner or break frequency. For a quadratic factor with
a damping ratio of .707, the difference between the asymp-
totic and actual Bode curves at the break frequency is also
3 db. Straight line asymptotic approximations are easy to
construct and are often satisfactory for determining the
system stability. If the system has first or second order
factors with break frequencies in the area of interest, then
it is important to apply the asymptotic corrections or let
the computer do the plotting. Examples showing both the
straight line Bode asymptotic curves and actual curves are
presented in texts like References 16 and 17.

References 12 and 38 discuss using Bode siggy and Bode
root plots to augment the information on standard root locus
and Bode plots. The standard Bode plot is not convenient

TABLE 7-1
COMMON BODE FACTORS

Type Factor	Num or Denom	Factor Form	Break Point	Magnitude Value db	Magnitude Slope db/dec	Phase Deg
gain	N	K	None	$20\log_{10}K$	0	0
	D	$1/K$	None	$-20\log_{10}K$	0	0
integral & derivative	N	jw^n	$w=0$	$f(w)$	$+20n$	$+90n$ constant
	D	$1/(jw)^n$	$w=0$	$f(w)$	$-20n$	$-90n$
first order	N	$1+jwT$	$w=1/T$	$f(w)$ $w>1/T$	$+20$	$0\text{-->}+90$ $\phi=45°@w=1/T$
	D	$1/(1+jwT)$	$w=1/T$	$f(w)$ $w>1/T$	-20	$0\text{-->}-90$ $\phi=-45°@w=1/T$
quadratic	N	$1+2\ jw/w_n+(jw/w_n)^2$	$w/w_n=1$	$f(w/w_n)$ $(w/w_n)>1$	$+40$	$0\text{-->}+180$ $\phi=+90°@w/w_n=1$
	D	$1/(1+2\ jw/w_n+(jw/w_n)^2)$	$w/w_n=1$	$f(w/w_n)$ $(w/w_n)>1$	-40	$0\text{-->}-180$ $\phi=-90°@w/w_n=1$

for determining the closed loop poles locations. The stand-
ard root locus plot can be used to determine closed loop
root location but is not convenient for studying gain sensi-
tivity of the closed loop poles. Reference 38 notes that it
is best to think of the Bode siggy and Bode root locus as a
root locus plotted on a Bode plot. The Bode siggy uses only
the real part of $S = \sigma + jw$, which explains the name. The
Bode root locus corresponds to a complex conjugate pair.
Program CC uses different plotting symbols to distinguish
between stable and unstable siggy and Bode root loci.

117

The standard plotting notation (Reference 38) is summarized below:

————————————	stable siggy,	$\sigma < 0$
— — — — — — — —	unstable siggy,	$\sigma > 0$
• • • • • • • •	stable Bode root locus,	$Re(S) > 0$
• • • • • • • •	unstable Bode root locus,	$Re(S) < 0$

Bode plots can be used to determine the system gain and phase margins. Bandwidth, a term used frequently in the new proposed helicopter handling qualities specification, is also defined in terms of the closed loop Bode plot. Figure 7-2 illustrates Bode plot criteria important to helicopter controllability studies. For system stability, both phase and gain margins have to be positive.
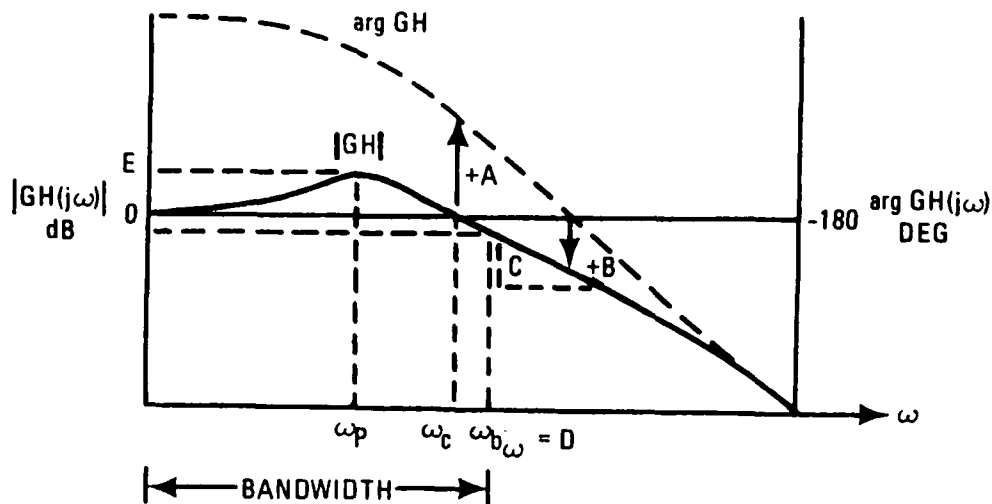

Figure 7-2 Bode Plot Criteria

118

A = Phase margin. It is the number of degrees that the phase curve [arg GH(jw)] is above minus 180 degrees, at the frequency corresponding to zero magnitude in dB (also referred to as the gain crossover frequency). Phase margin is indicative of relative stability and, for satisfactory control system performance, should be between 30 degrees and 60 degrees (Reference 17). Phase margin is related to system damping and Reference 17 notes that for damping ratios $(\zeta) \leq 0.7$, that $\zeta = 0.01\phi_{pm}$. This approximation is valid for second order systems or for higher order systems with transient response due to a pair of dominant underdamped roots.

B = Gain margin. It is the number of dB that the magnitude curve $|GH|$ is below zero dB at the frequency corresponding to minus 180 degrees phase (also referred to as the phase crossover frequency). The gain margin is also indicative of relative stability and should be greater than approximately 6 db for satisfactory system performance.

C = Slope of the Bode magnitude curve. In the region of gain crossover frequency, it is desirable to have a "fair stretch" of -20 db/decade slope for stability considerations.

D = Bandwidth. The bandwidth is usually defined as that frequency at which the closed-loop Bode magnitude curve is

down -3 db from the low frequency value. The Background
Information and User's Guide (BIUG) (Reference 34) for
proposed MIL-H-8501B defines the gain bandwidth as the
lowest frequency at which 6 dB of gain margin exits. The
phase bandwidth is defined as the lowest frequency at which
a phase margin of 45 degrees exists. Bandwidth is indica-
tive of system speed of response and, as the bandwidth
increases, the system rise time to a step input decreases.
Reference 16 notes that the specifications for bandwidth are
determined by the ability to reproduce the input signal
(speed of response) and the necessary filtering required for
high frequency noise. To track arbitrary inputs accurately,
a high bandwidth is required. A high noise environment,
especially at high frequencies, will dictate a lower band-
width. A design compromise is required to get the best
system for the opposing specifications.

E = Resonant peak. The resonant peak, M_{pw}, is indicative
of the system overshoot to a step input.

   b. **Nyquist Analysis.** Nyquist stability criterion was
first published by H. Nyquist in a Bell System Technical
Journal in 1932. The stability criterion is based on the
theory of complex variable and the development involves
conformal mapping of s plane functions into the F(S) plane.
The Nyquist polar plot is constructed by plotting magnitude

of GH(jw) and phase angle of GH(jw) as w varies. Recall
the closed loop system characteristic equation:

$$1 + G(S)H(S) = 0 \qquad\qquad (7\text{-}15)$$

$$\text{or } G(S)H(S) = -1 \qquad\qquad (7\text{-}16)$$

The Nyquist criteria relates system stability to the
number of encirclements of Z = - 1 point in the complex
plane. It is usually expressed as :

$$Z = N + P \qquad\qquad (7\text{-}17)$$

where (from Reference 16),

Z = number of right-half S plane [1 + G(S)H(S)] zeros

N = number of CW encirclements of -1+j0 point

P ∙ number of right-half S plane poles of G(S)H(S)

If P = 0, there are no G(S)H(S) poles in the right-half

S plane, and for stability there must be no encirclement

of the -1+j0 point by the G(jw)H(jw) locus.

If P ≠ 0, there are G(S)H(S) poles in the right-half S

plane, and Z must equal 0, or N must equal -P, for stabili-

ty. Since N = number of CW encirclements of the -1 point,

then there must be P counterclockwise encirclements of the

-1+j0 point for stability. The Nyquist plot can be used

to determine the relative stability of a feedback control
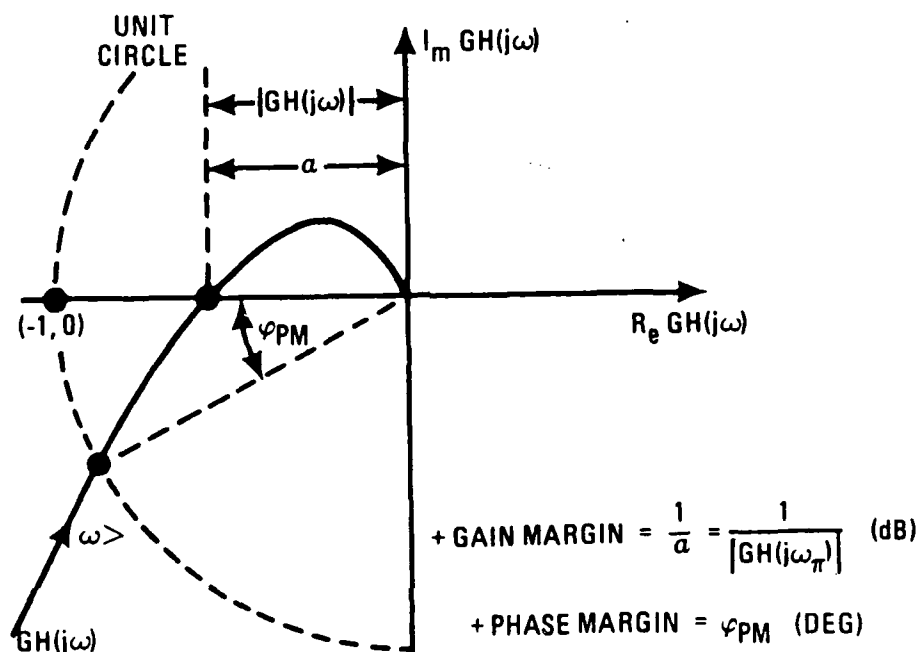
system as shown in Figure 7-3.

Figure 7-3 Nyquist Plot Criteria

c. **Nichols Chart Analysis.**

The Nichols Chart, a modification of the Bode and Nyquist plots, was developed by N.B. Nichols and documented in a "Theory of Servomechanisms" publication in 1947 (Reference 39). It consists of plotting db magnitude of G(jw) versus phase' angle of G(jw) in degrees in rectangular coordinates, as frequency w is varied. Gain margin and

122

phase margin on the db magnitude versus phase angle plot correspond to axis crossings, as shown in Figure 7-4. The Nichols chart also has contours of constant M (db) and N (deg) lines superimposed on the rectangular coordinate system. These M and N lines represent lines of constant

magnitude $\left|\dfrac{C}{R}(jw)\right| = \left|\dfrac{G(jw)}{1 + G(jw)}\right|$ in db and phase

Arg $\dfrac{C}{R}(jw)$ in degrees, respectively. Using the M and N contours, the closed loop frequency response can be determined by reading the magnitudes and phase angles at various frequency points.
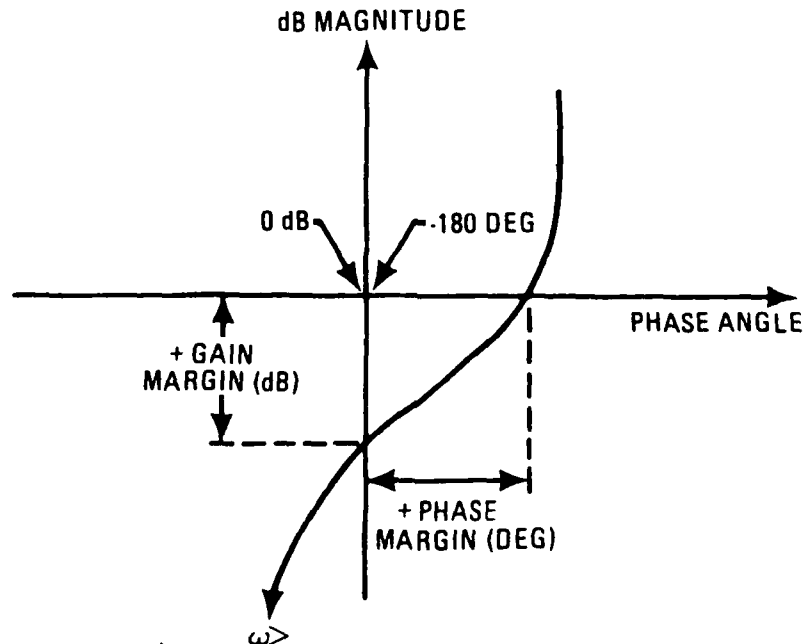

Figure 7-4   Nichols Plot Criteria (M and N Contours Not Shown)

4.   Transient-Response Analysis

Helicopter control system design requirements are often presented in terms of time-domain quantities. These quantities are usually related to the response of a second order system to a unit step input with zero initial conditions. Parameters of interest are shown in Figure 7-5.
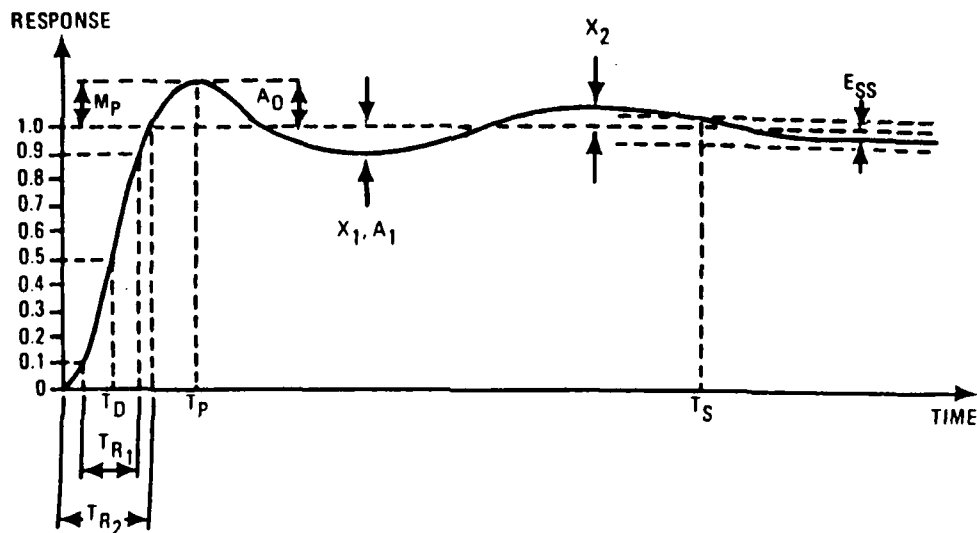

Figure 7-5   Transient Response Criteria

where from Figure 7-5:

T_D = Delay time. It is the time required for the response to reach 50% of it final valve.

T_R = Rise time. It is the time required for the response to reach either 90% (overdamped) or 100% (underdamped) of its final valve.

T_p = Peak time. It is the time required for the response to reach the peak overshoot.

T_s = Settling time. It is the time required for the response to settle within bounds of either 5% or 2%.

M_p = Maximum percent overshoot. It is the peak valve of the response.

E_{ss} = Steady State Error. It is the amount by which the steady state response fails to stabilize on unity.

Reference 34 notes that the subsidence ratio and transient peak ratio are used to determine an effective second-order damping ratio for proposed MIL-H-8501B requirement verification, where for an "ideal second order system" (unit numerator)

$$\frac{X_2}{X_1} = e^{-\frac{\pi}{\sqrt{1 - \zeta^2}}} = \text{Subsidence ratio} \qquad (7\text{-}18)$$

125

$$\frac{A_1}{A_0} = \text{Transient peak ratio (TPR)} = \frac{1 - e^{\left\{-\frac{2\pi}{\sqrt{1 - \rho^2}}\right\}}}{1 + e^{\left\{-\frac{\pi}{\sqrt{1 - \rho^2}}\right\}}} \qquad (7\text{-}19)$$

and

$$\rho = \left[\frac{\left[\ln \frac{X_2}{X_1}\right]^2}{\pi^2 + \left[\ln \frac{X_2}{X_1}\right]^2} \right]^{1/2} \qquad (7\text{-}20)$$

The requirement is to achieve rapid response with minimum overshoot and steady state error. Speed of response is determined by T_D, T_R, and T_P. Accuracy of the response is a function of M_P, T_S, and E_{SS}. Rise time and maximum overshoot requirements conflict with each other and both parameters can not be made smaller at the same time. Again, a compromise is required between speed of response and accuracy of response.
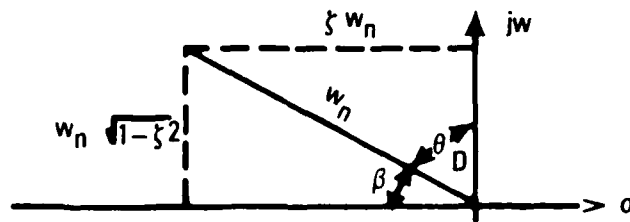
The parameters shown in Figure 7-4 may be picked off of a personal computer generated time response plot. The values may also be calculated for second order systems based on equations presented in References 16 and 17 and summarized in Figure 7-6.

$$T_R = \frac{\pi - \beta}{w_d}$$

Definition of β
(From Reference 16)

$$T_P = \frac{\pi}{w_d}$$

ρ = Damping coefficient

w_n = Undamped natural frequency

$$M_P = e^{-\left[\sqrt{\dfrac{\rho}{1 - \rho^2}}\right]\pi}$$

w_d = Damped natural frequency = $w_n\sqrt{1 - \rho^2}$

= System time constant = $\dfrac{1}{\rho\, w_n}$

$$T_{S2\%} = \frac{4}{\rho\, w_n} \qquad\qquad T_{S\,5\%} = \frac{3}{\rho\, w_n}$$

Figure 7-6   Transient Response Definitions

The transient response relations of Figure 7-6 are valid for second-order systems. The relations also give good approximations for higher order systems that are characterized by a pair of dominant roots. Reference 17 notes that the second order relations can be applied to third order systems as long as the real part of the dominant roots is less than 0.1 of the real part of the third root. Reference 17 also points out that the second order relations are

127

only valid for transfer functions without finite zeros. Finite zeros located near the dominate poles will significantly effect the transient response. For higher order systems or systems without a clearly dominant pair, it is best to let the computer calculate and plot the step response.

5.   Compensation

Compensation can be used to improve the basic helicopter handling qualities including controllability. The type of compensation required will depend on the aircraft mission, the mission environment, and on applicable specification requirements. Specification requirements are generally presented in terms of system accuracy, stability, and/or speed of response. Requirements may be presented in the frequency domain or time domain. Compensators may be added in series with the plant transfer function or they may be added as part of a feedback loop. Reference 16 notes that, in general, series compensation will be simpler than feedback compensation. Series compensators come in the form of lead, lag, or lag-lead networks. These compensators increase the system order.

Compensators are often designed using a trial-and-error approach and iterating until a given specification has been met. The result of the trial-and-error process may only be

a compromise between the relative stability and steady-state error requirement of the system. Compensation design techniques discussed in References 16 and 17 may be used to speed up the process of meeting a given specification. If the specifications are given in the frequency domain (phase margin, gain margin, bandwidth, etc.), it is convenient to use a frequency domain approach like the Bode analysis. It is also convenient to use a frequency domain approach when analyzing special problems like high frequency structural or noise problems. If the specifications are given in time domain (rise time, maximum overshoot, settling time, etc.), it is convenient to use the root locus approach for compensation design. Note that adding zeros to the open-loop transfer function tends to pull the root locus to the left in the S plane making the system more stable. It also tends to speed up the transient response of the system. On the other hand, adding poles to the open-loop transfer function tends to pull the root locus to the right in the S plane making the system less stable.

a. **Lead Networks**. If the compensator is given as:

$$G_c(S) = \frac{K(S + Z)}{S + P} \qquad (7\text{-}21)$$

and if $|Z| < |P|$, the compensator is referred to as a lead compensator. The lead compensator is also referred to as an

approximate differentiator since for $|P|$ much larger than $|Z|$ and $Z \approx 0$, the compensator is expressed as:

$$G_C(S) = \frac{K}{P} S \qquad (7-22)$$

Lead tends to increase the phase on the Bode argument plot, hence the phase margin. Lead can also be used to increase the system bandwidth and hence speed of response. On the other hand, lead, which is basically a high pass filter, tends to reduce the system low frequency gain. Reference 16 points out that a single lead compensator should not be designed to produce more than about 60 degrees phase lead because of the resulting high system gain requirements. Lead compensators may be used in series if more than 60 degrees phase lead is required. Reference 16 also notes that if the slope of the system open loop Bode phase angle plot decreases rapidly near the gain crossover frequency, lead compensation becomes ineffective.

    b. **Lag Networks.** If the compensator is given as:

$$G_C(S) = \frac{P}{Z} \frac{(S + Z)}{(S + P)} \quad \text{with } |Z| > |P| \qquad (7-23)$$

it is referred to as a lag compensator. The factor P/Z is the gain adjustment. If a system has satisfactory transient response but poor steady-state characteristics, a lag

network may be required. The lag compensator is also referred to as an approximate integrator or low-pass filter. It passes low frequencies, thus permitting high gains which reduce steady-state errors. A lag network attenuates at high frequencies and will shift the gain crossover frequency to a lower frequency. The gain crossover frequency shift is accomplished with only a small change in the phase angle plot at the crossover frequency. The lower crossover frequency will thus have an increased phase margin. In the S plane, the pole and zero of the lag compensator are placed close to the origin. This means that the net root locus angle contribution from the pole and zero will be very small ($\leq$ 5 degrees, Reference 16) and the system transient response will be effectively unchanged.

c. **Lag-Lead Networks.** If the compensator is given as:

$$G_c(S) = \frac{(S + Z_1)\ (S + Z_2)}{(S + P_1)\ (S + P_2)} \quad \text{where } |P_1| > |P_2| \quad (7\text{-}24)$$

with $Z_1 Z_2 = P_1 P_2$ for implementation, the compensator is referred to as a lag-lead compensator. A lag-lead compensator can be used for improvements in both the transient and steady-state response. The lag-lead compensator combines the advantages of both lead and lag networks into a single network, and results in:

131

- Increased phase margin (stability)

- Increased bandwidth (speed of response)

- Reduced steady-state error (increased low frequency gain)

- Reduced high frequency noise and structure problems

d. **Notch Filters.** Notch filters are sometimes used on modern helicopters with digital flight control systems to eliminate high frequency resonance problems. The resonance problems would otherwise require modification of the aircraft control flight system or aircraft basic structure. Reference 21 describes a resonant problem with the UH-60A Advanced Digital Optical Control System (ADOCS) program during forward flight climbs and descents. High aircraft structural vibration would feed through the pilot's arm into the multi-axis side-stick controller (SCC) and result in pilot induced oscillations (PIO). The pilot/airframe coupling was documented as occurring at 6.5, 6.34, and 5.8 Hz in the collective, directional, and longitudinal axes, respectively. Digital notch filters were used to eliminate the PIO tendencies. A notch filter has the basic form:

$$G_c(S) = \frac{(S^2 + 2\zeta_n w_n S + w_n^2)(s + a)}{(S^2 + 2\zeta_d w_n S + w_n^2)(s + a)} \qquad (7\text{-}25)$$

132

where

W_n is the frequency to be eliminated

ζ_n is the numerator damping coefficient

ζ_d is the denominator damping coefficient

  a is the break frequency of the first order term
used to give the filter TF a -20 db/dec slope
$(a \approx 3\ W_n)$

$\dfrac{\zeta_n}{\zeta_d}$ determines the height of the notch

A notch filter can be easily implemented on personal computer programs like Program CC using a low value for ζ_n (for example, 0.001), a nominal value for ζ_d of 0.5, and setting $a = 3W_n$ so it would not have any effect on the area of interest. The notch filter increases the order of the system and the system cost. Also, if the resonant frequency (W_R) varies as a function of operating condition, then W_n would have to track W_R for the notch filter to work. A wide notch or band-reject filter would work for some variation in W_n, but this type filter system would be relatively complex.

6. Example Using Analytical Procedures

The analytical procedures used for a specific AFCS problem will depend on the problem requirements, problem information available, and available analysis equipment. Consider the open loop transfer function presented in equation 7-26.

133

$$G(S) = \frac{150\,(S + 2)}{S(S + 10)(S^2 + 4S + 16)} \qquad (7\text{-}26)$$

The closed loop transfer function can be expressed as

$$\frac{C(S)}{R(S)} = \frac{G(S)}{1 + G(S)} = \frac{150(S + 2)}{S^4 + 14S^3 + 56S^2 + 310S + 300} \qquad (7\text{-}27)$$

From equation 7-27, the characteristic equation 1 + G(S) is

$$CE = S^4 + 14S^3 + 56S^2 + 310S + 300 = 0 \qquad (7\text{-}28)$$

Figure 7-7 presents the roots of equation 7-28, and shows that the closed loop system is stable. The Routh criteria can also be used, as shown in Figure 7-8, to calculate the stable range of gains (0 to 2.36) for the transfer function.
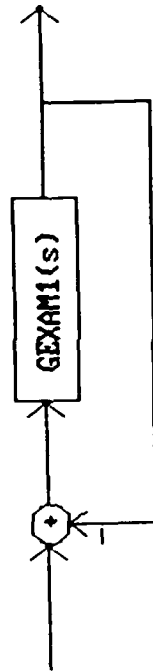
Equation 7-26 can be expressed as

$$G(S) = \frac{150k(S + 2)}{S(S + 10)(S + 2 + j3.464)(S + 2 - j3.464)} \qquad (7\text{-}29)$$

which is suitable for root locus hand sketches or computer plots, as shown in Figure 7-9. Information on root locus plot construction is shown in Figure 7-10.

In the frequency domain, equation 7-26 can be expressed as

$$G(jw) = \frac{150(jw + 2)}{jw(jw + 10)((jw)^2 + 4jw + 16)} \qquad (7\text{-}30)$$

CC>stability,gexam1

Closed loop characteristic polynomial:

$$p(s) = s^4 + 14s^3 + 56s^2 + 310s + 300$$

ZEROS: -1.1414069680907169
        -11.2616424492б846
        -.7984752949121861   +j 4.7645842472273987
        -.7984752949121861   -j 4.7645842472273987

The analog closed loop system is STABLE

Figure 7-7 Stability of Transfer Function (TF) GEXAM1

135

CC>dis,gexam1

$$GEXAM1(s) = \frac{150(s +2)}{s(s +10)(s^2 +4s +16)}$$

CC>routh,gexam1

Stable for gain ranges : 0 to 2.360126

Figure 7-8   Routh Criteria for TF GEXAM1

136

$$\text{GEXAM1} = k_{RL} \frac{150(s + 2)}{s(s + 10)(s^2 + 4s + 16)}$$

ROOT LOCUS FOR TF GEXAM1

k = 2.36
Closed loop poles:
-5.71923SE-05 -j 6.059243
-5.71923SE-05 +j 6.059243
-12.45111
-1.548775

k_{RL} = 2.36

Real s
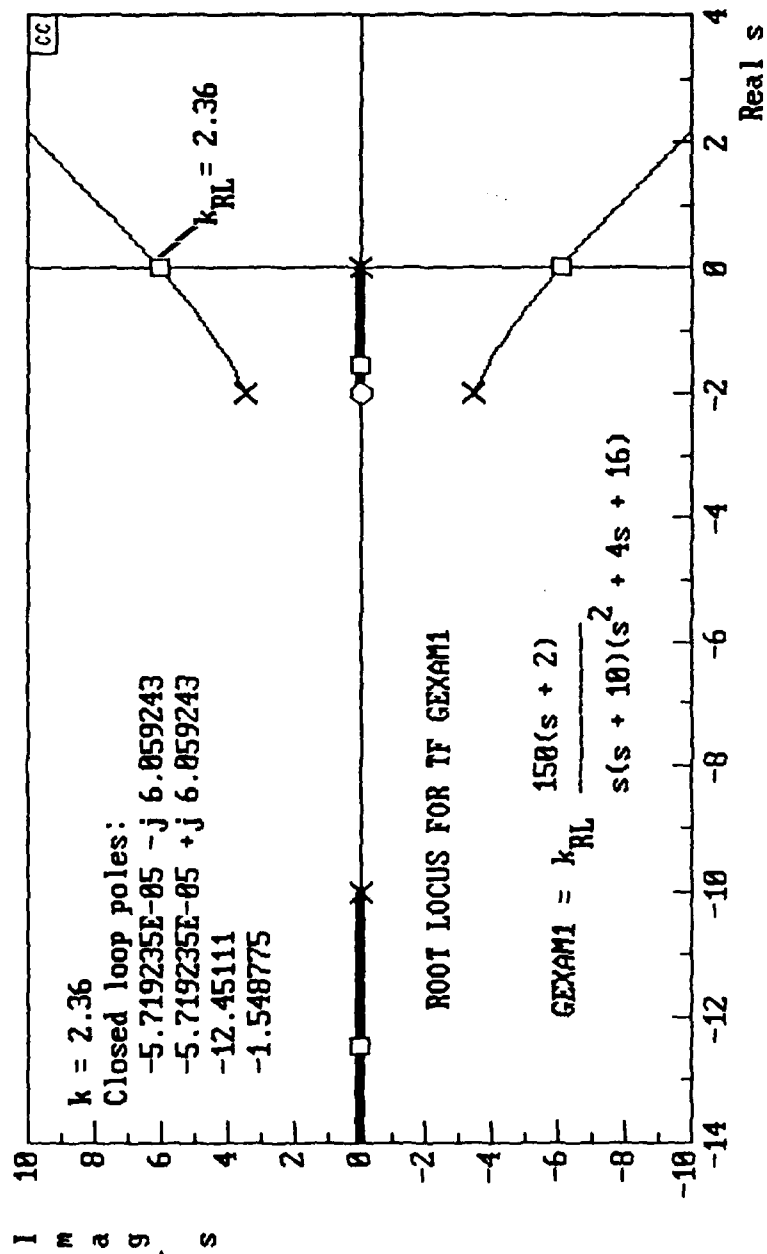
Figure 7-9 Root Locus Plot for TF GEXAM1

Open loop poles, Angle of departure

0	-180
-10	-180
-2 +j 3.464102	36.6
-2 -j 3.464102	-36.6

Center of gravity = -4
Asymptotic infinite patterns = 3
Angles :-60 60 180

Open loop zeros, Angle of arrival

-2	0

Breakpoints, Gain

None

ROOT LOCUS PLOTTING INFORMATION FOR TF GEXAM1

$$GEXAM1 = \frac{150(s + 2)}{s(s + 10)(s^2 + 4s + 16)}$$

Figure 7-10 Root Locus Plotting Information for TF GEXAM1

138

CC

and, in Bode form, equation 7-30 becomes

$$G(jw) = \frac{150(2)}{(10)(16)} \frac{(jw/2 + 1)}{jw(jw/10 + 1)[-(w/4)^2 + jw/4 + 1]} \quad (7\text{-}31)$$

where $\dfrac{150(2)}{(10)(16)} = 1.875 \equiv K_B =$ Bode gain and in decibels

$$K_B = 20\log_{10} 1.875 = 5.46 \text{ db}$$

Using equation 7-31 and Table 7-1, the Bode magnitude and phase plots for the individual transfer function terms can be sketched as shown in Figures 7-11 and 7-12. Note that the break points on the phase plot, Figure 7-12, occur at frequencies $(.2)(1/T)$ and $(5)(1/T)$ where from Table 7-1, $w = 1/T$. It is easier and more accurate to sketch the Bode phase using designed plotting templates. The individual Bode plot magnitude and phase components are added together for the composite plots. The Bode composite plot shown in Figure 7-13 can be readily constructed if tabular data on the magnitude and phase as a function of frequency is available. Tabular Bode data for composite plots can be generated by either hand calculator or PC programs as shown in Table 7-2.

A PC program, like Program CC, can be used to supplement the standard root locus and Bode plots with siggy and Bode root locus plots, as shown in Figure 7-14.
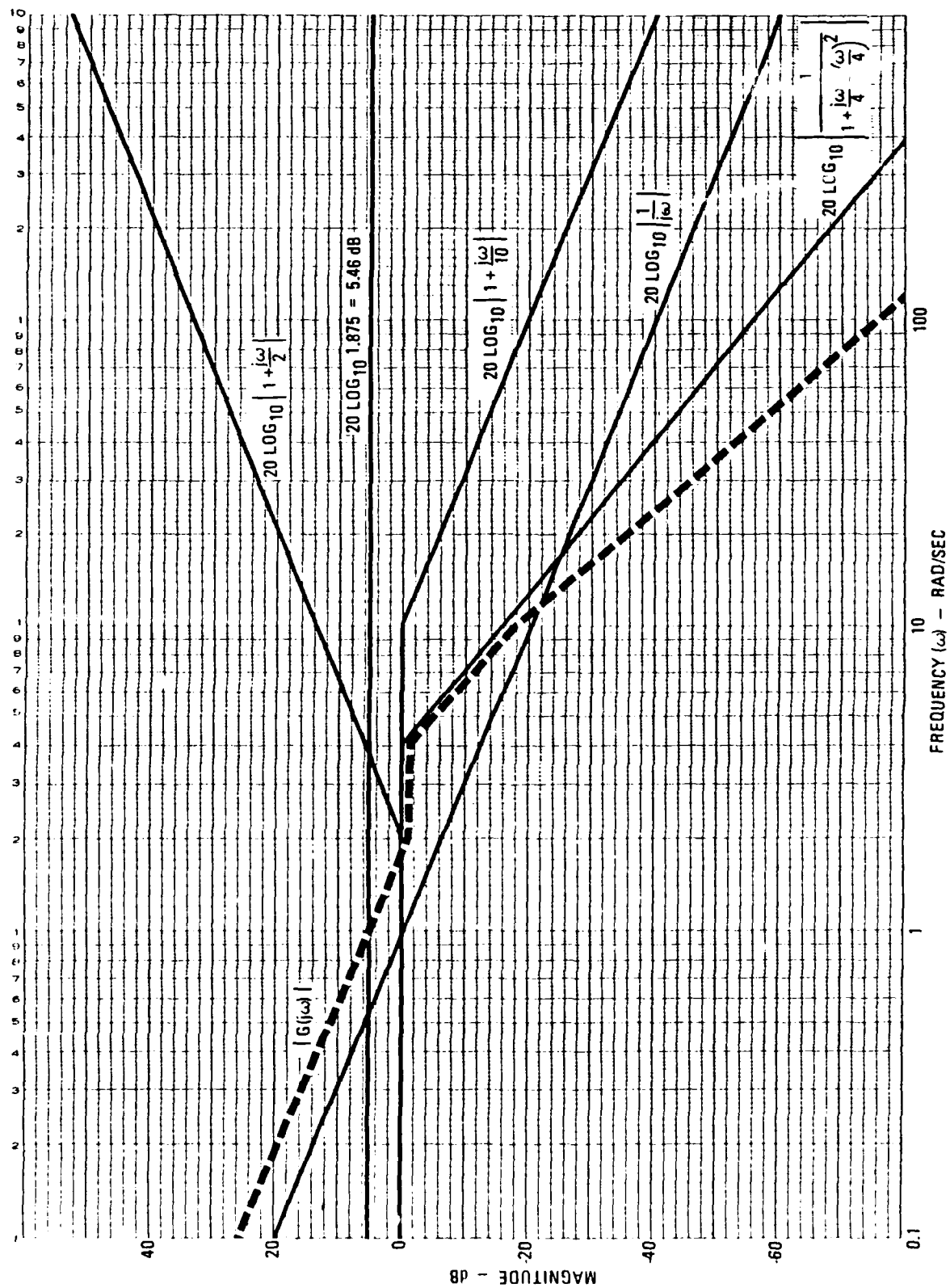
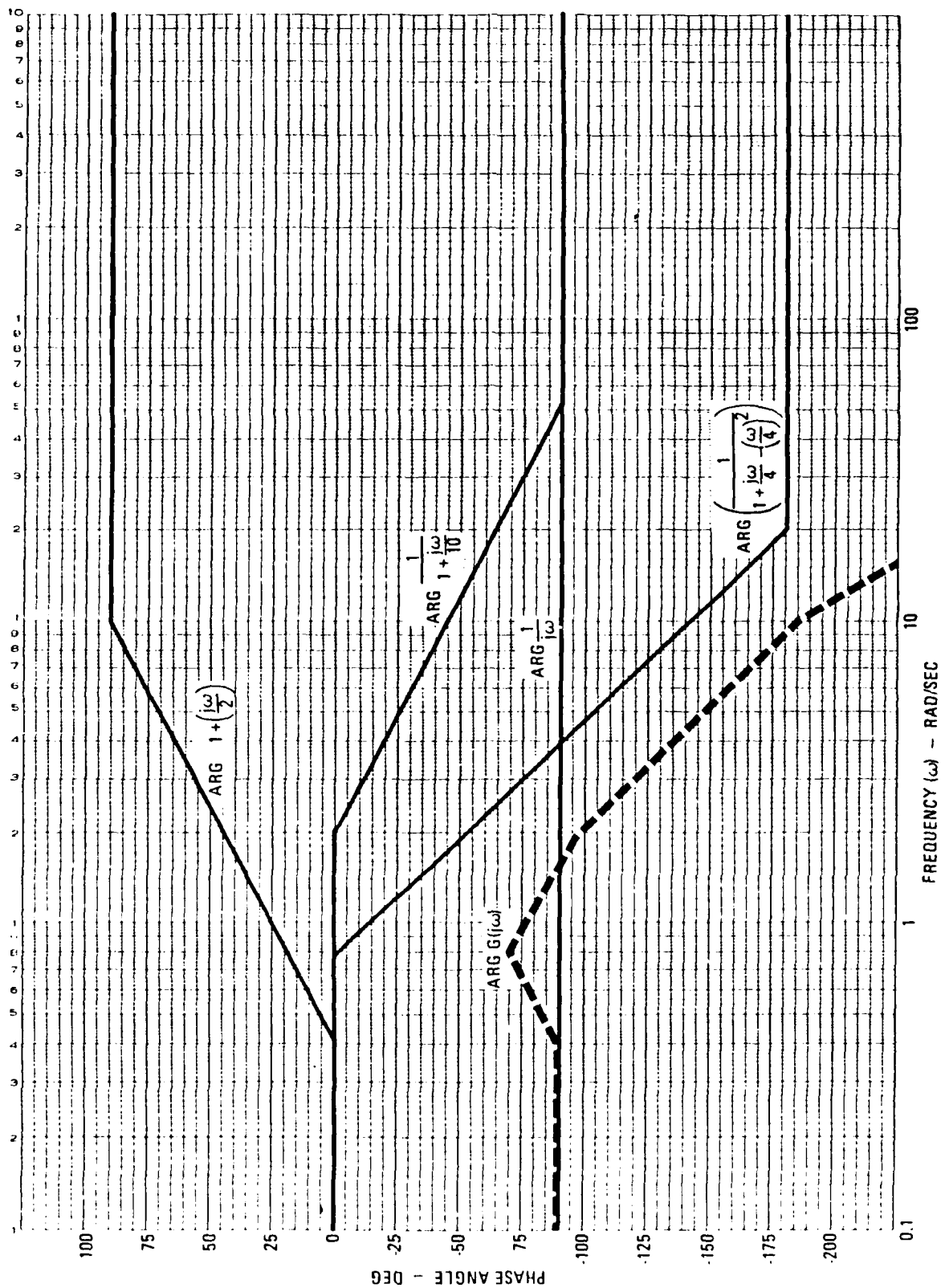Figure 7-11 Bode Magnitude Plot for TF GEXAM1
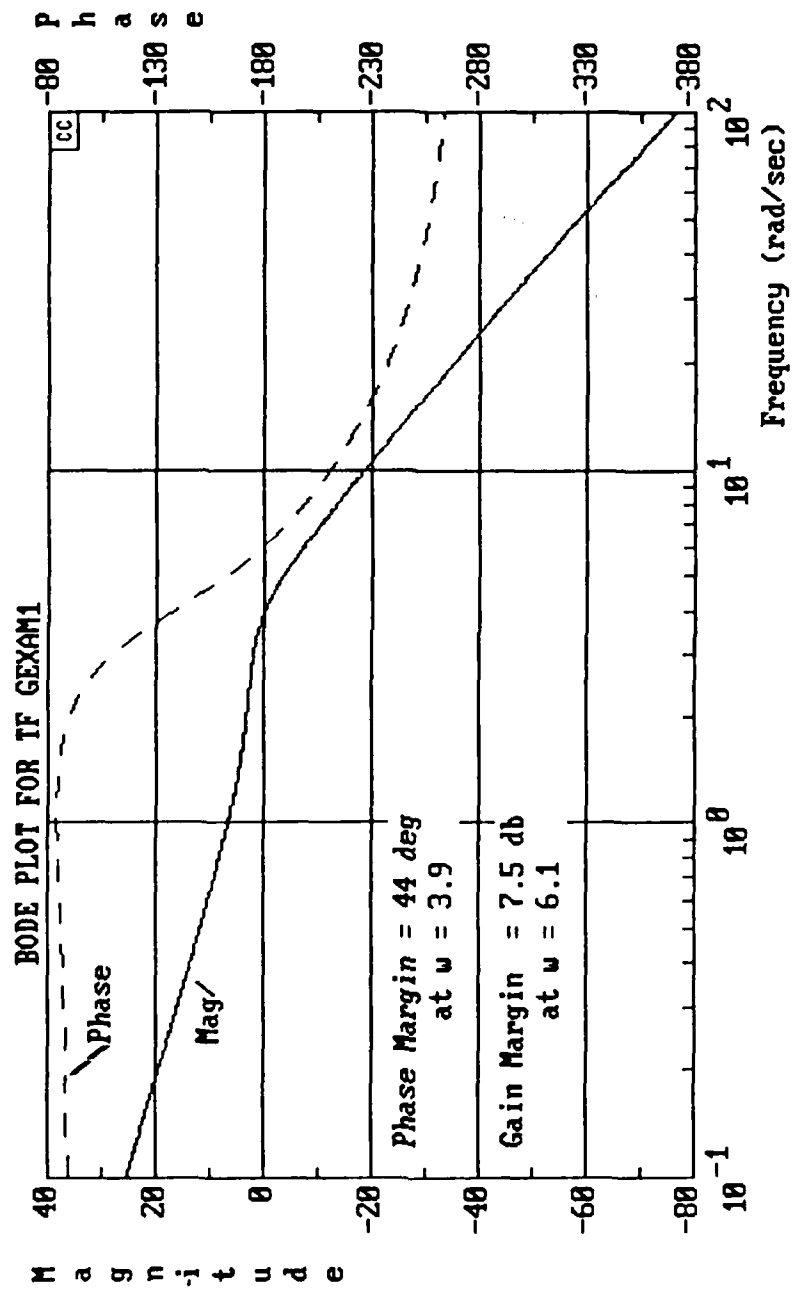
140

Figure 7-12   Bode Phase Plot for TF GEXAM1

141

Figure 7-13 Bode Magnitude and Phase Plot for TF GEXAM1

142

TABLE 7-2
TABULAR DATA FOR TF GEXAM1

| (index)	(real)	(imag)	(magnitude)	(phase)
1.000000E-01	2.806942E-01	-1.877625E+01	1.877835E+01	-89.1435
1.124210E-01	2.805474E-01	-1.670789E+01	1.671025E+01	-89.0380
1.263848E-01	2.803618E-01	-1.486882E+01	1.487146E+01	-88.9198
1.420831E-01	2.801271E-01	-1.323381E+01	1.323677E+01	-88.7874
1.597312E-01	2.798303E-01	-1.178041E+01	1.178373E+01	-88.6393
1.795714E-01	2.794549E-01	-1.048867E+01	1.049239E+01	-88.4738
2.018760E-01	2.789799E-01	-9.340886E+00	9.345051E+00	-88.2893
2.269510E-01	2.783788E-01	-8.321289E+00	8.325944E+00	-88.0839
2.551406E-01	2.776178E-01	-7.415891E+00	7.421086E+00	-87.8561
2.868317E-01	2.766540E-01	-6.612268E+00	6.618053E+00	-87.6042
3.224590E-01	2.754327E-01	-5.899394E+00	5.905820E+00	-87.3269
3.625117E-01	2.738840E-01	-5.267486E+00	5.274601E+00	-87.0236
4.075393E-01	2.719183E-01	-4.707873E+00	4.715719E+00	-86.6944
4.581597E-01	2.694207E-01	-4.212879E+00	4.221485E+00	-86.3408
5.150678E-01	2.662430E-01	-3.775714E+00	3.785089E+00	-85.9665
5.790443E-01	2.621930E-01	-3.390381E+00	3.400504E+00	-85.5779
6.509675E-01	2.570203E-01	-3.051594E+00	3.062399E+00	-85.1856
7.318242E-01	2.503963E-01	-2.754705E+00	2.766062E+00	-84.8062
8.227240E-01	2.418863E-01	-2.495632E+00	2.507327E+00	-84.4640
9.249147E-01	2.309105E-01	-2.270800E+00	2.282510E+00	-84.1937
1.039798E+00	2.166873E-01	-2.077068E+00	2.088340E+00	-84.0442
1.168952E+00	1.981530E-01	-1.911660E+00	1.921902E+00	-84.0821
1.314147E+00	1.738474E-01	-1.772053E+00	1.780560E+00	-84.3969
1.477378E+00	1.417527E-01	-1.655811E+00	1.661867E+00	-85.1069
1.660883E+00	9.908534E-02	-1.560289E+00	1.563432E+00	-86.3663
1.867181E+00	4.206735E-02	-1.482089E+00	1.482686E+00	-88.3742
2.099103E+00	-3.417824E-02	-1.416059E+00	1.416471E+00	-91.3826
2.359833E+00	-1.351571E-01	-1.353575E+00	1.360306E+00	-95.7022
2.652948E+00	-2.648207E-01	-1.280108E+00	1.307213E+00	-101.6881
2.982471E+00	-4.196804E-01	-1.173653E+00	1.246432E+00	-109.6763
3.352923E+00	-5.786535E-01	-1.009601E+00	1.163673E+00	-119.8192
3.769390E+00	-6.978730E-01	-7.798007E-01	1.046478E+00	-131.8266
4.237586E+00	-7.315363E-01	-5.157103E-01	8.950433E-01	-144.8174
4.763937E+00	-6.723114E-01	-2.770371E-01	7.271535E-01	-157.6051
5.355667E+00	-5.570635E-01	-1.054911E-01	5.669640E-01	-169.2769
6.020894E+00	-4.303148E-01	-3.857021E-03	4.303321E-01	-179.4865
6.768749E+00	-3.182336E-01	4.649645E-02	3.216124E-01	-188.3125
7.609496E+00	-2.290713E-01	6.569319E-02	2.383050E-01	-196.0019
8.554670E+00	-1.619230E-01	6.809247E-02	1.756577E-01	-202.8079
9.617247E+00	-1.128784E-01	6.239277E-02	1.289744E-01	-208.9313
1.081181E+01	-7.775090E-02	5.346148E-02	9.435747E-02	-214.5124
1.215474E+01	-5.296324E-02	4.388044E-02	6.877934E-02	-219.6420
1.366448E+01	-3.569926E-02	3.493020E-02	4.994553E-02	-224.3761
1.536175E+01	-2.382343E-02	2.716405E-02	3.613089E-02	-228.7486
1.726983E+01	-1.575100E-02	2.073652E-02	2.604030E-02	-232.7805
1.941492E+01	-1.032586E-02	1.559316E-02	1.870214E-02	-236.4873
2.182644E+01	-6.718243E-03	1.158142E-02	1.338895E-02	-239.8825
2.453751E+01	-4.342167E-03	8.514652E-03	9.557914E-03	-242.9800
2.758531E+01	-2.790507E-03	6.207800E-03	6.806152E-03	-245.7953
3.101168E+01	-1.784694E-03	4.495016E-03	4.836352E-03	-248.3450
3.486365E+01	-1.136820E-03	3.236659E-03	3.430499E-03	-250.6471
3.919406E+01	-7.217216E-04	2.320022E-03	2.429688E-03	-252.7199
4.406236E+01	-4.569385E-04	1.656890E-03	1.718743E-03	-254.5822
4.953534E+01	-2.886541E-04	1.179811E-03	1.214609E-03	-256.2520
5.568813E+01	-1.820175E-04	8.381110E-04	8.576481E-04	-257.7470
6.260516E+01	-1.146083E-04	5.942452E-04	6.051962E-04	-259.0837
7.038134E+01	-7.207954E-05	4.206991E-04	4.268292E-04	-260.2777
7.912340E+01	-4.528991E-05	2.974764E-04	3.009043E-04	-261.3434
8.895133E+01	-2.843583E-05	2.101430E-04	2.120582E-04	-262.2937
9.999997E+01	-1.784318E-05	1.483356E-04	1.494049E-04	-263.1409

143
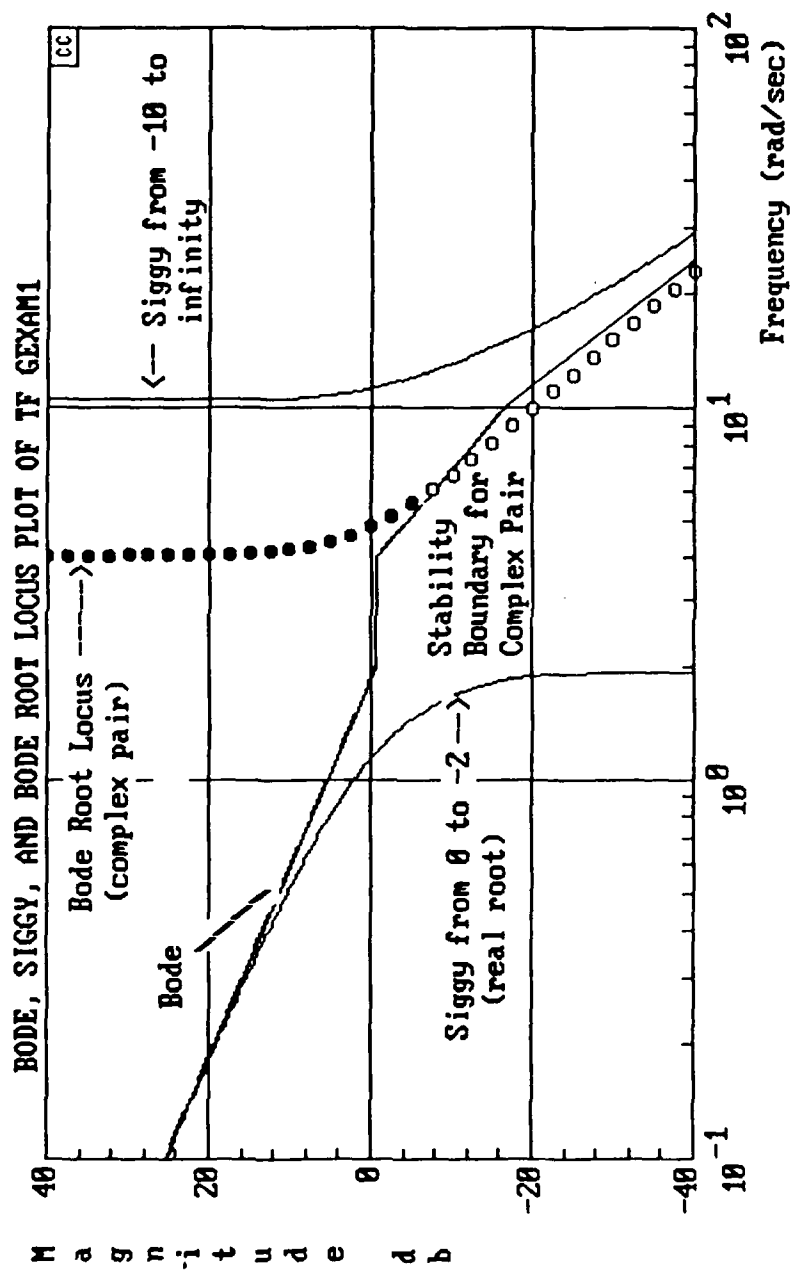
Figure 7-14   Bode, Siggy, and Bode Root Locus for TF GEXAM1

The tabular magnitude and phase data as a function of frequency can also be used to construct Nyquist and Nichols plots as shown in Figures 7-15 through 7-17. Note that the phase margin (44 deg) and the gain margin (7.5 db) from all the frequency response methods agree.

The transient response to a closed loop unit step input is shown in Figure 7-18. Values for each oscillation are tabulated so that transient response criteria can be calculated.
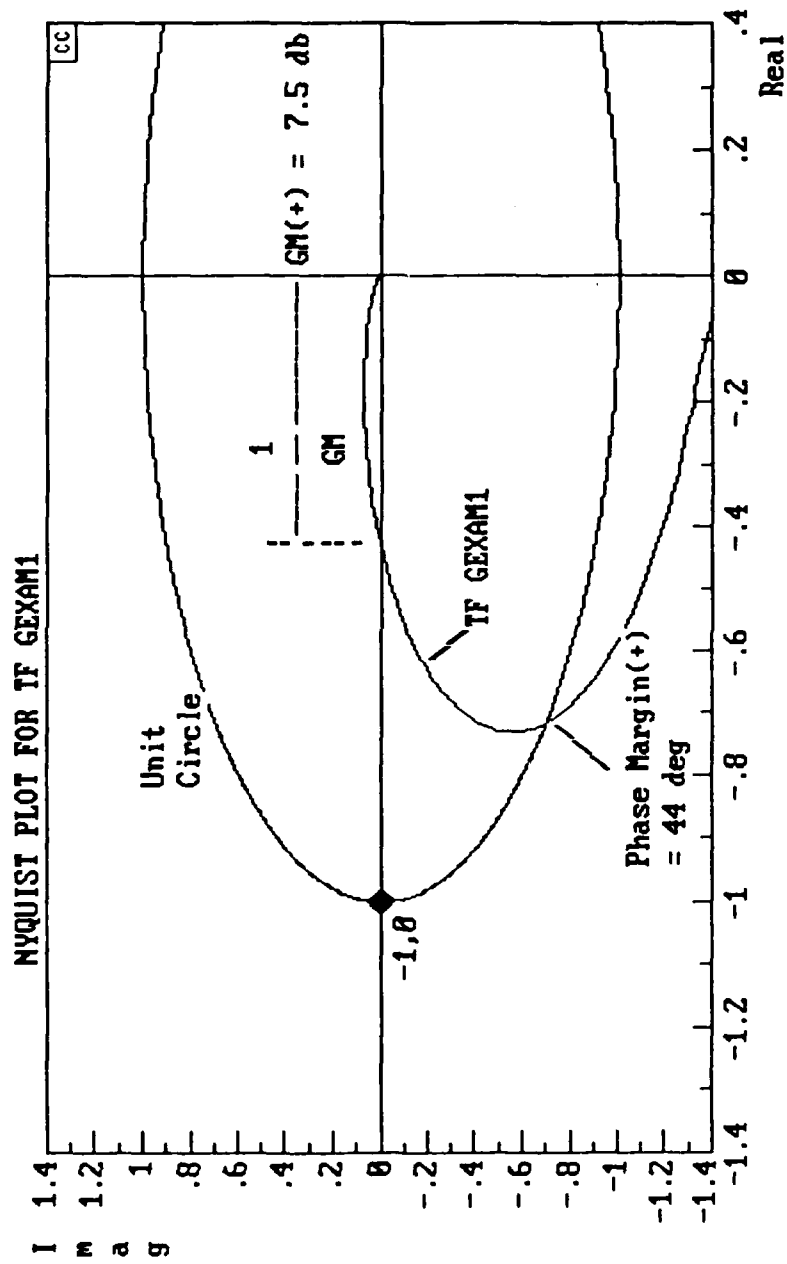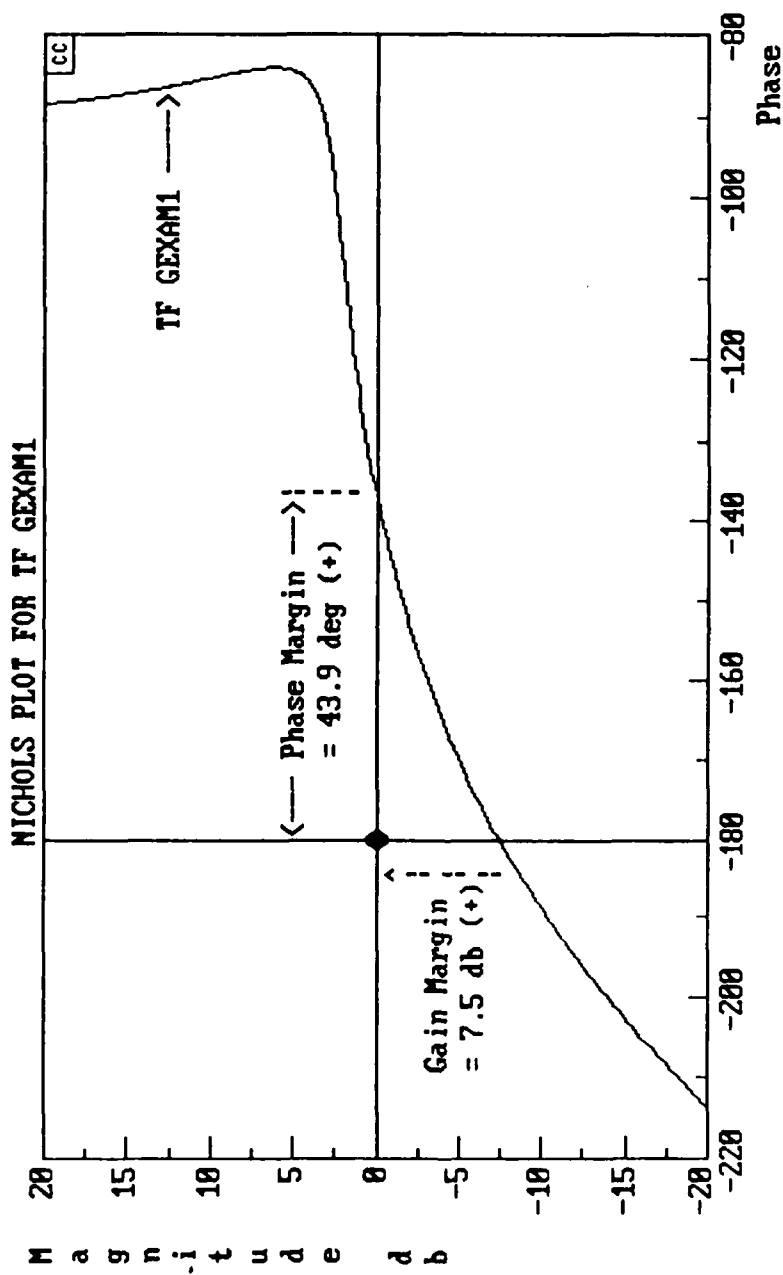
Figure 7-15 Nyquist Plot for TF GEXAM1
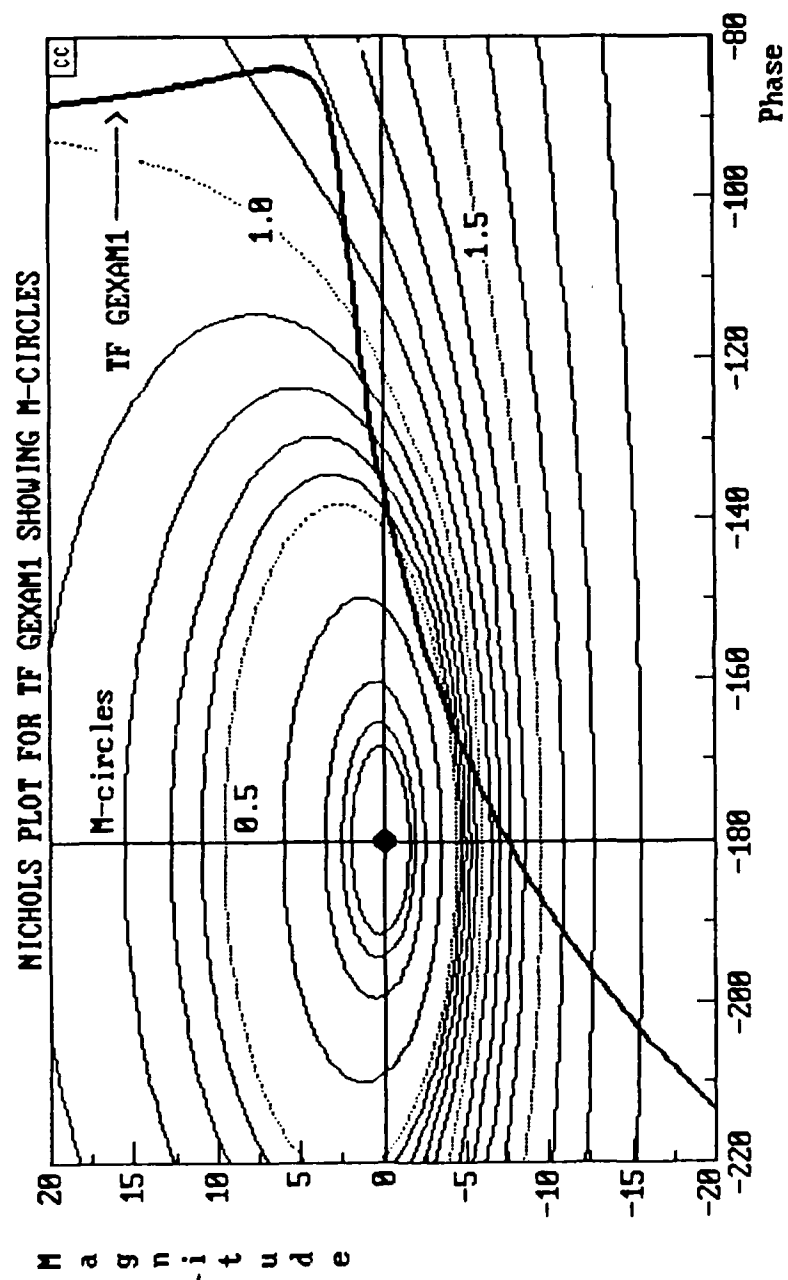
Figure 7-16 Nichols Plot for TF GEXAM1

147

Figure 7-17   Nichols Plot for TF GEXAM1 Showing Constant
Magnitude M-Circles

TF GEXAM1 RESPONSE TO UNIT STEP INPUT (CLOSED LOOP)

Number	Time	Amplitude
1	.83	1.11
2	1.39	.725
3	2.10	1.06
4	2.76	.916
5	3.42	1.03
6	4.09	.973
7	4.76	1.01

Time

Output

1.2
1
.8
.6
.4
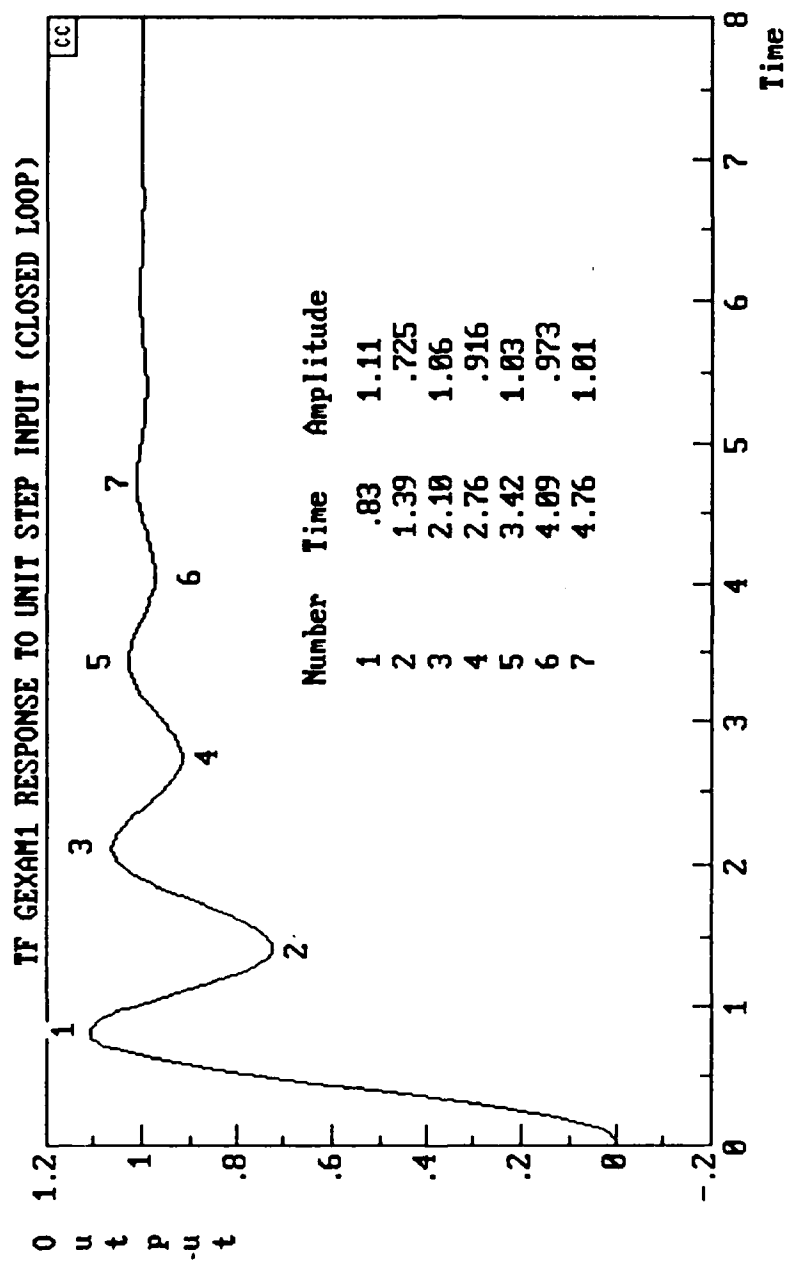.2
0
-.2

0 1 2 3 4 5 6 7 8

Figure 7-18 Time Response to Unit Step Input for TF GEXAM1

C. SIMULATION

Simulation can be used to evaluate the feasibility of an automatic AFCS design, to determine control system design enhancements, and to verify that the system is ready for flight test. The process starts with a good understanding of the physical system or helicopter to be simulated, including mission requirements and state-of-the-art AFCS design options. A mathematical model of the basic helicopter or plant is next developed/acquired and its stability requirements for the mission evaluated. System analysis can be performed using time history and frequency response matching in conjunction with the analytical graphical procedures discussed previously. Following the analysis of the basic helicopter stability requirements, the compensator or AFCS is added to the model. The system analysis process is repeated and the results compared to the design requirements. If the design requirements are met analytically the model should be implemented on a flight simulator to get qualitative pilot opinions of the system. This evaluation should include looking at any flight control failure modes or safety-of-flight items. Following the successful completion of the piloted simulation, a flight test program is the next step.

D. FLIGHT TEST

Flight testing is the final stage in the validation of an helicopter AFCS before it reaches the intended user. The length and scope of the flight test program will depend heavily on the thoroughness of the work accomplished during the analysis and simulation testing. Test team members should be familiar with the design specification requirements, AFCS system simulation results (especially failure analysis and lessons learned data), and basic aircraft flying qualities, performance, and mission requirements.

The initial test effort should focus on a human factors evaluation, including the AFCS cockpit layout, switch functions, and cockpit lighting. Prior to flight, an electromagnetic interference/vulnerability (EMI/EMV) evaluation should be conducted to verify that the AFCS does not interfere with other aircraft systems and vice versa.

The AFCS test aircraft should have a standard AFCS configuration and should have instrumentation to measure basic unaugmented FQ&P parameters plus AFCS switch and actuator positions. Testing should include the following:

- Basic switching transients and failure analysis
- Short term system performance
- Frequency sweeps

151

• Mission related tasks

• Reliability/Maintainability analysis

Switching the AFCS, or any channel/function of the AFCS, ON, or OFF should not produce undesirable transients. Failure possibilities in the form of rapid actuator hardovers, rate-limited hardovers, and oscillatory hardovers should be analyzed. Testing should be conducted using a gradual build-up in amplitude of the actuator hardover as set with a control input box. The aircraft response to the programmed actuator hardover should be recorded and evaluated in terms of mission accomplishment and specification compliance.

Short term system performance can evaluated using procedures described in helicopter test manuals, like Reference 8. Note that Reference 8 does not specifically address AFCS testing. Step, doublet, and pulse control inputs are commonly used to check the AFCS short term system performance. Aircraft response, with the AFCS engaged, can be compared to specification requirements and evaluated in terms of mission accomplishment. Reference 11 summarizes desirable aircraft response to step inputs in a hover, based on several flight test and simulation studies. The data presentation format, as shown in Figure 7-18, does not specify levels of flying qualities, but is convenient for

quickly evaluating flight test data. Level one handling

qualities (1 < HQR < 3.5) are desired for all mission tasks.

Rotorcraft AFCS test manuals and AFCS specifications which

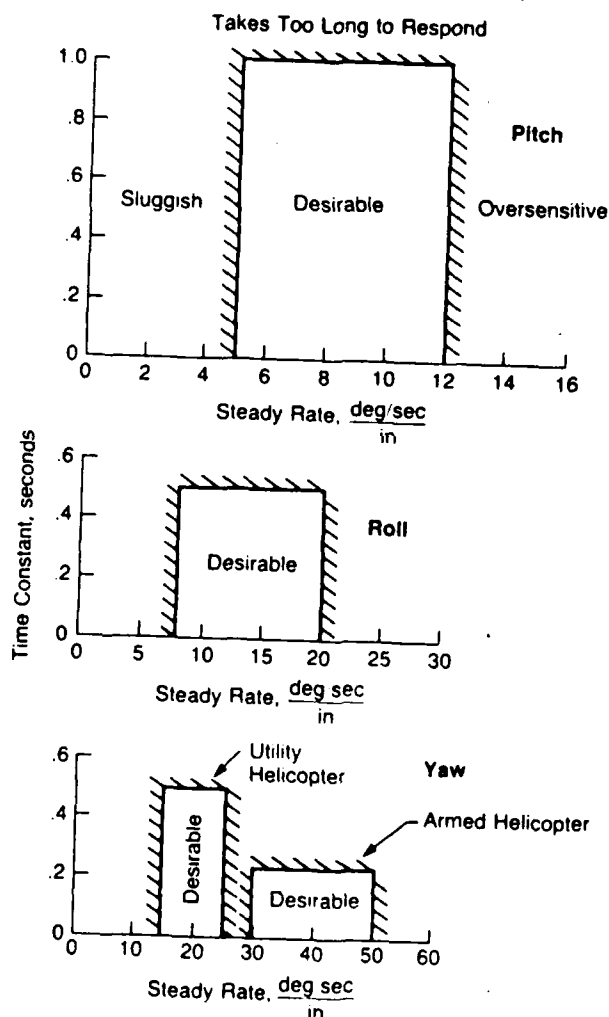reflect state-of-the-art equipment and procedures, are

needed.

Figure 7-18   Aircraft Response Options for Step Input in
Hover (From Reference 11)

Frequency sweeps can be used to evaluate the aircraft AFCS stability, to determine and isolate AFCS lags, to obtain information for parameter identification studies, and to get bandwidth data for the new proposed handling qualities specification. Sinusoidal control inputs of varying frequency can be used for magnitude and phase plots using Bode and/or other formats. Reference 40 describes frequency response testing with the XV-15 aircraft. Reference 34 describes procedures for using frequency sweeps to determine rotorcraft bandwidth for requirements in the proposed handling qualities specification MIL-H-8501B.

Mission-related tasks can be used to evaluate the long term AFCS performance as well as mission suitability. Operational missions may require tasks like long distance navigation or night automatic approach to hover over a point at-sea. Pilots can use the HQR scale presented in Figure 5-5 to evaluate each task and the overall mission.

It is important to keep data on the reliability and maintainability (R&M) of the AFCS both during the test program and during follow-on operational flying. The R&M information can be used to construct a lessons learned database and help prevent the same mistake from occurring twice.

Safety must be paramount in any flight test program. This is especially true for aircraft with high authority digital fly-by-wire flight control systems. Qualified personnel must be assigned at all levels of the program. Careful planning must be conducted, taking advantage of lessons learned from previous programs. Standard test procedures must be utilized, with gradual build-up approaches. Careful monitoring must be performed on all test data. Table 7-3 summarizes some flight safety considerations for AFCS.

TABLE 7-3
FLIGHT SAFETY CONSIDERATIONS
From Lear Siegler, Inc., Brochure

• AS FLIGHT CONTROL SYSTEM AUTHORITY AND AIRCRAFT INSTABILITY INCREASE SO DOES THE

  PROBABILITY THAT ELECTRONIC FAILURES WILL HAVE CATASTROPHIC RESULTS

  – MISSION AND FLIGHT SAFETY DEPEND ON CONTINUOUS, FAILURE-FREE OPERATION

  – FLY-BY-WIRE AIRCRAFT ARE TOTALLY DEPENDENT ON THE FLIGHT CONTROL SYSTEM

• TO ENSURE FLIGHT SAFETY, FLIGHT CONTROL SYSTEMS MUST BE ABLE TO ACCOMMODATE FAILURES

  – "FAIL-SAFE" MEANS THAT FAILURES WILL BE DETECTED AND THE SYSTEM SAFELY DISENGAGED

  – "FAIL-OPERATE" MEANS THAT FAILURES WILL BE DETECTED BUT THE SYSTEM WILL CONTINUE

    TO OPERATE NORMALLY

• FAILURE DETECTION CIRCUITRY IS ESSENTIAL FOR SAFETY

• REDUNDANT COMPUTER CHANNELS DECREASE THE POTENTIAL OF CATASTROPHIC FAILURE

• REDUNDANCY LEVELS DETERMINED BY EITHER OR BOTH OF TWO FACTORS

  – DESIRE FOR EITHER "FAIL-SAFE" OR "FAIL-OPERATE" CHARACTERISTICS

  – LOSS OF MISSION OR LOSS OF AIRCRAFT PROBABILITY REQUIREMENTS

VIII. SIMULATION OF GENERIC HELICOPTER AND AFCS

A. CONTROL INPUT TRANSFER FUNCTIONS

Control input transfer functions can be studied to show basic helicopter stabilization and controllability requirements plus application of the analytical tools discussed previously.

1. Pitch Attitude Feedback - Hover

The feedback of pitch attitude to longitudinal cyclic in a hover is illustrated in the block diagram shown in Figure 8-1.
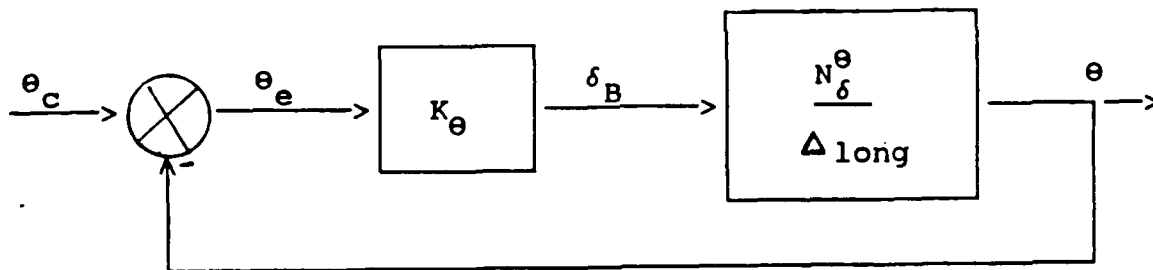

Figure 8-1   Block Diagram Showing Pitch Attitude Feedback to Longitudinal Cyclic in Hover

Recall from equation 4-5 that in a hover, the helicopter plunging mode (w) is uncoupled from airspeed (u) and pitch attitude (Θ). The longitudinal hover cubic was presented as equation 5-3. Using the Reference 12 notation discussed

previously, the open loop pitch attitude to longitudinal control transfer function for a generic single rotor hovering helicopter can be expressed as follows:

$$\frac{N_\delta^\theta}{\text{long}} = \frac{\theta(S)}{\delta_B(S)} = \frac{A_\theta(S + 1/T_\theta)}{(S + 1/T_1)(S^2 + 2\zeta w_n S + w_n^2)} \quad (8\text{-}1)$$

where $\zeta < 0$. Using stability derivatives of Reference 12 for a single rotor helicopter, equation 8-1 becomes

$$\frac{\theta(S)}{\delta_B(S)} = \frac{-6.65(S - .00109)}{(S + .874)(S^2 + (2)(-.25)(.473)S + .473^2)} \quad (8\text{-}2)$$

or

$$\frac{\theta(S)}{-\delta_B(S)} = GLHE1(S) = \frac{6.65(S - .00109)}{(S + .874)(S^2 - .2365S + .22373)} \quad (8\text{-}3)$$

Standard sign convention are used where back stick (+) (or up elevator (-) in fixed wing terms) produces a nose up (+) pitching moment. Equation 8-3 has a relatively low frequency unstable complex pair plus a numerator factor $(1/T_\theta)$ close to the origin and in the right hand plane. The open loop system is thus unstable and is characterized by a divergent oscillation as shown in Figure 8-2. Feeding back pitch attitude can stabilize the system as shown in the Figure 8-3 root locus plot. This effect of pitch attitude in stabilizing the aircraft may help explain the reason for
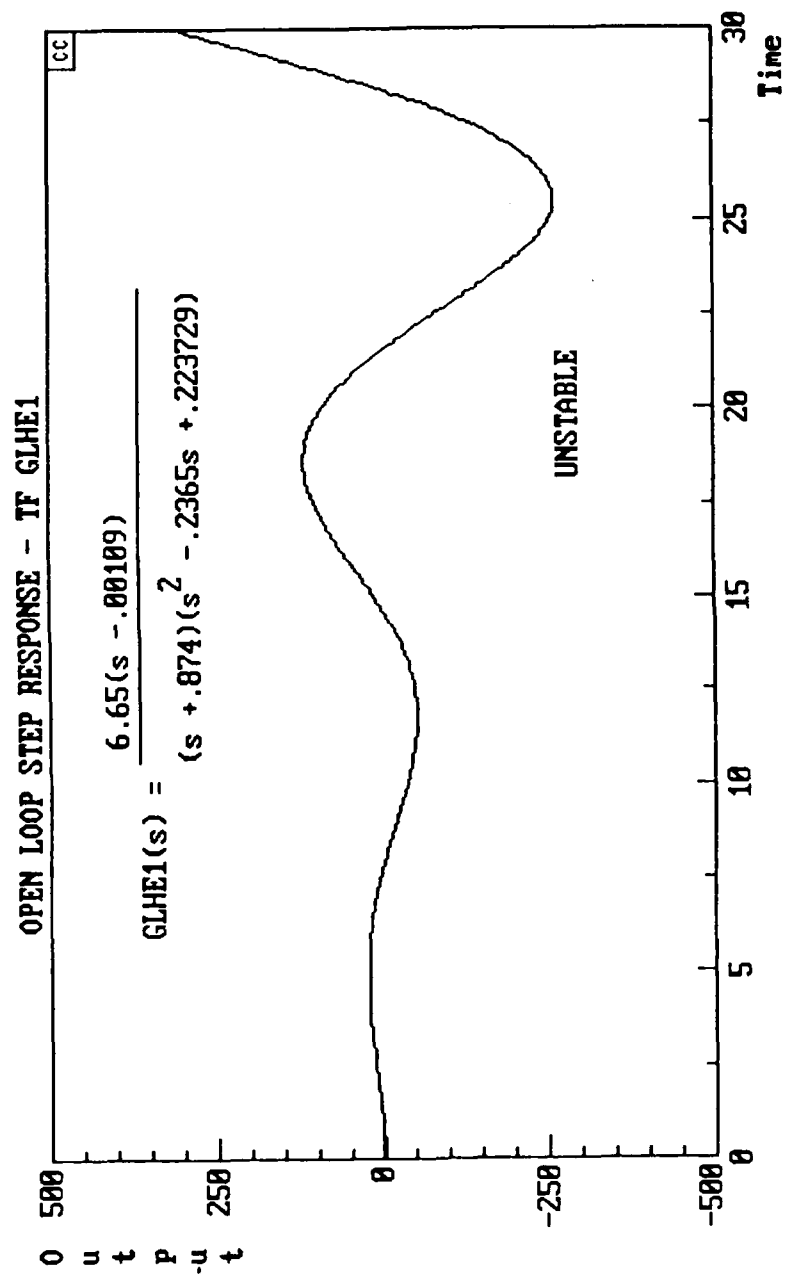
OPEN LOOP STEP RESPONSE - TF GLHE1

$$GLHE1(s) = \frac{6.65(s - .00109)}{(s + .874)(s^2 - .2365s + .223729)}$$

UNSTABLE

Figure 8-2 Open Loop Step Response for TF GLHE1

159

ROOT LOCUS PLOT FOR TF GLHE1

SHOWS CLOSED LOOP ROOTS
FOR TWO VALUES OF ROOT
LOCUS GAIN

$k_{RL2} = .1584 \longrightarrow$

$k_{RL1} = .1814 \longrightarrow$

k_{RL1} k_{RL2}

$$GLHE1 = \frac{k_{RL} \; 6.65 \; (s - .00109)}{(s + .874)(s^2 - .2365s + .223729)}$$

Real s

Imag s

1.5
1.25
1
.75
.5
.25
0
-.25
-.5
-.75
-1
-1.25
-1.5

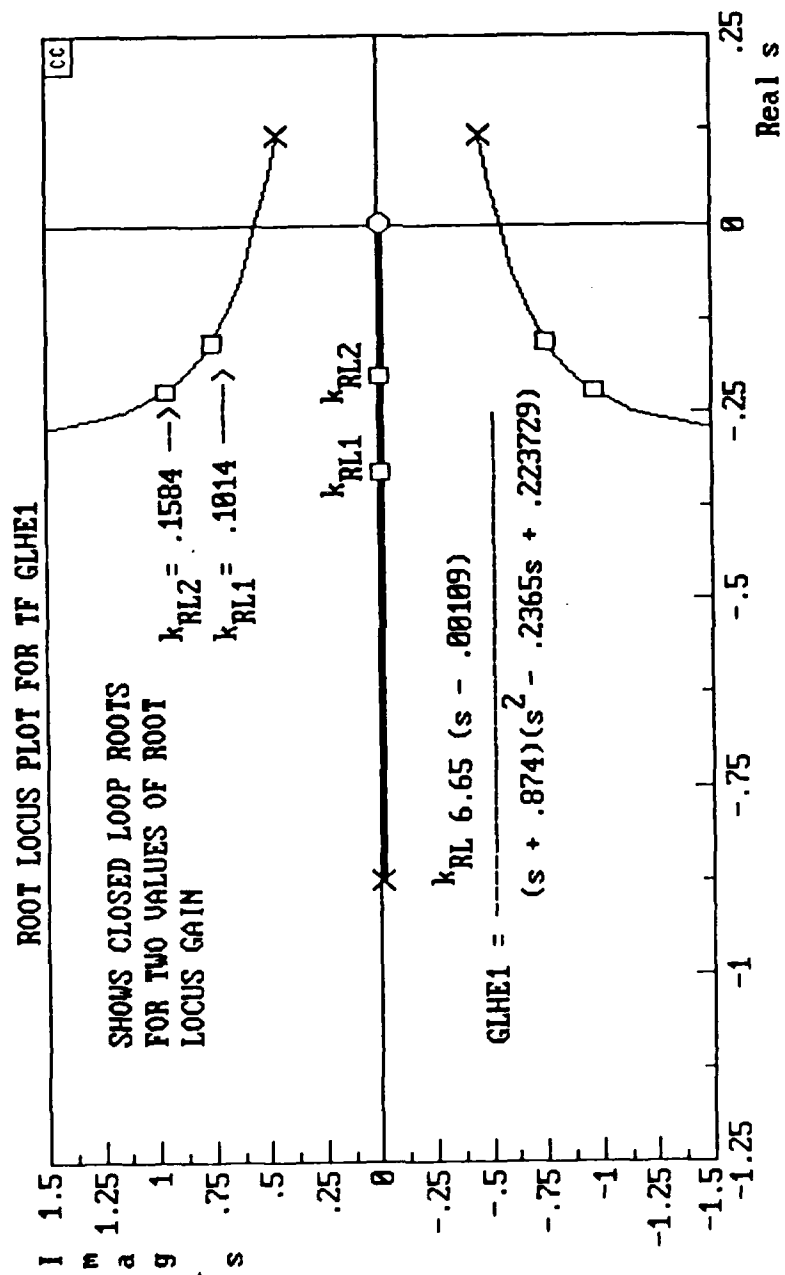-1.25   -1   -.75   -.5   -.25   0   .25

cc

Figure 8-3   Root Locus Plot for TF GLHE1

160

large attitude indicators commonly seen in helicopters. If
the root locus gain is increased above $k = 27$, the system
becomes unstable. The instability is caused by a closed
loop root crossing into the right half S plane as it ap-
proaches the open loop zero, as shown in Figure 8-4. Also
note that with attitude feedback alone it is not possible to
get a damping ratio greater than approximately $\zeta = .225$ for
the complex pair as shown in Figure 8-5.

Reference 12 notes that both pitch attitude and pitch
rate feedback are required for most helicopters and VTOL
aircraft, as shown in Figure 8-6.
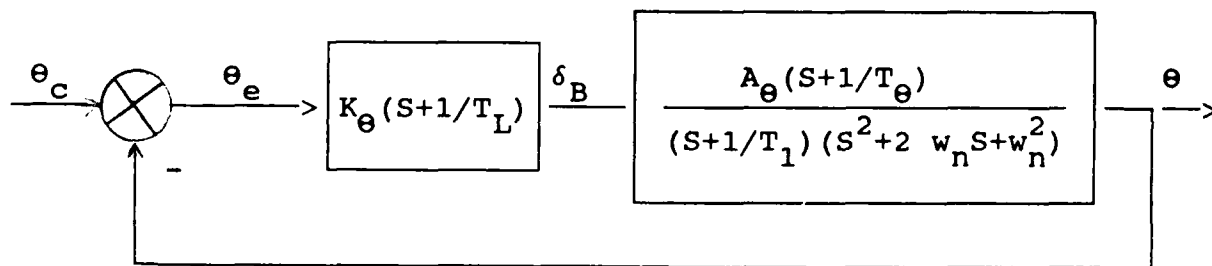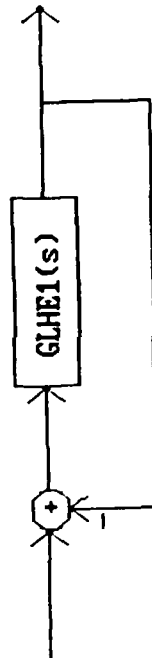

Figure 8-6   Block Diagram Showing Pitch Attitude and Pitch
             Rate Feedback to Longitudinal Cyclic in Hover

For simplicity, we let $1/T_L = 1/T_1 = -.874$, $K_\theta = 1$, and
$G_1 = GLHE1(S + .874)$.   The equivalent open loop transfer
function becomes

$$GLHE1(s) = \frac{6.65(s - .00109)}{(s + .874)(s^2 - .2365s + .223729)}$$

CC>STABILITY,GLHE1

Closed loop characteristic polynomial:

$$p(s) = s^3 + .6375s^2 + 6.667028s + .1882906$$

ZEROS: -2.831532497845312D-02
         -.3045923375107734   +j 2.560664414929179
         -.3045923375107734   -j 2.560664414929179

The analog closed loop system is STABLE
for gain ranges : 4.348956E-02 to 26.9765
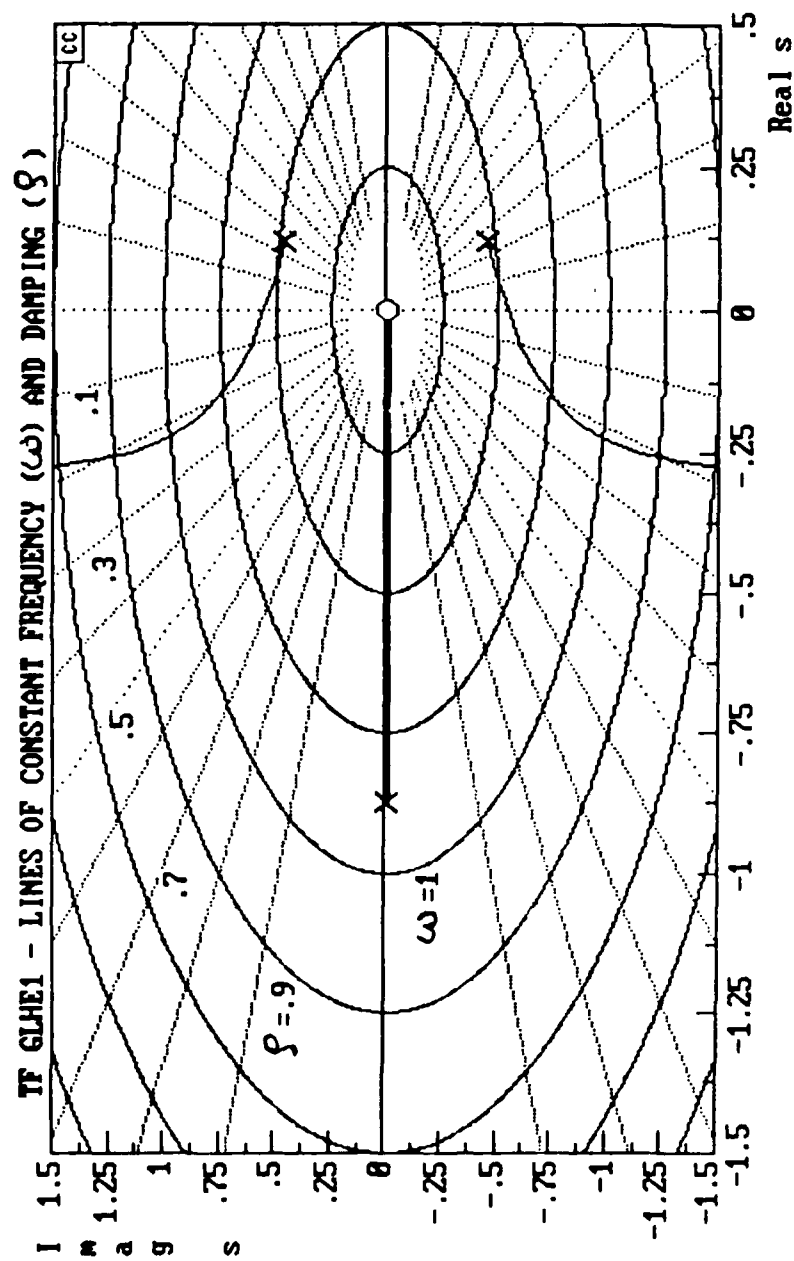
Figure 8-4 Stability of TF GLHE1

162

Figure 8-5   Root Locus Plot for TF GLHE1 Showing Lines of
Constant Frequency and Damping

163

$$G_{equiv} = \frac{6.65(S - .00109)}{s^2 - .2365S + .223729} = GL1 \qquad (8-4)$$

which effectively reduces the denominator of equation 8-3 to
second order. A root locus plot for transfer function GL1
is presented in Figure 8-7. This figure shows that initial
increases in root locus gain tend to stabilize the system
plus increase system damping. Figure 8-7 also shows the
closed loop roots for two values of gain. The first pair of
closed loop roots are complex and correspond to a constant
second order damping or zeta of approximately 0.707. A
small increase in gain brings the complex roots to the real
axis, as shown by the second pair of closed loop roots.
Increasing the gain will eventually drive the system unsta-
ble due to the numerator root or zero in the right half S
plane. The open-loop Bode plot presented in Figure 8-8
shows a "fair stretch" of -20 db/dec magnitude curve slope
in the vicinity of the gain crossover frequency. The Bode
phase plot starts at +90 degrees and goes to +270 degrees as
a result of the roots in the right half S plane (non-minimum
phase). Figure 8-9 presents the Bode magnitude asymptotes,
Bode root locus, and siggy curves. This graph shows the
closed loop root movement. It shows at what gain the closed
loop roots cross into the left half S plane, and when the
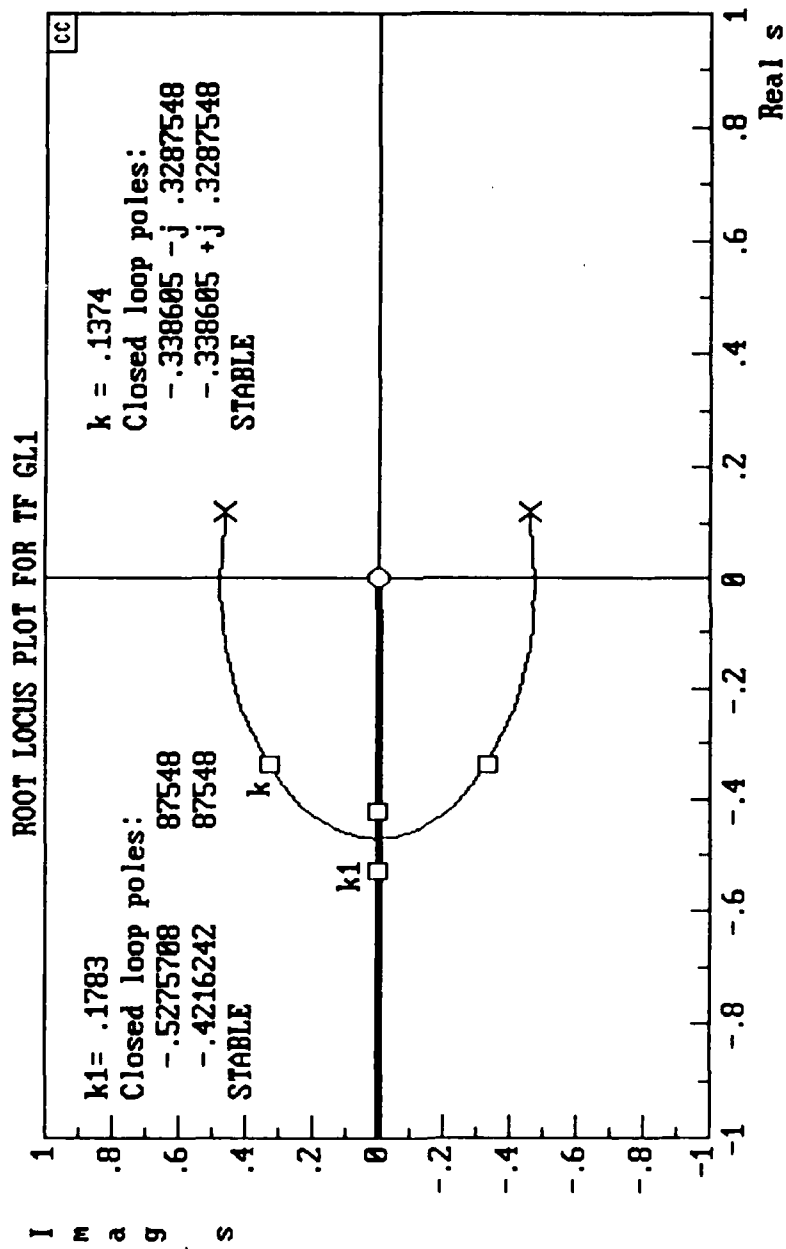closed loop roots reach the real axis.
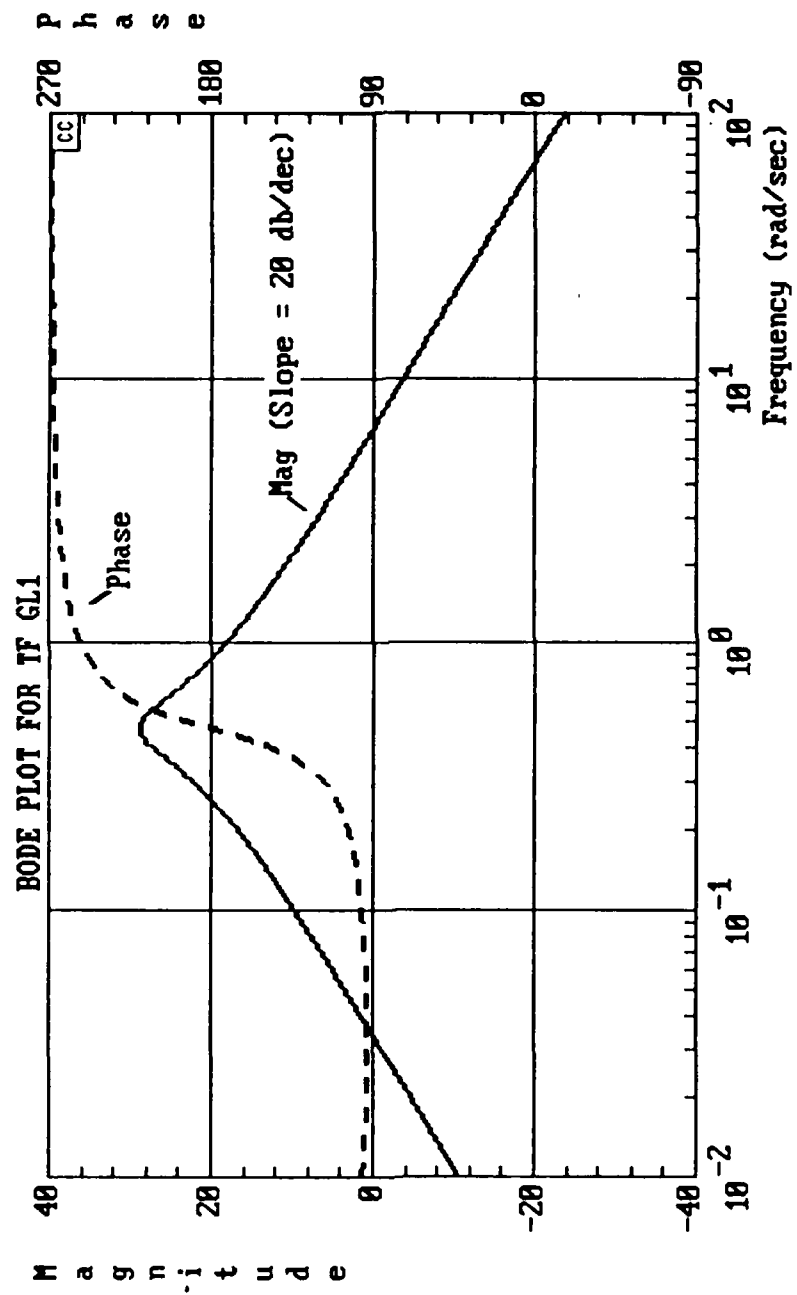
Figure 8-7 Root Locus Plot for TF GL1
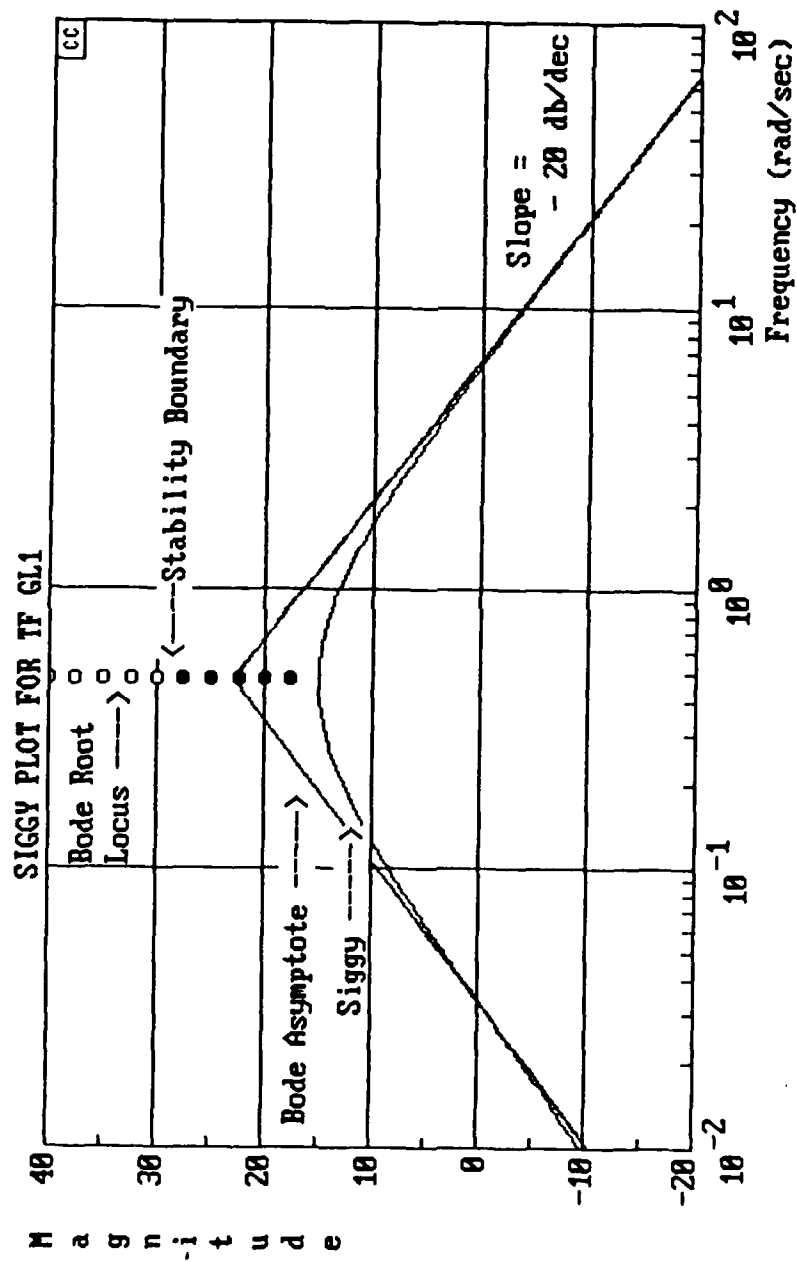
Figure 8-8   Bode Plot for TF GL1

166

Figure 8-9 Siggy Plot for TF GL1

167

2.   Pitch Attitude Feedback - Forward Flight

In forward flight the aircraft longitudinal, verti-
cal, and pitching motion is coupled as shown in equation
4-7. The characteristic equation is fourth order with two
pairs of complex roots which resemble conventional aircraft
short period (ζ_{sp}, w_{sp}) and phugoid (ζ_{p}, w_{p}) modes of mo-
tion. Unlike the conventional "well behaved" aircraft of
Reference 12, the low frequency complex pair from the
example helicopter is located in the right hand plane.

The feedback of pitch attitude to longitudinal control is
shown in Figure 8-1. The open loop pitch attitude to longi-
tudinal control transfer function in forward flight can be
expressed as

$$\frac{N_{\delta}^{\theta}}{\triangle_{long}} = \frac{A_{\theta}(S + 1/T_{\theta 1})(S + 1/T_{\theta 2})}{(S^2 + 2\zeta_{p}w_{p} + w_{p}^2)(S^2 + 2\zeta_{sp}w_{sp} + w_{sp}^2)} \qquad (8-5)$$

Using the Reference 12 stability derivatives for a single
rotor helicopter in forward flight at approximately 70 kt

$$\frac{\theta(S)}{\delta_{B}(S)} = \frac{-7.1(S + .0249)(S + .843)}{(S^2 - .0329S + .1444)(S^2 + 1.9068S + 1.1025)} \qquad (8-6)$$

$$\frac{\theta(S)}{-\delta_{B}(S)} = \frac{7.1(S + .0249)(S + .843)}{(S^2 - .0329S + .1444)(S^2 + 1.9068S + 1.1025)} \qquad (8-7)$$

Figure 8-10 presents the root locus plot for pitch attitude feedback transfer function in forward flight and shows closed loop roots for two values of root locus gain. This plot shows that feeding back pitch attitude tends to stabilize the "phugoid" roots, but reduces the "short period" root damping. The corresponding Bode plot is shown in Figure 8-11.

Reference 12 also notes that pitch rate can be fed back to improve short period damping. Pitch angle and pitch rate feedback is discussed for high altitude, high speed fixed-wing aircraft flight, and is called "almost universal" in modern aircraft automatic flight control systems.

Pitch attitude is obtained from an attitude gyro and can be considered a pure gain with no lag. Pitch rate can be obtained from a rate gyro, which has a second order lag with a natural frequency of approximately 20-30 Hz. The rate gyro can usually be considered a pure differentiator of the form $G_{RG} \doteq K_{\dot\theta}S$. The output from the attitude and rate gyro combination would have the form $G_C = K_\theta + K_{\dot\theta}S \doteq T_LS + 1$. Using lead compensation in the forward loop, equation 8-7 becomes

$$\left.\frac{\theta(S)}{-\delta_B(S)}\right|_{Comp} = \frac{7.1(S + 1/T_L)(S + .0249)(S + .843)}{(S^2 - .0329S + .1444)(S^2 + 1.9068S + 1.1025)} \qquad (8\text{-}8)$$

Reference 12 implies that, for the "well behaved" aircraft discussed, placing $1/T_L$ before $1/T_{\theta 2}$ could result in a low

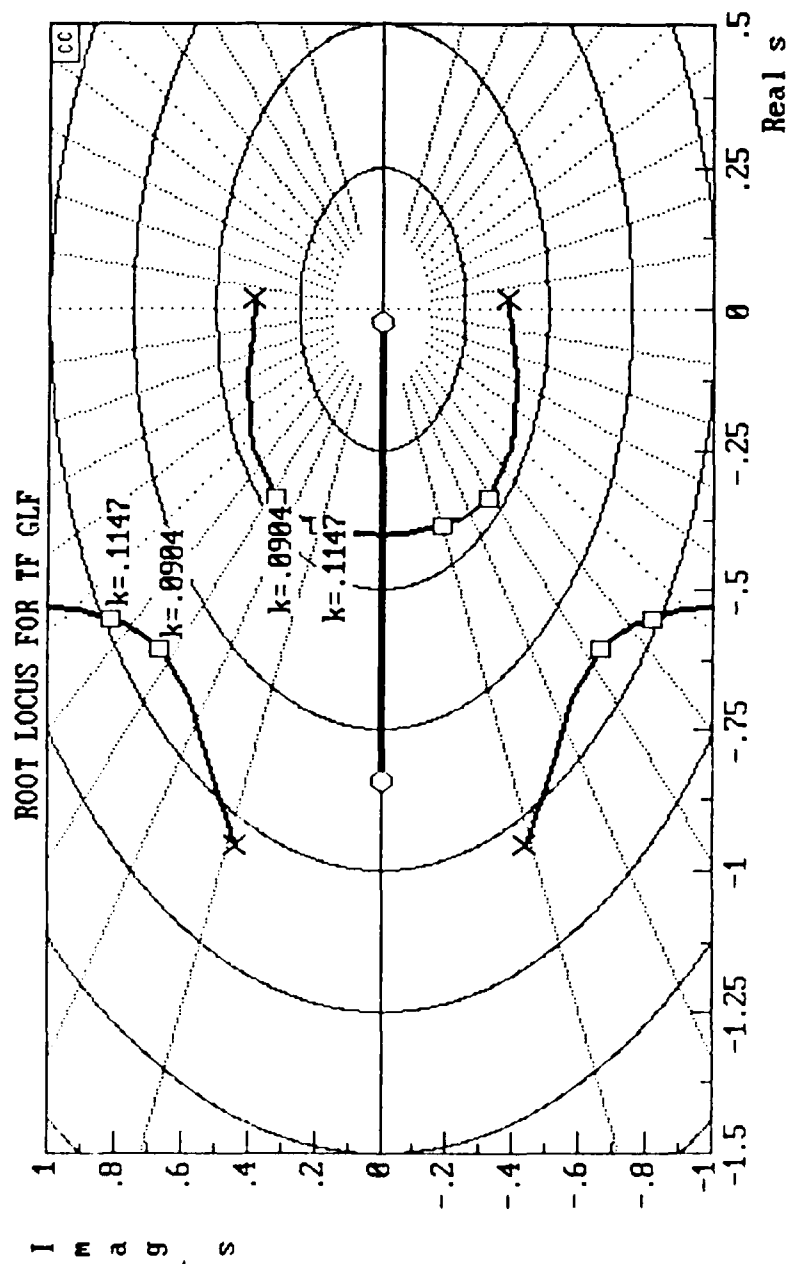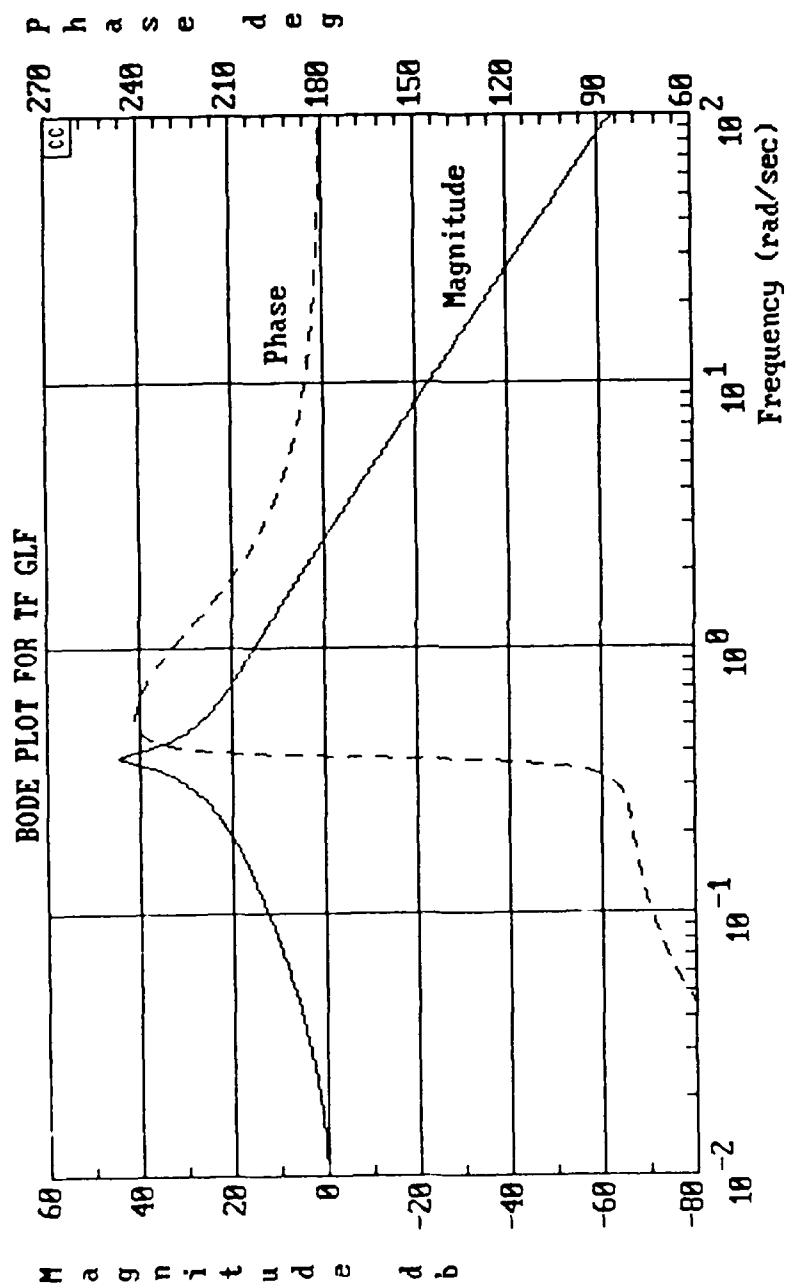Figure 8-10   Root Locus Plot for TF GLF

170

BODE PLOT FOR TF GLF

Figure 8-11   Bode Plot for TF GLF

171

dc gain and placing it after w_{sp} could result in stability problems. Selecting $1/T_L = -1.05$, gives the root locus plot shown in Figure 8-12. Note that the added lead effectively damps the so-called "phugoid" roots. With enough gain, both complex pair of roots can be driven down to the real axis.

3. Altitude Feedback - Forward Flight

Altitude control is important in helicopter missions ranging from nap-of-the-earth flight to long-distance, low-level navigation flight. It is also very important to basic take-off and landing phases of flight. The primary altitude controller in a helicopter is the collective control (δ_c), especially during low speed flight or for large altitude changes. Altitude changes in forward flight may also be made with the longitudinal cyclic control (δ_B). This study will consider using longitudinal cyclic to control altitude. The altitude to longitudinal control transfer function in forward flight is given in Reference 12 as

$$\frac{h(S)}{\delta_B(S)} = \frac{A_h(S + 1/T_h)(S^2 + 2\zeta_h w_h + w_h^2)}{S(S^2 + 2\zeta_p w_p + w_p^2)(S^2 + 2\zeta_{sp} w_{sp} + w_{sp}^2)} \quad (8-9)$$

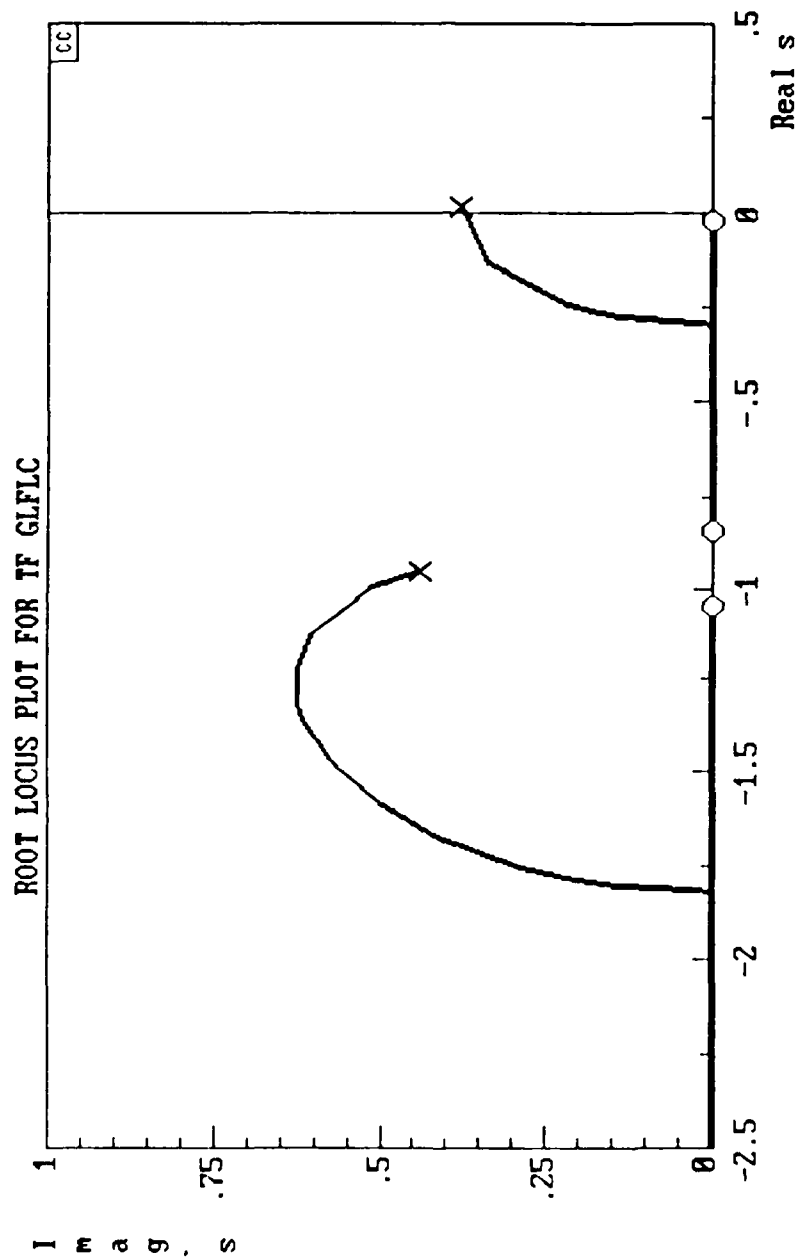and the stability derivatives for the Reference 12 single rotor helicopter are

Figure 8-12 Root Locus Plot for GLFLC

$$\frac{h(S)}{-\delta(S)} = \frac{92(S + .0560)[.183; 2.75]}{S [-.0433; .380][.908; 1.05]} \qquad (8\text{-}10)$$

where the shorthand notation $[\varphi; w] \equiv (S^2 + 2\varphi w + w^2)$ is used in Reference 12 as a concise way of writing second order Laplace factors.

Data showing the altitude to longitudinal control feedback are presented in Figures 8-13 through 8-16. Solving for the closed loop characteristic polynomial shows that the analog closed loop system is stable (see Figure 8-13). The Routh criteria can be used to determine the stability boundary of the system as shown in Figure 8-14. The root locus plot, Figure 8-15, shows that the free S in the altitude transfer function drives the already unstable "phugoid" complex pair further into the right half plane for low values of gain. The altitude transfer function complex numerator d⌣ pull the unstable "phugoid" pair back into the left half S plane for root locus gains greater than 0.3. Although the closed loop system is stable, as shown in Figures 8-13 and 8-14, the closed loop damping is very low. Figure 8-16 shows the transient response to a unit input. Basic altitude feedback is unsatisfactory, especially in gusty conditions. Improving the damping of this transfer function requires pulling the root loci from initially starting toward the right to initially starting toward the left. Since another complex pole is located just to the left, it is difficult to change the initial direction of

174

CC>STABILITY,GA
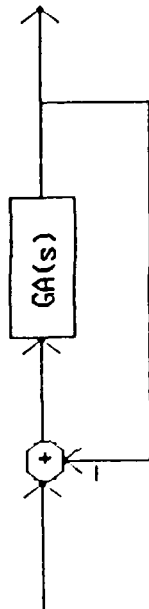
Closed loop characteristic polynomial:

$$p(s) = s^5 + 1.873892s^4 + 93.18415s^3 + 97.98906s^2 + 701.0947s + 38.962$$

ZEROS:

-5.5987907838648040D-02

-.51331884599960668   +j   2.8324225817296996

-.51331884599960668   -j   2.8324225817296996

-.3956332000846092   +j   9.15572973169543

-.3956332000846092   -j   9.15572973169543

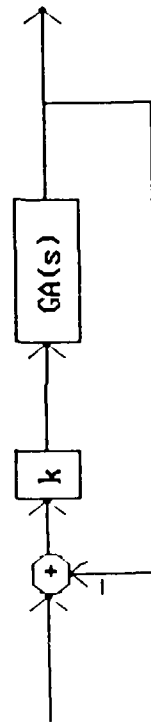The analog closed loop system is   STABLE

Figure 8-13   Stability of TF GA

CC>DIS,GA

$$GA(s) = \frac{92(s +.056)(s^2 +1.0065s +7.5625)}{s(s^2 -.032908s +.1444)(s^2 +1.9068s +1.1025)}$$

CC>ROUTH,GA

Stable for gain ranges : .306824 to infinity

Figure 8-14   Routh Criteria for TF GA
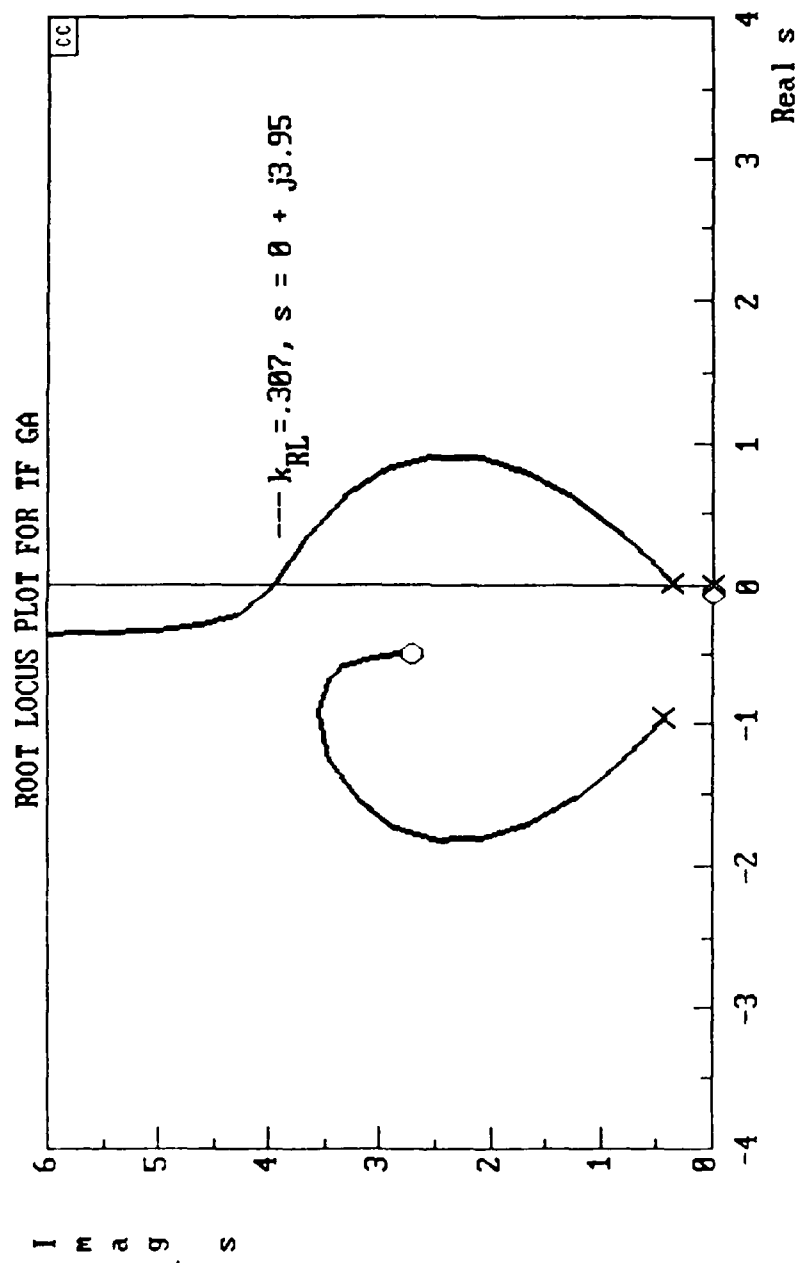
Figure 8-15 Root Locus Plot for TF GA

TF GA CLOSED LOOP STEP RESPONSE
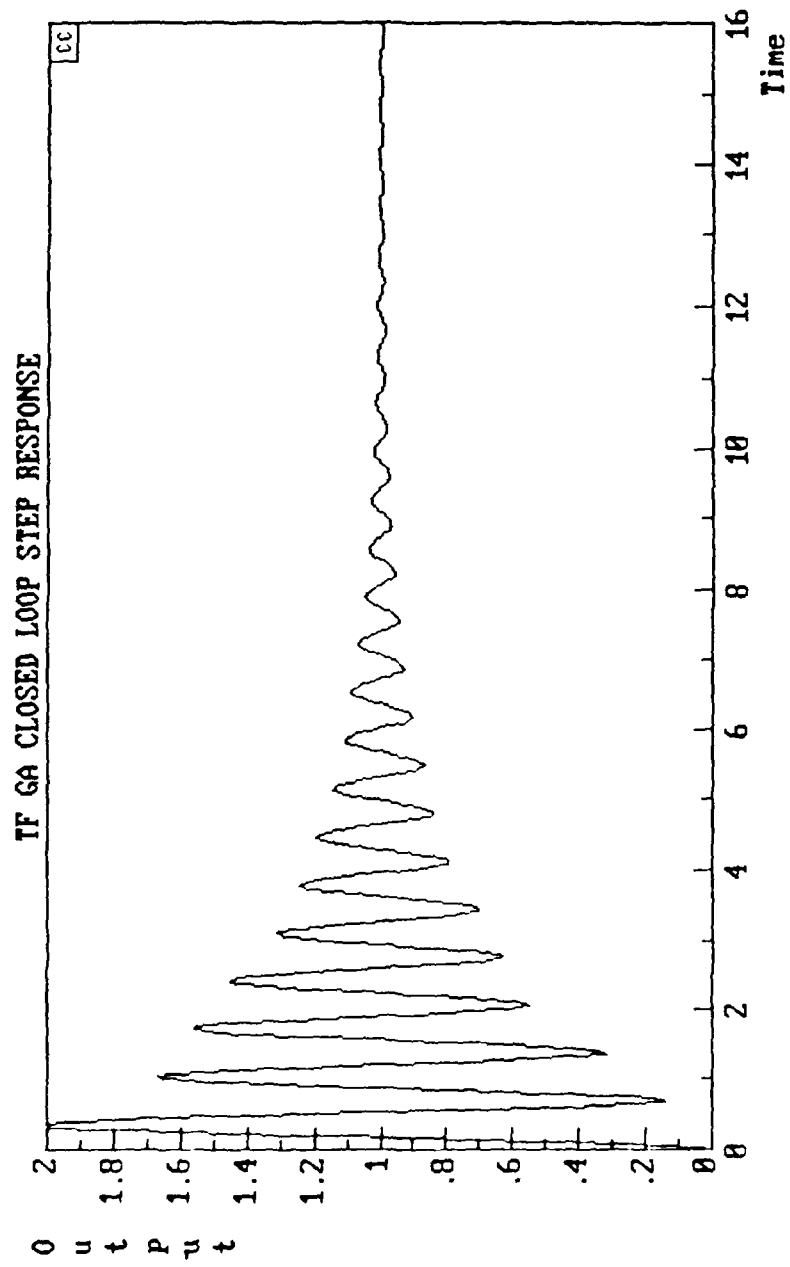
Figure 8-16   Closed Loop Step Response for TF GA

the root loci that travels into the right half plane. Altitude hold augmentation may use an altitude rate signal. Another option includes using pitch attitude feedback as an inner loop of a simple altitude hold autopilot.

B.   ALTITUDE HOLD AUTOPILOT

A simple altitude hold autopilot can be implemented by feeding back altitude and pitch attitude. Only one control point is used since both parameters are fed back to the longitudinal control. Reference 12 discusses factors controlling inner and outer loop choices like

- Relative bandwidth
- Closures characteristics
- "Subsidiary" loops
- "Interdependent" loops
- Multimode characteristics
- Equalization economy

Comparing pitch attitude and altitude shows that pitch attitude should be used as the inner loop. Recall that pitch attitude showed good single loop characteristics, although some lead was required. Pitch attitude can be used to increase bandwidth of any short period motion and can also serve in other modes of an autopilot. A block diagram for an altitude hold autopilot is presented in Figure 8-17.
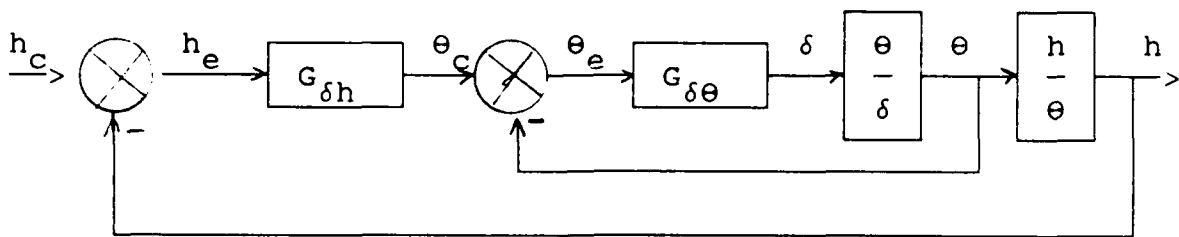
Figure 8-17   Block Diagram for Altitude Hold Autopilot

recall G = gain or equalization, $\delta = \delta_B$, and pitch
attitude to longitudinal cyclic control can be expressed as

$$\frac{\Theta}{\delta_B} = \frac{N_\delta^\Theta}{\Delta_{long}} \tag{8-11}$$

The altitude to pitch attitude transfer function can be
expressed as

$$\frac{h}{\Theta} = \frac{h}{\delta}\frac{\delta}{\Theta} = \frac{\dfrac{N_\delta^h}{\Delta}}{\dfrac{N_\delta^\Theta}{\Delta}} = \frac{N_\delta^h}{N_\delta^\Theta} \tag{8-12}$$

The transfer function for the inner loop of Figure 8-17 (pitch
attitude) is

$$\frac{\Theta}{\Theta_c} = \frac{G_{\delta\Theta}\, N_\delta^\Theta}{\Delta + G_{\delta\Theta}\, N_\delta^\Theta} \tag{8-13}$$

The Figure 8-17 block diagram can be reduced to
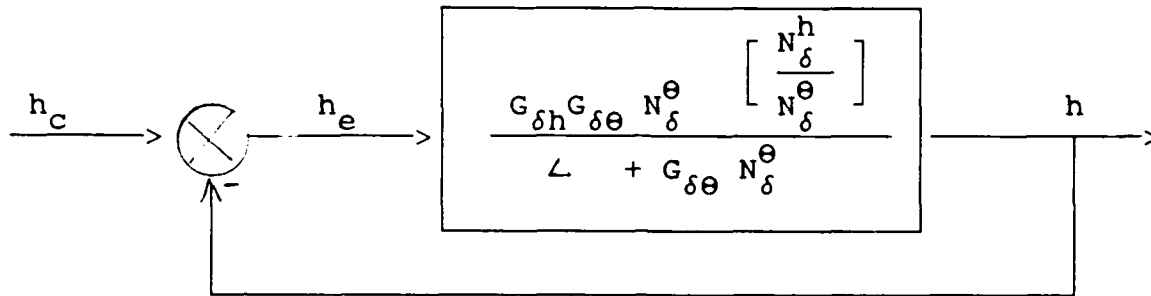
Figure 8-18   Simplified Block Diagram for Altitude Hold System

and the open loop altitude and closed loop pitch attitude
transfer function becomes

$$G_{equiv} = \left.\frac{h}{h_e}\right|_{\theta \longrightarrow \delta} = \frac{G_{\delta h}\ G_{\delta \theta}N_{\delta}^{h}}{\angle + G_{\delta \theta}N_{\delta}^{\theta}} \qquad (8\text{-}14)$$

where the denominator of equation 8-14 represents the closed
loop roots of the pitch attitude to longitudinal control at
a selected gain. The closed loop altitude transfer function
can be expressed as

$$\left.\frac{h}{h_c}\right|_{\theta \longrightarrow \delta} = \frac{G_{\delta h}G_{\delta \theta}N_{\delta}^{h}}{\angle + G_{\delta \theta}N_{\delta}^{\theta} + G_{\delta h}G_{\delta \theta}N_{\delta}^{h}} \qquad (8\text{-}13)$$

The closed loop pitch attitude roots are chosen at a gain
that drives the complex roots to the real axis. This im-

plies a higher gain and a higher crossover frequency for the altitude hold autopilot. For an open loop root locus gain, $K_{RL} = 0.4$, the closed loop pitch attitude transfer function roots are

$$T_1 = -2.5308$$
$$T_2 = -1.4723$$
$$T_3 = -0.6138$$
$$T_4 = -9.6975E-02$$

and the altitude hold transfer function becomes

$$\frac{h}{h_c} = \frac{G_{\delta\theta}A_h(S + 1/T_L)(S + 1/T_h)[\zeta_n;w_n]}{S(S + 1/T_1)(S + 1/T_2)(S + 1/T_3)(S + 1/T_4)} \qquad (8-16)$$

Recall from equation 8-9 that the altitude numerator (Reference 12) had the form:

$$N_\delta^h = \frac{A_h}{S}(S + 1/T_h)(S^2 + 2\zeta_h w_h + w_h^2) \qquad (8-17)$$

Including lead $(1/T_L = -.5)$, the altitude hold transfer function becomes:

$$\frac{h}{h_c} = \frac{G_{\delta\theta}A_h(S + 1/T_L)(S + 1/T_h)[\zeta_h;w_h]}{S(S + 1/T_1)(S + 1/T_2)(S + 1/T_3)(S + 1/T_4)} \qquad (8-18)$$

Substituting values,

$$\frac{h}{h_c} = \frac{(2.84)(92)(S + .5)(S + .056)(S^2 + 1.0065S + 7.5625)}{S(S + 2.531)(S + 1.472)(S + .614)(S + .097)} \qquad (8-19)$$

Root locus and Bode plots for the equation 8-19 altitude hold transfer function are presented in Figures 8-19 and 8-20.

ROOT LOCUS PLOT FOR TF GAH

Pitch Attitude Inner Loop

Altitude Outer Loop

Lead Compensation ($1/T_L = -.5$)

Real s

Imag, s

cc
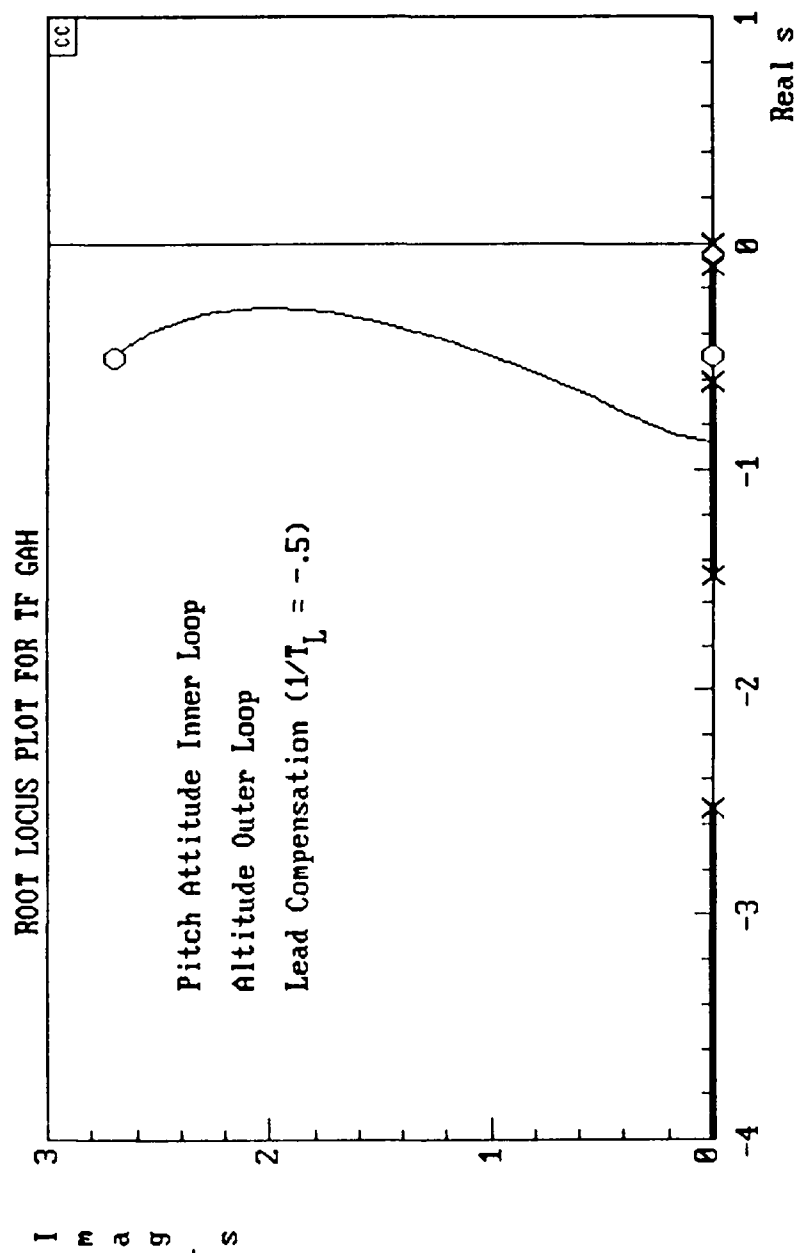
Figure 8-19 Root Locus Plot for TF GAH
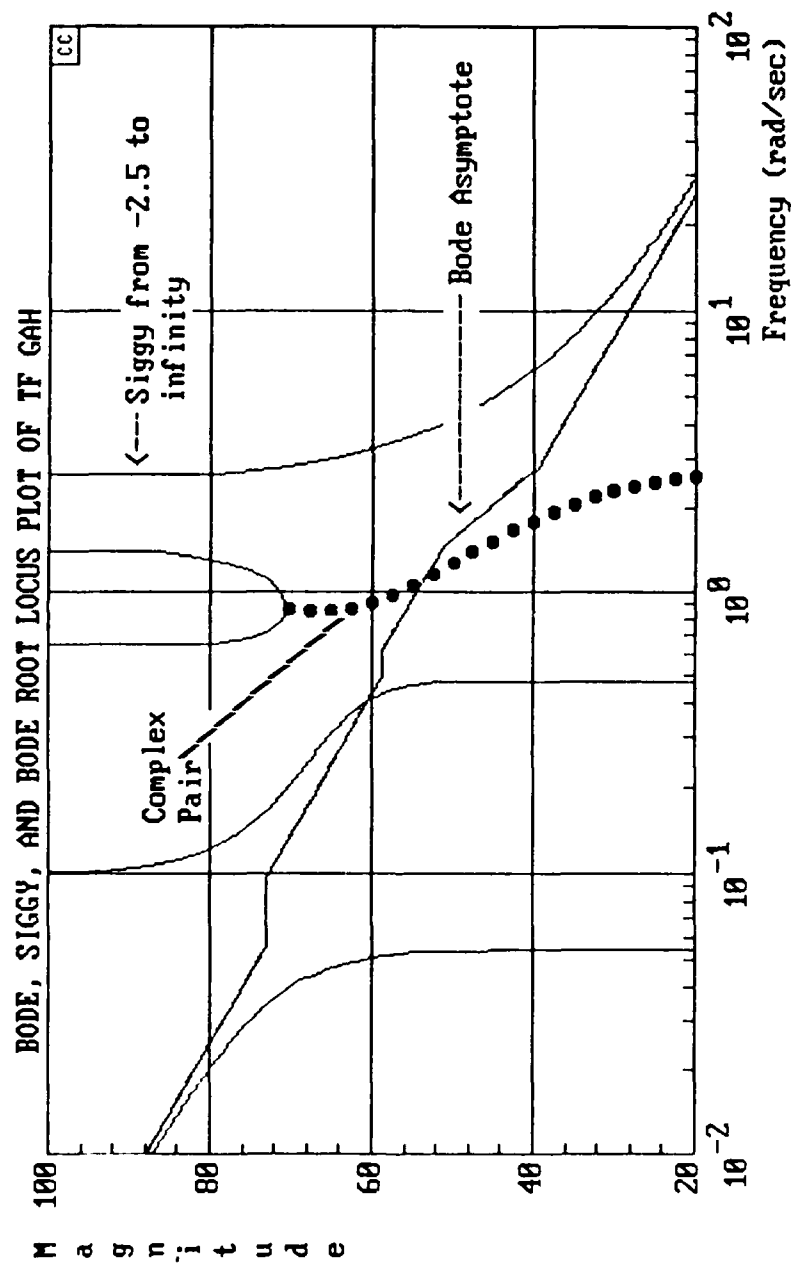
Figure 8-20   Bode, Siggy, and Bode Root Locus Plot for TF GAH

IX. CONCLUSIONS AND RECOMMENDATIONS

A. CONCLUSIONS

This thesis reviewed the many aspects of helicopter controllability. The review included helicopter development, configurations, linearized equations of motion, stability characteristics, flight control systems, evaluation techniques, and a generic simulation.

B. RECOMMENDATIONS

More emphasis should be placed on helicopter/rotorcraft flying qualities and flight control system courses. Rotorcraft flight control systems courses should touch on the theoretical validity of current and proposed specification requirements. Personal computer programs should be developed to aid students in control system design, analysis, and evaluation. A strong relationship should exist between airframe (aerospace) and control system (electrical) disciplines.

APPENDIX A.   SUMMARY CHRONOLOGY OF HELICOPTER AFCS DEVELOPMENT

HELICOPTER STABILIZATION HISTORY

BELL   HELICOPTER   TEXTRON   INTERNATIONAL (BHTI)

(Courtesy M. Murphy)

Date	Aircraft	System
1942	Bell Model 30	First flight with Bell Bar
1952	Bell Model 48	Artificial stabilization with AFL autopilot
1953	Bell Model 48	AFCS with hover/sonar coupler (fore-runner of HSL autopilot)
1954	HSL (tandem)	Four axis automatic flight control system (AFCS)
1968	Model 205	Hover Coupler (sonar ball and cable angle); four axis AFCS plus approach to hover and hover coupler for transition
1970	AH-1J/AH-1G-->S	Three axis stability and control augmentation system(SCAS)
1971	Model 206 Jet Ranger	Three axis SCAS
1972	UH-1N	Flying qualities evaluation with the stabilizer bar off
1972	UH-1N	Four axis AFCS plus hover coupler
1972	Model 212	Three axis AFCS
1972	Model 409	Three axis SCAS/force feel
1972	Model 214	Iranian model three axis AFCS
1976	XV-15	Three axis SCAS/force feel
1978	Model 222	Sperry Autopilot three axis AFCS

HELICOPTER STABILIZATION HISTORY

BHTI, continued

1979	Model 412	Three axis AFCS (Sperry)
1980	Model 214ST	Three axis AFCS with FBW horizontal stabilizer
1982	Model OH-58D	Digital 3-axis SCAS
1984	Model 249	Four valve fly-by-wire (FBW) Optical Control System
1986	AH-1W	Survivable tail rotor
1988	V-22	Triply redundant hybrid FBW system (Boeing Vertol/Bell)
1988	Model 4BW	Digital 3-axis SCAS, Fail/Operate-Fail/Safe

HELICOPTER FLIGHT CONTROL SYSTEMS DEVELOPMENT
HONEYWELL DEFENSE AVIONICS SYSTEMS DIVISION (DASD)
(Courtesy Carl Griffis)

Honeywell DASD (and under its former identity as part of the Sperry Corporation) has been involved in helicopter stabilization and flight control systems research, design and production dating back to the 1940's. Systems developed and produced have ranged from simple 1, 2, and 3-axis stability augmentation systems to 4 and 5-axis simplex and redundant automatic flight control systems with modes such as

- automatic terrain following
- navigation
- automatic landing
- approach to hover
- hover hold
- sonar cable angle hold
- automatic formation flight

Implementations have been both analog and digital. A partial listing of helicopters and VTOL aircraft types for which Honeywell DASD or Sperry Flight Systems has supplied flight control equipment is listed below:

- Sikorsky H-19, H-34, H-37, S-76
- Boeing-Vertol Model 44, CH-21, CH-46, CH-47, 234
- Lockheed AH-56
- Bell UH-1, 204, 205, 212, 214, 222, 412, 400, 406, OH-58
- Canadair CL-84
- Hughes OH-6
- McDonnell Douglas AH-64, AV-8

HONEYWELL DEFENSE AVIONICS SYSTEMS DIVISION (DASD)

- Aerospatiale 341, 360, 365, 350, 355
- Agusta 109, 212, 412
- MBB 1u5, 117

Systems currently in production at DASD include the SCAS for the OH-58D AHIP Scout Helicopter, DASE for the AH-64A Apache Attack Helicopter, SAAHS for the AV-8 Harrier VTOL Fighter Aircraft, and Drone Stabilization/Control Equipment for the QH-55 Target Drone. A sister division, Avionics Systems in Glendale, AZ., produces a variety of analog and digital flight control system equipment for commercial and foreign military helicopters.

HELICOPTER FLIGHT CONTROL EXPERIENCE
Over 30 Years Experience

DATE	APPLICATION	DESCRIPTION
1956	S-55	3-AXIS AUTO-STABILIZATION
1958	VERTOL MODEL 44 (SWEDISH NAVY)	4-AXIS AFCS WITH SONAR COUPLING
1958-62	CH-21	5-AXIS AFCS INCLUDING AUTO-HOVER
1962-63	CH-47A	3-AXIS, DUAL REDUNDANT SCAS
1968-70	AH-56 CHEYENNE	R&D SAS DESIGN, PRODUCTION YAW DAMPER/ HEADING HOLD
1968-71	UH-1B	R&D 4-AXIS TERRAIN FOLLOWING
1970	CL-84 TILT WING	3-AXIS DUAL-REDUNDANT SAS
1975-PRESENT	AH-64 APACHE	4-AXIS DIGITAL STABILIZATION SYSTEM WITH HOVER HOLD, BACK-UP FLY BY WIRE FUNCTIONS (OVER 500 PRODUCED TO DATE)
1981-PRESENT	OH-58D AHIP	3-AXIS SCAS WITH HEADING HOLD (OVER 100 PRODUCED TO DATE)

191

HELICOPTER FLIGHT CONTROL EXPERIENCE

Over 30 Years Experience

DATE	APPLICATION	DESCRIPTION
1975–82	VARIOUS COMMERCIAL HELICOPTERS: SA–341 BO–105 B–212 A–109A SA–360C B–222 SA–365C S–76 B–412 AS–350D AS–355F BV–234	2 & 3–AXIS ANALOG AFC, FD SYSTEMS (SIMPLEX, DUAL, TRIPLEX) (1st SINGLE PILOT IFR CERTIFICATION)
1983–PRESENT	SA–365N S–76 B–222 B–400 AB–212 AB–412 BK–117 B–214ST	3 & 4–AXIS DIGITAL AFC/ FD SYSTEMS (SIMPLEX, DUAL) (SAR AND ASW VERSIONS WITH DOPPLER APPROACH TO HOVER AND SONAR CABLE ANGLE HOLD)

APPENDIX B. MIL-H-8501 HANDLING QUALITIES SPECIFICATION SUMMARY
(From NAVAIRTESTCEN Notes)

Topic: Hover Handling Qualities

Paragraph Number	Specification Requirement
3.2.1	Margin of control power (longitudinal)
3.2.2	Longitudinal control for hover
3.2.10	Longitudinal stability characteristics
3.2.10.2	Longitudinal trim changes
3.3.2	Sideward flight
3.3.3	Lateral control .or hover
3.3.4	Lateral hover control power
3.3.6	Yaw hover control power
3.3.17	Lateral trim change
3.4.1	Collective control for hover
3.4.2	Collective mechanical characteristics
3.4.3	Collective control forces
3.5.2	Ground turn-up without chocks
3.5.4	(all subparagraphs) Takeoffs and landing
3.6.1.2	Longitudinal Dynamic Stability (IFR)
3.7.1	Vibration
3.7.3	Mechanical instability

Flight Tests Required for Specification Compliance

1.	Pilot effort in a hover
2.	Vertical damping
3.	Critical azimuth
4.	Lateral flight from hover
5.	Vertical takeoffs and landings
6.	Running takeoffs and landings
7.	Transitions to and from a hover
8.	Longitudinal flight
9.	Trim changes with power
10.	Longitudinal hover dynamics
11.	Lateral hover dynamics
12.	Mechanical characteristics of collective control system:

    a. Breakout plus friction
    b. Collective creep
    c. Maximum forces
    d. Force gradients
    e. Control pump, freeplay

APPENDIX B. MIL-H-8501 HANDLING QUALITIES SPECIFICATION SUMMARY
(From NAVAIRTESTCEN Notes)

Topic: Control Power, Control Effectiveness,
       Control Sensitivity, Control Margin and Damping

Paragraph Number	Specification Requirement
3.2.1	Margin of control power (longitudinal)
3.2.9	Response delay time (longitudinal)
3.2.11.1	Maneuver Stability characteristics
3.2.12	Normal acceleration during maneuver
3.2.13	Longitudinal control power
3.2.14	Longitudinal damping
3.3.1	Margin of control power (lateral)
3.4.1	Directional control power
3.4.2	Critical azimuth
3.3.7	Directional control sensitivity
3.3.15	Lateral control effectiveness
3.3.16	Response delay time (lateral/directional)
3.3.18	Lateral control power
3.3.19	Lateral directional damping
3.6.1.1	IFR control power damping

Tests for Specification Compliance

1.   Control effectiveness, delay time, maneuvering
            characteristics
              a. step inputs

2.   Control sensitivity and damping
              a. Control reversal technique
              b. Hold for three seconds

APPENDIX B. MIL-H-8501 HANDLING QUALITIES SPECIFICATION SUMMARY
(From NAVAIRTESTCEN Notes)

Topic: Longitudinal Flying Qualities

Paragraph   Specification Requirement
Number

3.2.1	Longitudinal control static margin
3.2.3	Longitudinal control forces at trim
3.2.4	Longitudinal control forces gradient
3.2.6	Longitudinal control forces
3.2.7	Breakout and friction
3.2.10	Static longitudinal control stability
3.2.10.2	Excessive longitudinal trim changes
3.2.11	Longitudinal dynamic stability
3.2.11.2	Gust response
3.5.9	(c and d) Control forces/stability ASE
3.5.10	Freeplay
3.5.11	Mechanical coupling
3.6.1.2	Longitudinal dynamic stability (IFR)
3.6.3	Static longitudinal force/position stability (IFR)

Tests for Specification Compliance

1.   Trimmed control position characteristics (level flight)
2.   Trimmed control position characteristics (vertical speed variation)
3.   Static longitudinal stability
4.   Long trim dynamic stability (long period oscillation)
5.   Short term dynamic stability (gust response)
6.   Short term dynamic stability (period determination)
7.   Longitudinal control short term response
8.   Control trim/force characteristics

APPENDIX B. MIL-H-8501 HANDLING QUALITIES SPECIFICATION SUMMARY
(From NAVAIRTESTCEN Notes)

Topic: Lateral and Directional Flying Qualities

Paragraph Number	Specification Requirement
3.3.8	Coordinated autorotative turns
3.3.9	Directional stability
3.3.10	Lateral and directional control forces at trim
3.3.11	Lateral control force characteristics
3.3.12	Directional control force characteristics
3.3.13	Breakout and friction
3.3.14	Transient coupling forces
3.3.17	Lateral trim change with power
3.5.9	(c and d) control forces/stability of basic airframe
3.5.10	Freeplay
3.5.11	Control coupling
3.6.1	Lateral-directional oscillations
3.6.2	Control force stability

Tests for Specification Compliance

1. Control force/trim characteristics
   a. Trim capability and self centering
   b. Control-jump
   c. Lateral-directional control force characteristics
2. Trimmed control position characteristics (level flight)
3. Trimmed control position characteristics (vertical speed variation)
4. Static lateral-directional stability
5. Cyclic only turns
6. Pedal only turns
7. Short term lateral and directional dynamics (gust response)
8. Dynamic lateral-directional stability (Dutch roll)
9. Spiral Stability
10. Coordinated turns in autorotation

196

APPENDIX B. MIL-H-8501 HANDLING QUALITIES SPECIFICATION SUMMARY
(From NAVAIRTESTCEN Notes)

Topic: Maneuvering Stability

Paragraph   Specification Requirement
Number

3.2.5   Quick stop and acceleration
3.2.11.1   Maneuvering Stability Characteristics
3.2.12   Normal acceleration response
Figure 1   Normal acceleration and pitch rate response

Tests for Specification Compliance

1.   Turning maneuvering stability (constant power)
2.   Turning maneuvering stability (constant altitude)
3.   Sudden pull-ups
4.   Steady pull-ups
5.   Quick stops and accelerations

APPENDIX B. MIL-H-8501 HANDLING QUALITIES SPECIFICATION SUMMARY
(From NAVAIRTESTCEN Notes)

Topic: Sudden Engine Failure and Autorotation Entry

Paragraph   Specification Requirement
Number

3.5.4.3   Autorotative landing at ground speeds up to 35 kt
3.5.4.4   Stopping distance
3.5.5   Autorotation entry and delay
3.5.5.1   Altitude changes following sudden power varia-
             tions
3.5.6   Control forces during autorotation entry
3.5.7   Autorotative landings

Tests for Specification Compliance

1. Delay times in: a. level flight
                    b. descent
                    c. climb
                    d. turning flight

2. Determination of attitude/altitude changes

APPENDIX B. MIL-H-8501 HANDLING QUALITIES SPECIFICATION SUMMARY
(From NAVAIRTESTCEN Notes)

Topic: Stability Augmentation

Paragraph   Specification Requirement
Number

3.3.1   Ground handling
3.5.1   Rotor engagement and disengagement
3.5.3   Droop stops
3.5.8   Boost failures
3.5.9   Stability augmentation failures
3.6.1   General Stability Requirements

Tests for Specification Compliance

1.   Hydraulic servo failure
2.   ASE failure
3.   Ground tests

APPENDIX C.   A CHRONOLOGY OF EVENTS LEADING TO MIL-F-87242

Courtesy Mr. D. Rubertus, Wright-Patterson AFB

Feb 1955 - MIL-F-9490 issued (6 Feb 55)

Mid 1955 - Amendment 1 to MIL-F-9490 issued

Aug 1957 - MIL-F-9490B issued (7 Aug 57)

Mid 1958 - Amendent 1 to Mil-F-9490B issued

Mar 1964 - MIL-F-9490C issued (13 Mar 64)

Mar 1966 - Amendment 1 to MIL-F-9490C issued

Jun 1972 - AFFDL contracted with Boeing/Wichita to prepare a revision to MIL-F-9490C

Aug 1973 - AFFDL requested industry comments on MIL-F-9490D (1st draft)

Mar 1974 - AFFDL requested industry comments on MIL-F-9490D (2nd draft)

Aug 1974 - AIAA paper No. 74-914 "Impact of New MIL-F-9490DRequirements on Future Flight Control Developments", James L.Townsend, Boeing and Paul E. Blatt, AFFDL

Jan 1975 - Publication of AFFDL-TR-74-116, BACKGROUND INFOR-MATIONAND USER GUIDE FOR MIL-F-9490D, Flight Control Systems - Design, Installation and Test of Piloted Aircraft, General Specification for, January 1975, (DTIC No. AD A029074)

Jun 1975 - Publication of MIL-F-9490D(USAF), MILI-TARY SPECIFICATION: FLIGHT CONTROL SYSTEMS - DESIGN, INSTAL-LATION AND TEST OF PILOTED AIRCRAFT, GENERAL SPECIFICATION FOR, 6 June 1975

Aug 1975 - Deputy Secretary of Defense Memorandum on Specifications/Standards Applications. Agencies are to control   blanket   contractural   imposition   of specifications/standards; tailor requirements to essential operational needs (4 Aug 1975)

Nov 1976 - ASD designated Flight Control Systems as a Prime
Air Vehicle Specification (AFFDL/FG is the REO); Flying
Qualities of Piloted Aircraft as a Prime Air Vehicle Standard
(AFFDL/FG is the REO)

Apr 1977 - Publication of DOD Directive 4120.21, SPECIFICA-
TIONSAND STANDARDS APPLICATION, required procuring organiza-
tions to control, review, certify, and document the tailoring
of specifications and standards (9 April 1977)

Apr 1977 - Publication of AFFDL-TR-77-7, VALIDATION OF
MIL-F-9490D- GENERAL SPECIFICATION FOR FLIGHT CONTROL SYSTEM
FOR PILOTED MILITARY AIRCRAFT, April 1977
   VOL   I: Summary of YF-17 and C-5A Validation
   VOL   II: YF-17 Lightweight Fighter Validation
   VOL III: C-5A Heavy Logistics Transport Validation

Jul 1979 - AFFDL contracted with Northrop to prepare a
revision to MIL-F-9490D

Jan 1980 - Publication of AFFDL-TR-74-116 Sup. 1, APPENDIX
TO "BACKGROUND INFORMATION AND USER GUIDE FOR MIL-F-
9490D" AFFDL-TR-74-116 (DTIC No. AD094717)

Sep 1980 - AFWAL contracted with Northrop to upgrade MIL-F-
9490D to Flight Control System MIL-PRIME-Specification

May 1981 - MIL-F-9490E submitted; not released due to im-
pending conversion of MIL-F-9490D to a MIL-PRIME-Specifica-
tion in 1982

Dec 1981 - AFWAL requested industry commments on draft FCS
PRIME Specification

Mar 1982 - Combined symposium on DESIGN CRITERIA FOR THE
FUTURE OF FLIGHT CONTROLS covering planned upgrades on
MIL-F-8785C and MIL-F-9490D to PRIME Standard and Specifica-
tion, respectively

Jul 1982 - Publication of AFWAL-TR-82-3064, DESIGN CRITERIA
FOR THE FUTURE OF FLIGHT CONTROLS: Procedings of the Flight
Dynamics Laboratory Flying Qualities and Flight Control
Symposium 2-5 Mar 1982 (July 1982)

Dec 1984 - Publication of AFWAL-TR-84-3114, PROPOSED MIL-PRIMEFORMATTED FLIGHT CONTROL SYSTEM SPECIFICATION, December 1984

Dec 1984 - Transfer of responsibility for MIL-F-9490D and the upgrade to MIL-PRIME-Specification from AFWAL/FIGL to ASD/ENFTC

May 1985 - ASD mandated review of all MIL-PRIME-documents by Aerospace Industry Association (AIA)

Jul 1985 - ASD submitted draft Flight Control System MIL-PRIME-Specification to AIA for review

Mar 1986 - Approval of MIL-F-87242(USAF), MILITARY SPECIFICATION FLIGHT CONTROL SYSTEM, GENERAL SPECIFICATION FOR, 31 Mar 1986

Mar 1986 - Decision to retain MIL-F-9490D as a military specification as long as any aircraft built to its requirements remained in operational use

REFERENCES

1.   Johnson, Wayne, <u>Helicopter Theory</u>, Princeton University Press, 1980.

2. Boulet, Jean, <u>History of the Helicopter</u>, Editions France-Empire, 1984.

3.   Gessow, Alfred and Myers, Garry C. Jr., <u>Aerodynamics of the Helicopter</u>, Frederick Ungar Publishing Co., 1967.

4.   "Vertiflite", The American Helicopter Society, Vol. 30, Number 4, May/June 1984.

5.   Burke, J. A., "A Close Look at Mast Bumping", U. S. Army Aviation Digest, January 1977.

6.   Layton, Donald M., <u>Helicopter Performance</u>, Matrix Publishers, Inc., 1984.

7.   Heffley, Robert K., et al, <u>A Compilation and Analysis of Helicopter Handling Qualities Data, Volume One: Data Compilation, Volume Two: Data Analysis</u>, NASA Contractor Reports 3144 and 3145 of August 1979.

8.   Daughaday, Hamilton and Parrog, Michael L., <u>Helicopter Stability and Control Theory and Flight Test Techniques</u>, Calspan Report No. 6645-F-10 of November 1983.

9.   Seckel, Edward, <u>Stability and Control of Airplanes and Helicopters</u>, Academic Press, 1964.

10.   Bramwell, A. R. S., <u>Helicopter Dynamics</u>, John Wiley and Sons, 1976.

11.   Prouty, Raymond W., <u>Helicopter Performance, Stability and Control</u>, PWS Publishers, 1986.

12.   McRuer, Duane, Ashkenas, Irving, and Graham, Dunstan, <u>Aircraft Dynamics and Automatic Control</u>, Contract No. NOw62-0781-c, Systems Technology, Inc., Hawthorne, Ca., August 1968.

13.   O'Neil, Hugh James, <u>Calculation of the Longitudinal Stability Derivatives and Modes of Motion for Helicopter Aircraft</u>, M.S. Thesis, Naval Postgraduate School, Monterey, California, October 1982.

14. Advanced Flight Control System Concepts for VTOL Aircraft, Phase I Technical Report TRECOM TR 64-50, October 1964.

15. Hilbert, Kathryn B., "A Mathematical Model of the UH-60 Helicopter", NASA Technical Memorandum 85890 of April, 1984.

16. Ogata, K., Modern Control Engineering, Prentice-Hall, Inc., 1970.

17. Dorf, Richard C., Modern Control Systems, Addison-Wesley Publishing Company, 1967.

18. DiStefano, Joseph J. III, Stubberud, Allen R., and Williams, Ivan J., Feedback and Control Systems, Schaum's Outline Series, McGraw-Hill Book Company, 1967.

19. Wolkovitch, Julian and Walton, Richard P., VTOL and Helicopter Approximate Transfer Functions and Closed-Loop Handling Qualities, STI Technical Report No. 128-1 of June 1965.

20. Report No. NADC-85017-60, 4-Valve Fly-by-Wire/Optical Control System, Bell Helicopter Textron, October 1984.

21. Glusman, Steven I., et. al., "Handling Qualities Evaluation of the ADOCS Primary Flight Control System", 42nd Annual Forum of the American Helicopter Society, Washington, D. C., June 2-4, 1986.

22. Murphy, R. D., "CH-53E Digital Automatic Flight Control System", American Helicopter Society (AHS) Meeting on Helicopter Flight Controls, 11-13 October 1978.

23. Masters, George W., Communications System Test and Evaluation, Airborne Systems Course Textbook, United States Naval Test Pilot School, 1 January 1981.

24. Glickman, H., Flight Control System Criteria for Advanced Aircraft for Incorporation into an Updated Military Specification, Grumman Aerospace Corporation, February 1981.

25. Kaniuka, W. W., et al, New Flight Control Technologies for Future Naval Aircraft, Report No. NADC-82240-60, September 1982.

26. Kaniuka, W. W., et al, New Flight Control Technologies for Future Naval Aircraft (Update), Report No. NADC-84088-60, June 1984.

27. <u>NATOPS Flight Manual</u>, NAVAIR 01-110HCE-1, 1 July 1985.

28. Corliss, L. D. and Carico, G. Dean, "A Flight Investi-
gation of Roll-Control Sensitivity, Damping, and Cross
Coupling in a Low-Altitude Lateral Maneuvering Task," NASA
Technical Memorandum 84376 of December 1983.

29. Livingston, C. L. and Murphy, M. R., "Flying Qualities
Considerations in the Design and Development of the Hueyco-
bra", Journal of the American Helicopter Society, Vol. 14,
January 1969.

30. Siegel, R. B., "A Case Against Computer-Aided Flight
Testing", Symposium on Computer-Aided Flight Testing, Report
Number 26, Plainview, New York, 5-7 October 1970.

31. Salmirs, Seymour and Tapscott, Robert, "The Effects of
Various Combinations of Damping and Control Power on Heli-
copter Handling Qualities during both Instrument and Visual
Flight", NASA Technical Note D-58, October 1959.

32. Goldstein, Kevin, "VTOL and VSTOL Handling Qualities
Speciations: An Overview of the Current Status", NASA Con-
ference Publication 2219, Helicopter Handling Qualities
Workshop, NASA Ames Research Center, Moffett Field, Cali-
fornia, 14-15 April 1982.

33. Key, David L., "A Critique of Handling Qualities Speci-
fications for U. S. Military Helicopters", AIAA Paper 80-
1592, 7th Atmospheric Flight Mechanics Conference, Danvers,
Massachusetts, 11 August 1980.

34. Hoh, Roger H., et al, <u>Proposed Specification for Han-
dling Qualities of Military Rotorcraft, Volume II -- Back-
ground Information User's Guide (BUIG)</u>,(DRAFT), USAAVSCOM
Technical Report 87-A-3 of May 1988.

35. Glickman, H., <u>Flight Control System Criteria for Ad-
vanced Aircraft for Incorporating into an Updated Military
Specification, Report No. NADC-78124-60</u>, June 1980.

36. Thaler, G. J., <u>Automatic Control Systems</u>, West Publish-
ing Company, St. Paul, Minn., October 1988.

37. Wood, Roy L. Jr., <u>Microcomputer Based Linear System
Design Tool</u>, M.S. Thesis, Naval Postgraduate School, Monter-
ey, California, September 1986.

38. Tompson, Peter M., <u>Program CC Version 4 Tutorial and
User's Guide</u>, of 27 May 1988.

39.   James, H. M., Nichols, N. B., and Phillips, R. S.,
Theory of Servomechisms, McGraw-Hill, New York, 1947.

40.   Tischler, Mark B., et al, "Frequency-Domain Identifica-
tion of XV-15 Tilt-Rotor Aircraft Dymanics in Hovering
Flight", AHS/IES/SEPT/SFTE/DGLR 2nd Flight Testing Confer-
ence, Las Vegas, Nevada, November 1983.

INITIAL DISTRIBUTION LIST

No. Copies

1. Defense Technical Information Center
   Cameron Station
   Alexandria, VA 22304-6145

   2

2. Library, Code 0142
   Naval Postgraduate School
   Monterey, CA 93943-5002

   2

3. Chairman, Code 62
   Department of Electrical and Computer Engineering
   Naval Postgraduate School
   Monterey, CA 93943-5000

   1

4. Professor George J. Thaler, Code 62Tr
   Naval Postgraduate School
   Monterey, CA 93943-5000

   2

5. Professor H. A. Titus, Code 62Ts
   Naval Postgraduate School
   Monterey, CA 93943-5000

   1

6. Chairman, Code 67
   Department of Aerospace Engineering
   Naval Postgraduate School
   Monterey, CA 93943-5000

   1

7. Professor Donald M. Layton
   44 Seca Place
   Salinas, CA 93908

   2

8. Mr. C. N. Jubeck, Code RW04
   RWATD
   NATC
   Patuxent River, MD 20670-5304

   1

9. Dr. Larry Mertaugh, Code RW04A
   RWATD
   NATC
   Patuxent River, MD 20670-5304

   1

10. Mr. Robert Miller, Code TP60A
    USNTPS
    NATC
    Patuxent River, MD 20670-5304

    1

11. Mr. Hank Agnew, Code AIR-53014D   1
    NAVAIRSYSCOM
    Washington, DC 20361-5301

12. Mr. Dean Carico, Code RWO4B   5
    RWATD
    NATC
    Patuxent River, MD 20670-5304

13. Mr. Jerry Higman   1
    NPS SMC #1359
    Monterey, CA 93943-5000

14. Mr. Tony Cricelli, Code 67Cr   1
    Naval Postgraduate School
    Monterey, CA 93943-5000